

POLITECNICO DI TORINO

Collegio di Ingegneria Energetica

**Corso di Laurea Magistrale in
Ingegneria Energetica e Nucleare (Energy and Nuclear Engineering)**

**EIT InnoEnergy Master in Environmental Pathways for Sustainable
Energy Systems (SELECT)**

Tesi di Laurea Magistrale

3D printing of advanced functional materials for sustainable energy systems



Supervisors

Prof. Vincenzo Esposito

Prof. Federico Smeacetto

Candidate

Lin Zhang

September 2018

Preface

This master thesis has been performed within the framework of the InnoEnergy Master's School program: M.Sc. SELECT – Environmental Pathways for Sustainable Energy Systems. The thesis work “3D printing of advanced functional materials for sustainable energy systems” was completely conducted with internally funding at the Technical University of Denmark (DTU), Department of Energy Conversion and Storage (DTU Energy), Risø Campus, Roskilde, Denmark from April 30, 2018 to September 7, 2018 under the supervision of Prof. Vincenzo Esposito from Technical University of Denmark and Prof. Federico Smeacetto from Politecnico di Torino.

Acknowledgements

I would like to start expressing my sincere gratitude to my supervisor Prof. Vincenzo Esposito from Department of Energy Conversion and Storage at Technical University of Denmark. Though extremely busy, he was always able to support me whenever I was lost in literatures or ran into trouble spots during experiment. His consistent motivation and professional suggestions are invaluable for the whole process of thesis.

Next, I would like to acknowledge Prof. Federico Smeacetto from Department of Energy at Politecnico di Torino, who offered me this great opportunity to develop such an interesting and leading-edge thesis work. I am obliged for his generosity and consultations, as well as his valuable comments on the thesis plan and writing.

Special thanks are also given to Dr. Jacob R. Bowen and Dr. Astri Bjørnetun Haugen, who continuously provided refreshing ideas and driving force towards the completion of this work. In addition, I would also like to say thanks to all my friends here in Denmark, especially the Chinese group, who kept me accompanied and made me life colorful during a fantastic 2018 summer.

Thank you Prof. Massimo Santarelli and Prof. Peter Hagström for the organization of SELECT master program and Kungliga Tekniska Högskolan and Politecnico di Torino for providing such a great platform to make everything happen.

My acknowledgment also goes to the SELECT family members, who are always innovative, brilliant, supportive and delightful. The amusing cultural exchange experience and adventurous journey we have been through together in seventeen European countries will for sure influence my whole life. I hope to meet you all again someday, somewhere in the world.

Finally, I must express my profound gratitude to my parents Yizhen Yue and Jianjun Zhang, who constantly support me throughout student life. The continuous mental encouragements I received from you are crucial to the completion of my master degree and to my future life.

All in one phrase, Thank you /Tack så mycket/Grazie mille/Mange tak/谢谢!

Lin Zhang

2018-09-07

Roskilde, Denmark

Abstract

Constant and secure energy supply plays a critical role in the stable development of one society and economy. The Paris agreement signed in 2015 by 174 countries has also acknowledged the importance of developing sustainable energy technologies for mitigating the global warming and reducing other effects caused by the climate change.

Among all advances, adopting new manufacturing methods for energy systems has been considered as a way to contribute to such progress. Additive manufacturing (AM), also known as 3D printing (3DP), has recently emerged as a practical strategy for optimizing fabrication process, innovating the design and enhancing energy systems' performance. By covering research and innovation from starting materials' formulation and complex structural design to printers' development and system integration, the 3DP technology is expected to give chances to the generation of various customized products with controlled structures and embedded functionalities. Despite 3DP in energy systems has great promises for future challenges, this technology has not been fully developed yet and a thoughtful analysis is thus needed to provide general criteria to link 3DP technology and energy technologies.

As a starting point, current research shows the significance of converting advanced functional energy materials into 3DP processable compounds to facilitate the production of 3D object with devised complex geometries and tailored microstructures. Enlighted by this idea, this thesis work is conceived to develop 3D printable hybrid piezoelectric materials that can be used in energy applications. As one of the most interesting 3DP techniques, fuse deposition modeling (FDM) was selected for our work due to its easy controllability and capability of producing high-resolution objects. The experimental approach included material synthesis (barium titanate production, spinning solution preparation, electrospinning and calcination), printing pastes preparation, 3D printing and post-processing. Characterization results show that barium titanate microfibers (BTMFs) with high-yield fabrication and consistent size were successfully produced. Simple CAD designed structures with inside controllable highly-oriented BTMFs were manufactured by FDM. An enhanced dielectric property of 31 was observed at 1 kHz in our 3D printed material, a value that is around 300% higher than pure PVDF polymer and about 50% higher compared to materials with same composition but produced by other techniques. At the end, a general study of the potential application of the prepared functional materials was conducted.

In conclusion, this master thesis summarizes the progress of energy technologies processed by 3DP and provides new perspectives in the manufacturing of high-performance, flexible hybrid materials that have promising applications in energy harvesting and sensing technologies.

Keywords: 3D printing; Functional Materials; Energy Harvesting; Fused Deposition Modelling; Piezoelectric Materials; Dielectric properties; Applications;

Table of content

PREFACE	I
ACKNOWLEDGEMENTS	II
ABSTRACT	III
LIST OF FIGURES	VI
LIST OF TABLES	X
ACRONYMS	XI
CHAPTER 1. INTRODUCTION	1
1.1 Background	1
1.2 Objectives	4
CHAPTER 2. STATE OF THE ART: 3D PRINTING OF FUNCTIONAL MATERIALS FOR ENERGY SYSTEMS	5
2.1 Overview of 3D printing techniques	5
2.1.1 Material extrusion (ME)	6
2.1.2 Vat polymerization (VP)	8
2.1.3 Powder bed fusion (PBF)	10
2.1.4 Material Jetting (MJ)	12
2.1.5 Binder jetting (BJ)	13
2.1.6 Sheet lamination (SL)	14
2.1.7 Directed energy deposition (DED).....	15
2.1.8 Summary of current 3D printing techniques	17
2.2 Overview of functional materials for energy systems	19
2.2.1 Materials by functionalities.....	19
2.2.2 Materials by microstructure.....	22
2.2.3 Summary of functional material for sustainable energy systems	24
2.3 Overview of 3D printing of functional material for energy systems	25
2.3.1 Solar energy systems.....	25
2.3.2 Thermoelectric energy systems	26
2.3.3 Wind energy systems	30
2.3.4 Energy storage systems.....	31
2.3.5 Super capacitors	33
2.3.6 Thermal energy systems	34
2.3.7 Fuel cells systems	35
2.3.8 Sensors	38
2.3.9 Summary of 3D printing of functional material for energy systems	40

CHAPTER 3. 3D PRINTING OF ADVANCED FUNCTIONAL MATERIALS FOR SUSTAINABLE ENERGY SYSTEMS: A CASE STUDY OF FERROELECTRIC COMPOSITES FOR ENERGY HARVESTING.....	41
3.1 Motivation.....	41
3.2 Experiment	45
3.2.1 List of equipment	45
3.2.2 List of materials	46
3.2.3 The 3D printer	47
3.3 Preparation of the starting materials: BaTiO₃ microfibers (BTMFs).....	49
3.3.1 Preparation of spinning solution.....	49
3.3.2 Electrospinning and calcination process.....	50
3.4 3D printing of the BTMFs/PVDF hybrid material	51
3.4.1 Computer aided design of printing object	51
3.4.2 Preparation of printing pastes	51
3.4.3 3D printing of designed objects	52
3.5 Characterizations	52
CHAPTER 4. RESULT AND DISCUSSION	54
4.1 Characterizations of the BTMFs.....	54
4.1.1 Thermal properties.....	54
4.1.2 Morphology.....	55
4.1.3 Crystallography.....	58
4.2 Characterizations of 3D printed BTMFs/PVDF hybrid materials.....	59
4.2.1 Rheology.....	59
4.2.2 Crystallography.....	62
4.2.3 Morphology.....	63
4.2.4 Dielectric property	65
CHAPTER 5. BUSINESS CASE ANALYSIS.....	69
5.1 Energy storage system	69
5.2 Smart wearable industry	69
5.3 Medical industry	70
5.4 Wind energy industry.....	72
5.5 Automotive industry	73
CHAPTER 6. OVERALL CONCLUSION	74
CHAPTER 7. FUTURE WORK	75
CHAPTER 8. REFERENCES.....	76

List of figures

Figure 2-1 Types of 3D printing techniques 5

Figure 2-2 Schematic illustration of material extrusion process 6

Figure 2-3 Schematic illustration of vat polymerization process 8

Figure 2-4 Comparison between 3D printed objects from a SLA printer (Left) and a FDM printer (right)[31] 9

Figure 2-5 Schematic illustration of powder bed fusion process 10

Figure 2-6 Schematic illustration of material jetting process 12

Figure 2-7 Schematic illustration of binder jetting process 13

Figure 2-8 Schematic illustration of sheet lamination process 14

Figure 2-9 Schematic illustration of direct energy deposition process 16

Figure 2-10 Schematic illustration of the hybridized 3Dceram CERAMAKER coupled with different printing techniques and multi-materials processing technique [58] 19

Figure 2-11 Schematic illustration of 3D geometrical optimized busbars for solar cells[74], with traditional rectangle busbars on the left and shape optimized busbar on the right 22

Figure 2-12 Schematic illustration of sol-gel process[81] 23

Figure 2-13 Schematic illustration of a simple electrospinning setup 24

Figure 2-14 Schematic illustration of a 3D printed light trapper with solar cells 25

Figure 2-15 Schematic illustration of a CAD designed light trapper for solar cells 26

Figure 2-16 Otego designed “oTEG”[100] 28

Figure 2-17 Example of 3D tailor-made TEGs for pipes, enlightened by Kim et al.[106] 29

Figure 2-18 A working proof of concept of 3D printed mobile wind turbines [109]	30
Figure 2-19 Representative configuration of 2D and 3D microbatteries	31
Figure 2-20 Schematic illustration of 3D interdigitated microbattery architectures, enlightened by Lewis’s research[116]	32
Figure 2-21 Schematic illustration of the preparation of 3D-printed electrodes for Li- ion batteries, enlightened by Hu et al.[119].....	33
Figure 2-22 3D printed supercapacitors with periodic macroporous structure, enlightened by Zhu et al.[121].....	34
Figure 2-23 3D printed functional RGO heater, enlightened by Hu et al.[122]	35
Figure 2-24 SEM observations of the inkjet printings of YSZ with 2-layer (up) and 5-layer (down) depositions after sintering at 1300 °C for 6 h. Reprinted from V. Esposito et al.[128]	36
Figure 2-25 Schematic illustration of the Cell3Ditor project[134]	38
Figure 2-26 Schematic illustration of 3D fabrication of ear prosthesis proposed by Suate-Gomez et al.[140]	39
Figure 3-1 3D printed objects with intended fibers alignment A). Device diagram of an FDM 3D printer B). Desired highly-aligned fibers produced by 3DP C). Random oriented fibers often found in other manufacturing techniques D). Enlarged view at printing needle	42
Figure 3-2 Design of two different printing scenario A). Overall view of one- direction-printing with same-aligned microstructure on each layer; B). Right- side view of one-direction-printing; C). Overall view of two-direction-printing with cross-aligned microstructure on each layer; D). Right-side view of two- direction-printing	43
Figure 3-3 Digital view of CELLINK INKREDIBLE on the left and CELLINK BIOX on the right	47
Figure 3-4 Adjusting Z axis for the 3D printer	48
Figure 3-5 Electrospinning solution preparation process A). Glassware arrangement B). Flow chart of the preparation of the viscous spinning solution	49

Figure 3-6 Flow chart of the electrospinning process and related post-processing procedures.....	50
Figure 3-7 Computer aided design of printing object A). Overview B). Front view C). Top view	51
Figure 3-8 Flow chart of the preparation of 3D printing paste	52
Figure 4-1 TGA/DTG analysis.....	54
Figure 4-2 Physical photos of A). as-spun material B). as-calcinated material	55
Figure 4-3 Electrospinning with applied voltage at 15 kV and binder concentration at A). 0.025 g/ml B). 0.050 g/ml.....	55
Figure 4-4 Electrospinning with binder concentration at 0.025 g/ml and applied voltage at A). 10 kV B). 15 kV C). 20 kV	56
Figure 4-5 SEM figures of A). B). as-spun BTMFs and C). D). calcinated BTMFs	57
Figure 4-6 SEM figure of grinded BTMFs	58
Figure 4-7 XRD characterization of the as-prepared materials (Left) and reference XRD pattern (Right)[85].....	58
Figure 4-8 Result of rheology test-viscosity test.....	59
Figure 4-9 Result of rheology test-double logarithmic power law plot for showing flow index	60
Figure 4-10 XRD pattern of pure PVDF, BTMFs and hybrid printing materials	62
Figure 4-11 Comparison of A). physical view of the one direction printed object (3 layers) after drying and its B). digital design model vs. B). physical view of the crossed printed object (3 layers) after drying and its D). digital design model	63
Figure 4-12 SEM figures showing the alignment of BTMFs in 3D-printed materials with different loading A). 4.5 vol% BTMFs C). 20 vol% BTMFs C). 25 vol% BTMFs	64
Figure 4-13 Sample of 3D printed BTMFs/PVDF hybrid material with silver electrodes for dielectric testing	65

Figure 4-14 Frequency dependence of the dielectric constant of the 3D printed hybrid material.....	66
Figure 4-15 Dielectric constant comparison of BTMFs/PVDF composites with different BTMFs loadings at 0.1 kHz, 1 kHz and 10 kHz, room temperature	67
Figure 4-16 Dielectric constant comparison between the 3D-printed BTMFs/PVDF hybrid material and the reported BTO/PVDF composites at 1 kHz, room temperature	68
Figure 5-1 PEH applications in smart shoes	70
Figure 5-2 3D printed ear prosthesis for temperature and pressure sensing by Gómez et al.[140] A). Computer-aided designed ear prosthesis B). 3D printed ear prosthesis	71
Figure 5-3 PEHs applications on heart to power defibrillator and pacemaker	71
Figure 5-4 PEHs applications on wind turbines A). PEHs using bending force B). PEHs using rotary motion.....	72
Figure 5-5 PEHs applications on automotive.....	73

List of tables

Table 2-1 A summary of advantages and disadvantages of 3D printing technology..... 17

Table 3-1 List of experiment equipment45

Table 3-2 List of experiment materials46

Table 4-1 Flow indexes for the pure PVDF, reference gel and the hybrid materials..... 61

Acronyms

3DP	Three-Dimension Printing
AM	Additive Manufacturing
ASR	Area Surface Resistance
BJ	Binder Jetting
BTO	Barium Titanate
BTMFs	Barium Titanate microfibers
CAD	Computer Aided Design
CAPEX	Capital Expenditure
CHP	Combined Heat and Power
CSP	Concentrated Solar Plant
DED	Direct Energy Deposition
DLP	Digital Light Processing
DOD	Drop on Demand
FDM	Fused Deposition Modelling
GHG	Greenhouse Gas
GO	Graphene Oxide
HVAC	Heating, Ventilation and Air Conditioning

LOM	Laminated Object Manufacturing
ME	Material Extrusion
MJ	Material Jetting
OPEX	Operational Expenditure
PBF	Powder Bed Fusion
PE	Piezoelectric Effect
PEH	Piezoelectric Energy Harvester
PV	Photovoltaic
PVDF	Polyvinylidene Fluoride
PZT	Lead Zirconate Titanate
RGO	Reduced Graphene Oxide
SEM	Scanning Electron Microscope
SL	Sheet Lamination
SLA	Stereolithography
SLM	Selective Laser Melting
SLS	Selective Laser Sintering
SM	Subtractive Manufacturing
SOFC	Solid Oxide Fuel Cell
TEG	Thermoelectric Generator

TGA	Thermogravimetric Analysis
UAM	Ultrasonic Additive Manufacturing
UV	Ultraviolet
VP	Vat Polymerization
XRD	X-Ray Diffraction
YSZ	Yttria-Stabilized Zirconia

CHAPTER 1. Introduction

1.1 Background

Ever since the industrial revolution, the human beings have been witnessing a drastic increase in energy-related consumption of fossil fuels, causing a disruptive amount of greenhouse gases (GHGs) emission that directly leads to the global warming crisis. A recent report from the International Energy Agency (IEA) revealed that a historic value of 32.5 gigatons (Gt) of CO₂ emission has been recorded in 2017, posing an extreme threat to global climate, public health as well as the natural ecosystem.[1] However, a constant and secure energy supply is crucial for the development of our society and economy.[2], [3] Therefore, finding proper methods to provide sufficient amount of energy while still control GHGs emission at the same time becomes a necessity.

Lots of progresses have been made in innovating functional materials, creating hybrid energy systems, introducing new policies for renewable energy integration, etc.[4]–[11] Among all solutions, developing inexpensive, reliable, CO₂ neutral energy harvesting and storage devices (e.g. photovoltaic panels, wind turbines, fuel cells, rechargeable batteries, etc.) is considered to be one of the key way-out.[12] Yet, it is reported that using conventional methods to fabricate such energy production and storage devices could, to some extent, compromise the performance of energy systems due to their intrinsic limitations in the ability of controlling the geometry and architecture of materials and products.[8] Nonetheless, very few attentions are paid to optimizing the manufacturing process of such energy devices.[13] An advanced fabrication technology that is both affordable and capable of producing sophisticated shape and designed structure is therefore needed. On the other hand, the concept of micro-power generation gained its popularity in the past few decades. By welcoming a decentralized generation of electricity and heat, individuals or local companies are expected to behave like “prosumers”, meaning that they are capable of internally generating power to fit their own needs and even feed the excessive power to their neighbor or to the grids. By doing this, an energy self-sufficient society can be created with zero waste of resources and an autonomous operation. However, this idea requires a cooperative operation inside the neighborhoods in order to achieve a better overall performance.[14] A wide-spread application of home-scale renewables that are inexpensive and easy-accessible is consequently necessary. As each residential family has different energy consumption pattern, tailored-made energy harvesters and management systems are thus needed to be designed and manufactured for each household. Yet, traditional common mass production methods are known to be inflexible for customized products as it is difficult

to alter the design or production process once the production lines are implemented, posing another problem to the energy industry.

Additive manufacturing (AM), also known as 3D printing (3DP), has thus emerged as an innovative approach to solve the problem. Ever since its first introduction by Charles Hull in mid-1980s from a process now known as stereolithography (SLA), the 3DP technology has continuously received enormous attention.[15]–[17] It is fundamentally different from traditional subtractive manufacturing (SM) methods as the core concept of this technology is to adopt a bottom-up approach where an object can be constructed into its digital designed shape by following a layer-by-layer step in three-dimension formations. By doing this, the number of production processes can be significantly reduced and procedures which are generally considered as time demanding and material or energy inefficient (e.g. molding, cutting, welding, etc.) can be avoided.[17] Recently, a significant cost reduction of printers caused by the patents expiry and technology progression has also attracted the attention from a variety of sectors.[13]

Due to the above-mentioned features, the 3DP technology possesses many intrinsic advantages over conventional methods. Several studies have already compared 3DP with traditional subtractive manufacturing methods and illustrated how 3DP can benefit the manufacturing process and the product. Obviously, different techniques have different advantages and disadvantages, but in general, 3DP has the following beneficial features[18]–[20]:

- Ability to rapid prototyping;
- Ability to produce customized objects with different features;
- Ability to create novel complex-shaped and light weight functional products (e.g. medical nano-scaffold, etc.);
- Ability to reduce material consumption;
- Ability to reuse/recycle waste materials;
- Ability to create more sustainable production process;
- Ability to improve existing manufacturing process as preparatory steps;
- Ability to cut capital expenditure (CAPEX) and operation expenditure (OPEX);
- Ability to enable more direct revenue streams and generate higher net revenue;
- Ability to promote more direct interactions between consumers and producers;
- Ability to increase production efficiency due to reduced design-to-market time;
- Ability to ensure safer operation due to less manual labor participation and more automation control (robotic production);
- Ability to empower a decentralized production with digital design;
- Ability to achieve innovative supply chains with optimized design concepts;
- Ability to create competitive business models via open source sharing.

Despite many people claims that 3D printing is a disruptive but simple process, in reality it suffers from many constrains.[8], [21] For example, the limited materials options of printing inks and the difficulty to select common post processing conditions largely hinder the employment of 3DP. Slow speed is another typical problem as the existing 3D printers can only produce very limited number of pieces in a certain period of time while conventional manufacturing methods can achieve mass production in a much more cost-effective manner. To have a better view of the disadvantage of current 3DP, some of the representative limitations are summarized below:

- Slow production speed;
- Limited material options;
- Possible costly machines;
- Need special training for computer aided 3D design;
- Difficult post processing might be required in some techniques;
- Poor surface finish and low resolution in some techniques;
- Poor mechanical properties in some techniques;
- Limited recyclability of product due to quality loss;
- Limited replication of business model to other sectors;
- Not suitable for multi-materials product in some techniques;
- Not suitable for mass production with the existing technologies.

Based on the above-discussed features that 3DP has, most people nowadays hold the view that this technology can only serve as a part of simple production, at least in the foreseeable future. It cannot either replace the whole traditional production process or become a mass production technique for all kinds of products. Nonetheless, some early adopters in the dental and medical industry, jewelry industry and aerospace industry have also set their long-term development goal to incorporate 3DP technology into their business.[20] Also inspired by its benefits, many industrial energy companies have also expressed interest in employing 3D printing into their production processes. However, when it comes to the application of 3D printing in the field of energy sector, such integration still mainly remains in the laboratory level and mostly unexploited.

As said by the economists, the implementation of 3D printing could empower things to be produced in a more economically manner with smaller numbers, more customization, higher flexibility and lower input of labor. Consequently, using 3D printing to prototype and customize new energy solutions is considered to be one of the keys to push forward the trend of power generation, especially from a micro side, which leads to the inspiration of this thesis.

1.2 Objectives

In this thesis, the potential and limitations of 3D printing for energy technologies were firstly explored by starting with a comprehensive literature review, which leads to a summary of current 3D printing technology and their roles in energy applications. This was followed by an analysis of suitable 3D printable functional materials for energy application. It was found out that the development of energy technologies go hand in hand with the advance of functional materials. Ranging from heat-storage ceramics for energy storage technology to ferroelectric oxides with high power conversion efficiency in PV systems, advanced functional ceramics materials (i.e. electro-ceramics), in particular, have been studied intensely for energy application.[22]–[24] A series of experiments of the fabrication and performance test of functional advanced ceramic-based composite materials were therefore designed and conducted by using 3D printing technology based on literature review. Lastly, a short study of the potential application of the prepared functional material in the energy sector was identified.

The scope of the work can be defined into three parts. Firstly, the state of the art, the benefits and limitation, the materials of the current 3D printing technologies in the field of energy technology were summarized. Secondly, attentions were paid to the experiment procedures, which included the processing of 3D printable functional materials such as raw materials synthesis, inks preparation and pastes characterization. The optimized condition for printing was tested and defined thereafter. Thirdly, a business analysis was conducted in order to point out the potential applications of the prepared materials.

CHAPTER 2. State of the art: 3D printing of functional materials for energy systems

Nowadays, finding out a proper manufacturing method for energy technology is of great importance as the conventional production of energy devices usually involves multiple inefficient processing procedures that are material-wasting, time-consuming and energy-demanding. The employment of 3D printing technology is believed to bring competitive improvement in terms of functionality embedment, performance enhancement and cost reduction.[21] In the following section, existing additive manufacturing techniques, 3D printing materials and some of their proposed applications are reviewed.

2.1 Overview of 3D printing techniques

Various 3D printing techniques have been developed in the past decades to facilitate the construction of objects. According to the ISO and ASTM international standard terminology document (ISO/ASTM 52900:2015), these techniques can be categorized into seven sub-groups, which are Material Extrusion, Vat Polymerization Powder Bed Fusion, Material Jetting, Binder Jetting, Sheet Lamination and Directed Energy Deposition.[25] Figure 2-1 shows the hierarchy of the seven additive manufacturing techniques as well as some of their representative subclass groups.

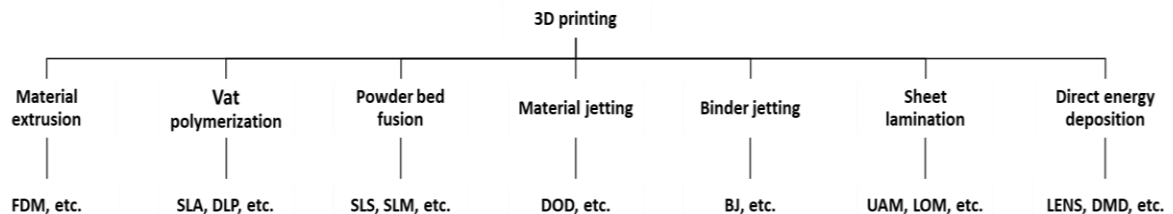


Figure 2-1 Types of 3D printing techniques

The difference between these techniques lies in the printing mechanism, the materials used during the processes and the way that layers are deposited. Parameters such as fabrication speed, surface resolution, build volume, production cost, mechanical strength are normally used to evaluate the performance of each 3D printing process. Hereby, all seven 3D printing processes are listed and discussed based on their characteristic, current available printers and potential applications.

2.1.1 Material extrusion (ME)

Among all AM technologies, extrusion-based additive manufacturing is considered to be the most versatile way to build 3D items due to its facile printing strategy and easy controllable fabrication process.[26]

The most common method of extrusion-based 3DP is fused deposition modelling (FDM), a method that uses thermoplastic polymer or low melting points composite filaments as its printing materials. In order to print objects, the FDM technique firstly uses the printer nozzle to heat up the as-received filaments and turn the viscous-elastic materials into semi-liquid form. Afterwards, material is pushed out onto the desired substrates layers by layers with the help of pressure pump. It should be noted that in order to maintain a proper shape of the designed product, the FDM material should be able to solidify quickly, either by itself or under the help of external sources such as UV curing. Apart from that, the materials should have also good binding ability with previous printed layers in order to obtain a solid one-piece part. Therefore, it is important for extruded materials to possess a proper melting point (typically at around 200 °C) and appropriate viscosity.

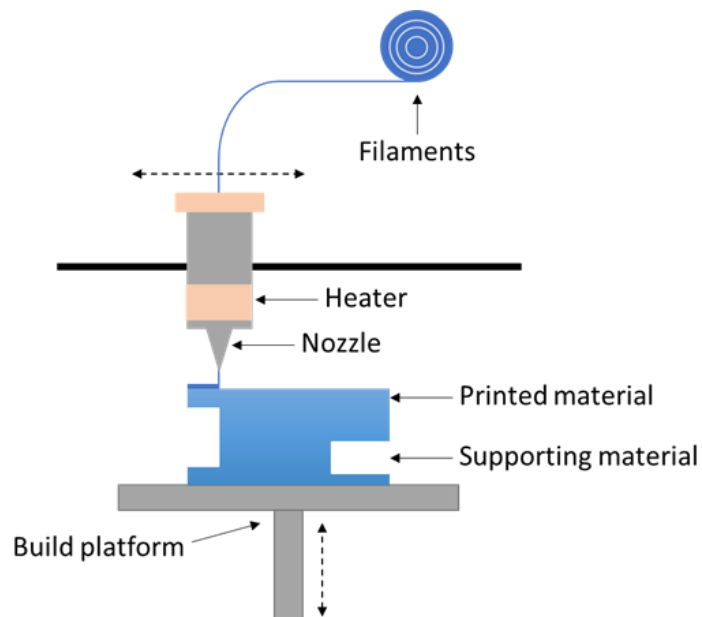


Figure 2-2 Schematic illustration of material extrusion process

Famous for its low-cost, easy-accessibility and simple-operation, FDM also stands itself out among many ME techniques by having the capability of processing multiple materials at one time. Recently, Gibbons *et al.* developed a novel AM system that can process various materials at the same time and print out a heterogeneous structure consist of variable compositions and different properties.[27] Similarly, David *et al.* constructed a hybridized FDM system that can deposit multiple materials by using a

combination of printing techniques. The designed system is also capable of controlling the thickness of different layers and the width of roads by the introduction of two legacy FDM machines.[28] Based on such multimaterials processing merit, a much wider range of industrial or research applications can be unlocked by FDM.

However, a limited number of thermoplastic material choices together with weak mechanical performances and poor surface quality of the obtained products hamper the application of extrusion-based 3D printing process. In this context, current research has been focusing on enriching thermoplastic filaments options, developing fiber-reinforced composites, and further constructing 3D printer that can produce high aspect ratio solids from multiple materials.[16]

As for now, the FDM technology has been found out to be widely used in a variety of companies such as Nestle from the food industry, Hyundai and BMW from the automobile industry and some drug-packaging firms from the pharmaceutical sector. In terms of available 3D printers, a project called REplicating RAPid prototype (RepRap) has to be particularly mentioned. Started by Dr. Bowyer in 2005 with an aim of developing low-cost printers, RepRap is a range of home-based 3D printers that predominantly associate themselves with FDM technique and target at designing self-replicable 3D printers. Based on this idea, the machines were designed to be consist of standard materials that are both cheap and easy accessible. This gives the possibility of a mass distribution of FDM based printers and spread the reputation of in-home extrusion-based printing technology.[29] When it comes to a commercial available product, a wide selection of types can be found in the market. Some well-known models are Replicator from MakerBot, Cube from 3D Systems Inc, Mojo from Stratasys and Inkredible from Cellink. The price of these modes largely depends on size and application and therefore varies from a few hundred euros to over thousands.

2.1.2 Vat polymerization (VP)

Vat polymerization is a general term that refer to techniques such as Stereolithography (SLA), Digital Light Processing (DLP) and other similar process that are driven by a reaction called photopolymerization. The photopolymerization is a phenomenon where various types of chemical compounds solidify because of a series of chemical reactions triggered by light illumination.

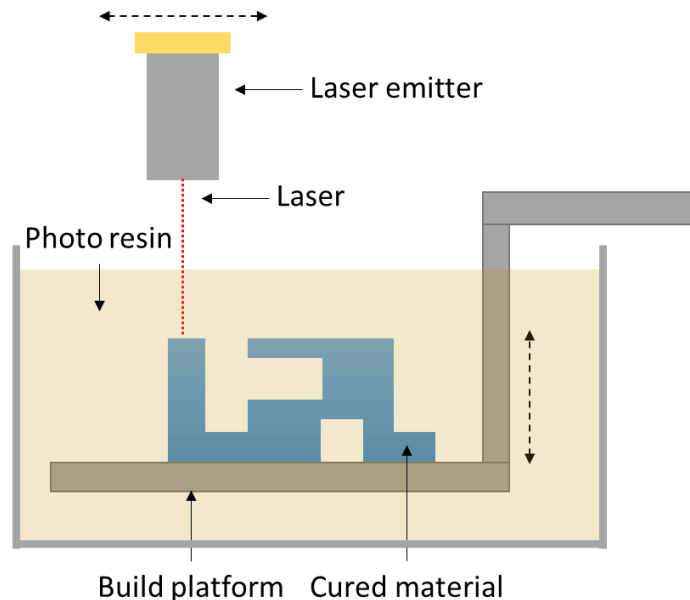


Figure 2-3 Schematic illustration of vat polymerization process

The most typical technology in the vat polymerization group is Stereolithography (SLA), a technique that was developed in mid-1980s. This technique uses monomer such as liquid resins as its original material. Sometimes ceramic particles are added to the virgin printing materials in order to obtain composites materials for functional purposes. High-energy light such as UV beam is utilized to harden the objects by initiating chain reactions in thin light-sensitive monomer layers. Such layers polymerize instantly once they are exposed to light while the unreacted parts stay in liquid form and are removed later. Post heat treatments are often required for SLA-based products in order to obtain desired mechanical strength. Compared to FDM, the printed parts from SLA usually possess higher resolution (e.g. from 100 to 300 μm in z-axis and from 200 to 400 μm in x/y-axis for FDM vs. from 25 μm to 100 μm in z-axis and from 50 to 180 μm in x/y-axis for SLA), but the product itself tends to be more expensive and most of the time becomes increasingly brittle over time.[30]

Similarly, Digital Light Processing (DLP) is another type of VP-based printing technique and uses the same mechanism during the printing process. However, there are some differences between SLA and DLP. One of the biggest distinctions is the way of

projecting light. While SLA uses single UV laser to draw rounded lines during printing, DLP uses a digital micro mirror device or a projector to control the direction of light for treating the surface at once. As the whole printed layer is cured simultaneously, the printing time of DLP can be much reduced.[32] However, a faster production speed of DLP results in a lower resolution of the product. Therefore, a tradeoff between speed and resolution is needed to be made.



Figure 2-4 Comparison between 3D printed objects from a SLA printer (Left) and a FDM printer (right)[31]

Even though the number of VP-based printing materials continues to increase, the VP printing technique is still intrinsically limited for multimaterials processing due to the design of using ink sink, which normally comprises one single resin at one time. This means that the fabrication of multimaterials product via VP-based printing process remains difficult. To solve this problem, works have been done on the development of automated systems that are capable of producing multimaterials objects by introducing exchangeable resin reservoirs.[33] On the other hand, in order to further improve the performance of VP-produced objects, some other advances were found in developing composite materials with good mechanical and electrical functionality, inventing different curing light sources conditions, etc.[34]–[36]

Although SLA is the oldest technique among all 3D printing choices, many printers available in the market can still be found to be based on this technique. 3D System Inc, for example, provides various types of SLA machines for both industrial and home-based customers.[37] Form 2 produced by Formlabs is another famous SLA printer that

has been continuously ranked as one of the greatest home use SLA machines.[38] CERA FAB 7500 & 8500 from Lithoz are other outstanding choices. By homogeneously dispersing ceramic powder into a UV-sensitive polymer matrix, high-performance ceramic parts can be selectively structured by this DLP-based machine. Likewise, 3Dceram is a French company that supplies printing services for ceramic-related products based on SLA. Alternatively, other DLP-based printers can be found as Micromake L2, Anycubic Photon, Envision Tec Ultra, Lunavast XG2, etc.

2.1.3 Powder bed fusion (PBF)

Powder bed fusion is another 3D printing technique that utilizes laser beam to fuse powder into a designed 3D solid structure. Once the first layer is completed, the powder bed lowers itself based on defined thickness and a new round of powder is dropped on the bed for the next fabrication. This technology is capable of printing materials including polymer, metals, alloy, composites and so on.

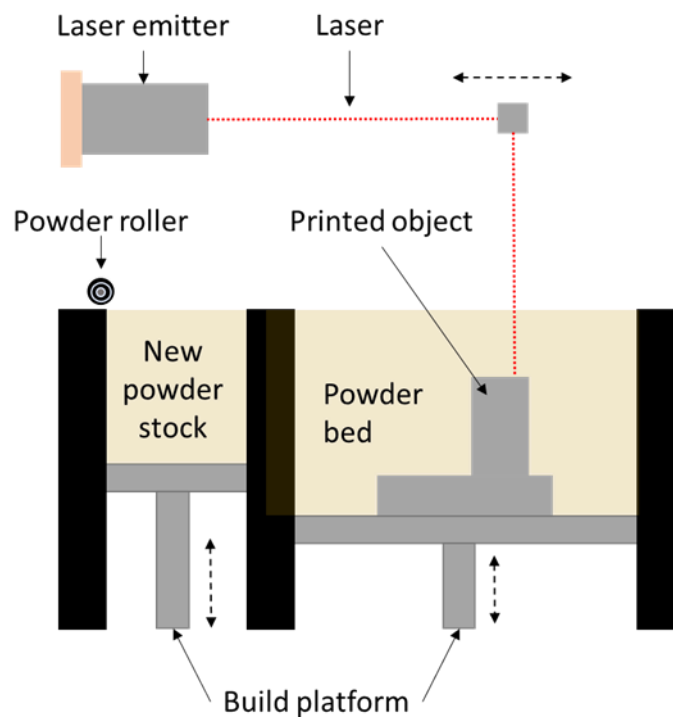


Figure 2-5 Schematic illustration of powder bed fusion process

The most two popular techniques in powder bed fusion are Selective Laser Sintering (SLS) and Selective Laser Melting (SLM). Although these two techniques use very similar concepts, fundamental differences can be found in their products as the material in SLM is fully melted while the material in SLS is only partially sintered. Such a distinction makes SLS and SLM suitable for different printing situations. Essentially, SLS can handle a variety of materials at one time as long as some parts of the material can fuse to “glue” the whole piece while the rest remains unchanged. This partially-melted feature often results in a porous surface, which can be tuned by varying the sintering

temperature. By contrast, SLM use laser to achieve a full melt and convert the whole dumped powder into one homogenous part. Therefore, the products from SLM exhibit a higher mechanical performance compared to those from SLS as the SLM-based objects have fewer voids and less porosity inside the printed structures. However, to have one fixed melting point, the material of SLM is limited to a selected choice of single metal powder such as steel and aluminum. That means mixed powder such as alloy is not applicable in this technique. This makes SLM more practical in single-material application but less viable when it comes to multimaterials processing. [39]–[43]

Generally speaking, fine resolution and wide range of material selection are the main advantages of power bed fusion. These merits make power bed fusion popular in shaping complex construction for applications like medical scaffolds, tooling, aircraft instruments and other area where small quantities of high-quality parts are needed. In addition, untreated materials are used to support the printed structures throughout the printing processes, thereby avoiding the repeated process of removing materials. However, many unsolved issues remain for power bed fusion technique. For instance, although many companies advocate that the materials used during the SLS/SLM process can be reused, this is not the true case when it comes to the real-life operation. The supporting materials that are exposed to high temperature for long period are reported to be prone to unpredictable chemical reactions. Report shows that in order to reuse the unreacted materials, around 50% of extra virgin powder must be additionally provided. For this reason, 3D printing with SLS/SLM technique is suggested to work with cost-insensitive fabrication. Besides, as discussed above, the inherently mechanism of powder bed fusion technology makes itself less competitive when dealing with multi-materials objects. Certainly, some people might state that different layers of powder can be added once at a time to print out product with different composition parts. However, in return, the fabrication processes might become too complicated and the virgin materials are no longer “pure” to be recycled.[44]

Currently, researchers are working on optimizing PBF printing by developing new material formulations that have slow oxidation rate and low resistance degradation during the prolonged heating, constructing multi-powder deposition printers to enable multi-materials processing, and analyzing the physical and metallurgical mechanisms throughout the printing procedure.[45]

In terms of the available 3D printers, most SLS/SLM-based printers are found out to be designed and manufactured for industrial company or academic groups rather than home-based amateurs. This is probably due to the requirement of high energy-demanding lasers during the printing process, which makes the printing process very expensive and difficult for the general public to operate. Nevertheless, an interesting project called Focus SLS printer was reported for improving the applicability of SLS-

based technique for home-based 3D printing. Regardless of some great progression, the project was forced to terminate in 2013 because of the slow production speed and high cost compared to other 3D printing technology.[46] Formiga P 110, on the other hand, was rated as the best commercial SLS machines according to 2018 3D printer guide. With the access to the most common polyamide materials and the capability to generate complex medium-sized prototype, this industrial SLS printer is marketed for professional printing businesses and is one of the top of its class.[38]

2.1.4 Material Jetting (MJ)

Material jetting technique has many other names: Inkjet printing, PolyJet, Drop on Demand (DOD), etc. It is a process that print items in a way similar to traditional two-dimensional printers. To begin with, the MJ printer usually carry a container, from which liquid droplets are pushed out and precisely positioned onto desired substrates. UV light treatment is then carried out to cure the materials. Once a thin layer is created, the process repeats itself by jetting following layers until the whole designed structure is created. Polymers and waxes are often chosen as the original materials due to their suitable viscosity to form drops and proper chemical and physical properties. The minimum resolution of MJ printed structure is restricted by the minimum volume of one droplet. Therefore, developing multimaterials object can be easily produced by simply switching the material containers during the building stage. Currently, it is popularly used for printing complex and advanced ceramic structures such as medical scaffolds.[16]

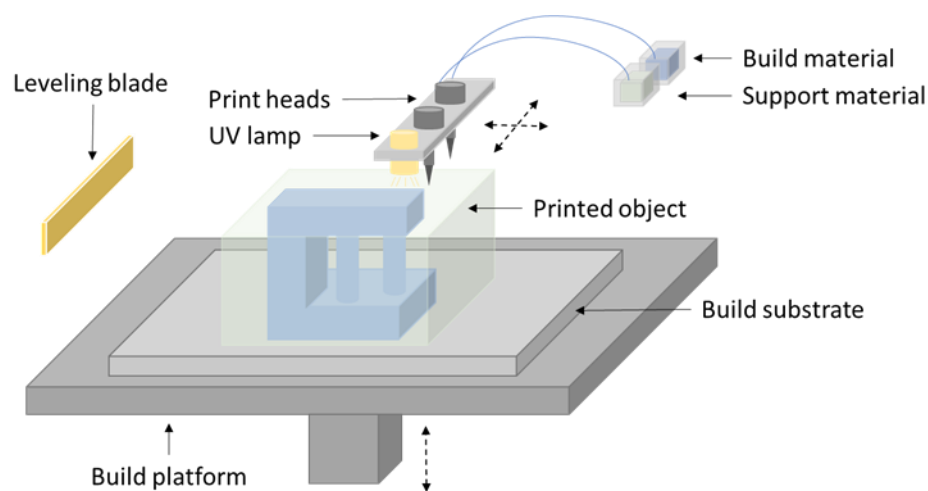


Figure 2-6 Schematic illustration of material jetting process

Compared to other technique, material jetting technology guarantees a minimum usage of materials and large-size production without compromising high printing accuracy. This is extremely beneficial to production associated with expensive materials. Plus, MJ printers are much cheaper as compared to other AM machines. High-speed fabrication

can also be achieved by using heads equipped with numbers of nozzles, By contrast, typical drawbacks of MJ are limited materials choices, low adhesion between layers, weak mechanical performance and degradation via light.[16], [47]–[49] As a result, some valuable works have been done on developing photo-robust long-lasting materials and developing multimaterials printers.[50]–[52]

2.1.5 Binder jetting (BJ)

Binder jetting is capable of using a wide selection of materials such as metal, ceramics and polymers during the printing process and its printing mechanism is also very similar to powder bed fusion. Firstly, a designed thickness of virgin materials is deposited onto desired substrate. This is followed by the jetting process which, instead of using laser to sinter or melt powder particles, deploys a liquid binder into powder bed for adhesion. The bound layers are later re-coated with a new layer of powder for next-step binder jetting until the final completion of the fabrication. For most cases, the printed products are left in the powder bed for some time to let the binder fully glue and make the product become mechanical strong. Post processing process are always necessary to remove the unbound powder and functional infiltration. Based on the materials used in the process, BJ processes can further be categorized into sand binder jetting, metal binder jetting, ceramic binder jetting etc. [48]

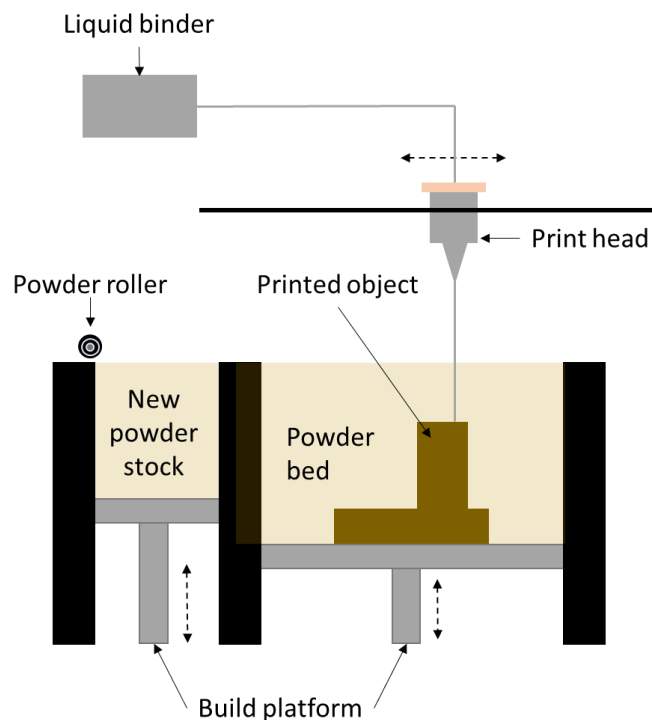


Figure 2-7 Schematic illustration of binder jetting process

The binder jetting technique has many similar advantages as powder bed fusion technique does such as self-supporting and wide selection of materials. In addition, compared to material jetting technique, binder jetting technique tends to have higher capability to deal with high-loading pastes, making it possible for producing high quality ceramic and metal parts. Another advantage is that BJ process can create accurate multi-material and multi-color prints that directly used for representing end products. That is one of the reasons why most BJ printed products are found in building multi-color structures for demonstration or aesthetic applications. Conversely, poor accuracy and low surface resolution are normally found among BJ printed products. Some additional post processing steps such as infiltration are also needed after printing to ensure good mechanical performance, adding significant extra time to the overall process. Due to the method of binding and related characteristics of printing material, BJ printed products are not usually considered for functional purposes.[35], [48], [49]

2.1.6 Sheet lamination (SL)

Sheet lamination is a process based on layer cutting and sheets lamination. Well-known subclasses of sheet lamination are ultrasonic additive manufacturing (UAM) and laminated object manufacturing (LOM). A schematic graph showing typical sheet lamination process can be found in Figure 2-8.

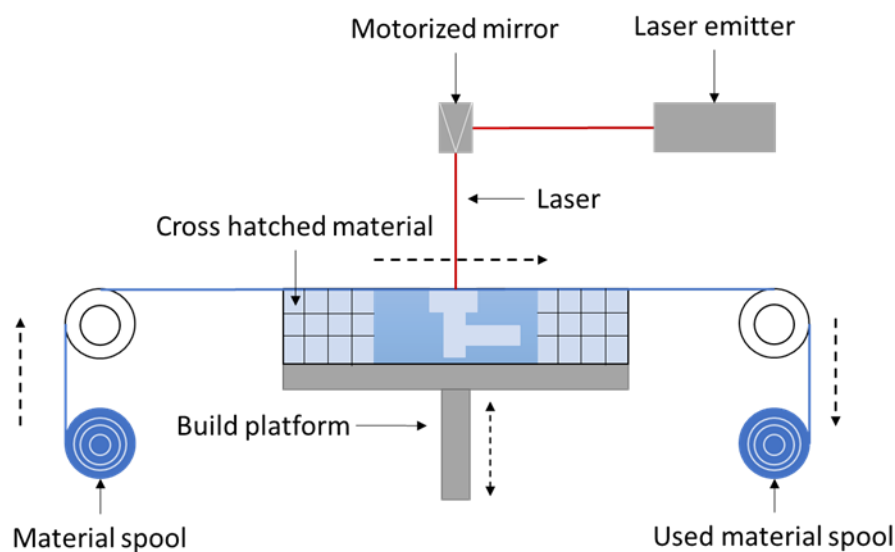


Figure 2-8 Schematic illustration of sheet lamination process

Generally, the sheet lamination process starts by placing a single layer of solid material (e.g. paper, PVC plastic, metal or ceramic) across the build surface, which is then followed by physical cutting by a laser or a mechanical knife. Two different process can be applied later. If the bonding treatment is applied immediately after cutting, the technique is called form-then-bond process (e.g. UAM). If it's vice versa, the technique

is named bond-then-form process, (e.g. LOM). The unused materials are left in place as supporting materials and diced into small cubes before they are separated from the desired shapes for recycling or disposal purposes. Post processing might be required depending on used materials or desired properties. The resolution of the printed materials completely depends on the thickness of each layer.[16], [53]

As a new subclass of SL technique, UAM uses ultrasonic to weld the metal sheets, making it particularly suitable for metal structures construction at low temperature. Based on this merit, UAM is used to create smart structures with designed cavities. These smart structures can be used to encapsulate functional components (e.g. solar panels, actuators and sensors) and build up compact customized electronics. By combining with direct writing technique, UAM is capable to produce electronic devices in a fully automated manner.[48] In comparison, LOM uses a similar approach but utilizes paper and adhesive. Since its printing materials are all paper-based, LOM is thus rarely considered when it comes to practical energy application but is mostly found in visual model creation such as 3D topographical maps.

In general, SL-based 3D printing requires relatively little energy, as the printed materials do not need to undergo any phase changing process. On the other hand, this technique is much faster than other 3DP techniques as it only requires some basic trimming to form cross-sectional layers. However, SL -based products are normally found out to be poor in surface quality and low in dimensional accuracy. Additionally, the removal of untreated materials from the inside of designed 3D shape is always time-consuming and sometimes troublesome, especially for the case of complex shape. Therefore, it is not recommended for creating sophisticated structural objects via sheet lamination.[16], [48]

As a less well-known printing technique, very few companies were found out to work with SL-based printers. Nonetheless, a Canadian company called Cubic Technologies is reported to be one of the main manufacturers of LOM printers while one Irish company named Mcor Technologies claimed to produce similar printers. Due to these reasons, SL technique is often found to be used by artists and architects to create affordable visual prototypes.[38]

2.1.7 Directed energy deposition (DED)

Also known as direct metal deposition (DMD) or directed light fabrication (DLF), Directed energy deposition is a process that create items by using focused energy source (e.g. an electron beam or high energy laser) to melt down feeding materials. This technique might sound like extrusion process, but in fact it is different because more energy is required for melting materials. In addition, as the nozzles of DED are designed to be movable in multiple directions, the deposition of layers in random orientations is

achieved. This feature makes DED suitable for applications such as repairing or retrofitting existing parts and beneficial to the reduction of preferential grain growth as well as undesired properties of anisotropy. The DED process might also sound similar to powder bed fusion process. However, in DED the materials are melted as they are being deposited while in PBF the materials are pre-laid in a powder bed. This difference brings advantages to DED over PBF, proved by one benchmark study showing that mid-size metal parts built by DED technology are averagely ten times faster and five times less costly than their correspondences built by PBF.[48], [54]

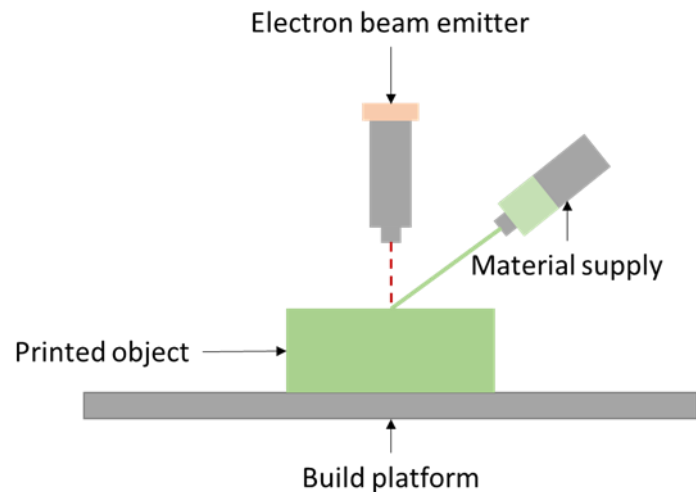


Figure 2-9 Schematic illustration of direct energy deposition process

By varying laser density, DED processes can produce dense objects with controllable microstructures. However, this technology is less viable when it comes to complex structures production due to the need for dense supporting materials. Therefore, currently DED technique is mostly found in applications such as repairing defect components (e.g. turbine engines) or adding new features to existing products. Some other niche applications in automotive and aerospace industry are also found to support traditional subtractive manufacturing methods.[16]

2.1.8 Summary of current 3D printing techniques

In summary, each of the AM process has its own advantages and disadvantages in terms of techniques, applicable materials, production speed, fabrication resolution, etc. Based on these features, a detailed list of advantages and disadvantages between different AM processes is created in Table 2-1.

Table 2-1 A summary of advantages and disadvantages of 3D printing technology

Process	Advantages	Disadvantages
Material extrusion	Low cost Easy controllability Versatile to customize Multimaterials processability	Low level of precise detail control Weak mechanical properties
Vat polymerization	Relatively high fabrication speed High resolution Good surface quality	Limit to photo-sensitive materials Expensive precursors Poor mechanical performance
Powder bed fusion	Powder acts as a supporting structure Wide material options	Relatively slow production speed Lack of structural integrity High power consumption Variable surface finish
Material jetting	No waste of materials High resolution Good surface quality Multimaterials processability Fast in production	Supporting materials are treated as a waste Mechanical strength degrades over time
Binder jetting	Parts can be made with various color choices Wide materials options	Not suitable for structural parts due to the use of binder materials Additional post processing adds significant extra time
Sheet lamination	Low cost Excellent for manufacturing large structure	Inferior surface quality Sheet thickness limit resolution Limitation of creating complex shape
Direct energy deposition	Excellent mechanical properties Controllable microstructures Excellent for repairing and retrofitting	Limitation of printing complex shape High energy demand Needs dense support materials Inferior surface quality

The material extrusion techniques, particularly the fused deposition modelling, is currently the most widely-used additive manufacturing technology due to its low cost, simplicity and high fabrication speed. Even though it might create poor mechanical performance objects, FDM is still widely selected among all 3D printing techniques. Powder bed fusion printed objects normally possesses higher resolution, but the production process is relatively more time-consuming. Vat polymerization (VP) is one

pioneering technology but the limitation of materials hinders its development, especially for those where high mechanical performance is demanded. Materials Jetting (MJ) is fast in fabrication but the products sometimes have issues in maintaining performances over time. Nevertheless, it is popularly used for 3D printing of ceramic materials. By contrast, Binder jetting (BJ) is capable of dealing with higher solid loadings pastes and have already been deployed for multicolor objects production in various industries for visual demonstration. Sheet lamination is based on layer-by-layer cutting followed by the lamination of sheets and is often used to build up smart-integrated structures or print large structures such as buildings. Direct energy deposition (DED) uses high energy sources to melt down materials with simultaneous deposition. This technique is different from ME and PBF as it is energy-demanding but does not need powder beds.[55]

However, as discussed in the previous section, the assembly of one energy device does not rely solely on one manufacturing technique or only on one functional material. This means that an ideal production process should take into consideration the capability of assembling multimaterials at the same time in order to achieve multifunctionalities. As a consequence, hybridized 3D printing (e.g. FDM+SLA) technique is sometimes needed to overcome the structural or functional shortcomings of printed objects by combining the benefits of several techniques and creating final parts made from various sources such as plastic, ceramic, steel, aluminum and virtually any type of printable material. To the best knowledge of the author, the CERAMAKER from 3DCeram is the only commercial hybrid 3D printer by far in the market. This hybridized 3D printer incorporates several 3D printing technologies together (e.g. material extrusion, nozzle jetting, powder bed fusion as well as stereolithography) and takes advantage of the specializations of each printing techniques. As a result, the CERAMAKER is capable of producing parts that are made of different types of ceramic or even from a combination of ceramic and metal. Together with a feature of large-parts printability, it is believed that CERAMAKER would give a solution with high potential for energy devices.[56] Meanwhile, some demands of physical performance or aesthetics requirement can also be met by hybridized systems. One example was found in the assembly produced by Baklund R&D, which integrated aluminum high wear sections onto a rifle magazine by using 3D hybridized printing.[57] The optimized printing process not only enable the company to have reduced time to the market, but also allow the product to withstand many required testing that simple 3D printed products fail to pass. In addition, hybrid AM process that is composed of additive manufacturing and subtractive technologies are also necessary in some fields.[49]

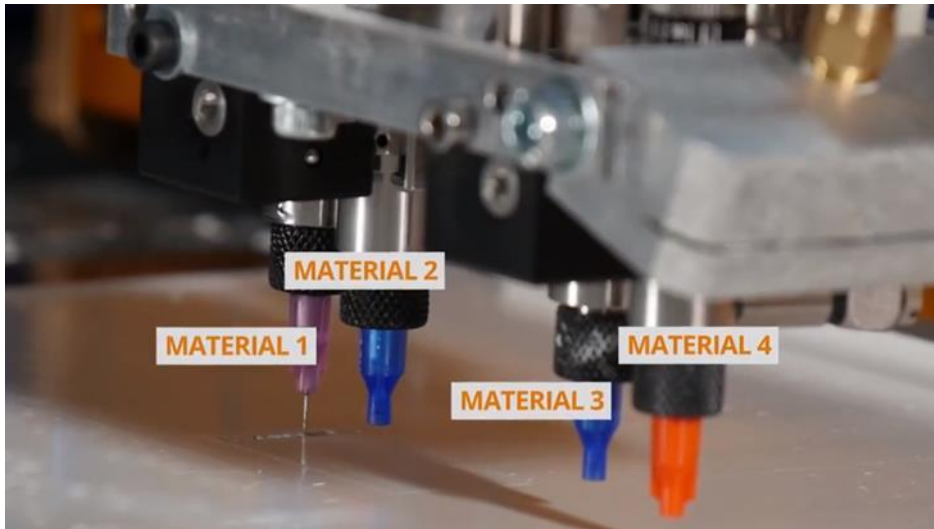


Figure 2-10 Schematic illustration of the hybridized 3Dceram CERAMAKER coupled with different printing techniques and multi-materials processing technique [58]

As this hybridization technique becomes a demanding technique, future work should be done on improving existing techniques and inventing new hybridization systems for creating more functional prototypes, as well as end-user products. This will eventually lead to an upgrade on designed products.

2.2 Overview of functional materials for energy systems

It is a common sense to all that the advance of one energy system goes hand in hand with the development of functional materials. These desired functional materials with specific electrical, thermal, mechanical and chemical properties can significantly enhance the overall performance of energy systems or even revolutionize the industry. The following sections aims at reviewing some representative functional materials that have been developed or are being developed for energy technologies.

2.2.1 Materials by functionalities

Various ways exist when it comes to dividing materials into groups. Based on their chemical or physical property, materials can be classified into organic or inorganic compound, metal or non-metal. Judging from their toxicity, materials can be sorted into toxic or non-toxic. Depending on their functionality or usage, materials can also be grouped based on their applications.

However, for energy technology, solely functional materials are not sufficient. Various auxiliary parts such as current collectors, supporting components and other passive elements (insulating, protecting, etc.) are also crucial for the assembly of one energy device. Thus, these materials should also be considered when one wants to design a

satisfying energy system. Therefore, in the following sections, materials are categorized into two groups to be reviewed, namely functional materials and auxiliary materials.

2.2.1.1 Functional materials for energy systems

Scientists and researchers have made enormous effort into developing functional materials for advanced energy systems. Herein, some representative examples are presented.

Silicon-based materials have been heavily studied for solar energy harvesting. In the meantime, well-designed conjugated polymers produced by using earth abundant elements and simple production methods are also reported for effective photovoltaic system.[59]–[61] Wu *et al.* designed water/alcohol soluble polymers based on diimide materials and obtained a power conversion efficiency of over 8% in single-junction polymer solar cells, making it the highest efficiency in this cell's group that has ever been recorded.[62] Bella *et al.* produced multifunctional fluorinated photopolymer coatings that can be put on the front of the solar cells and boosted the solar cells efficiency to almost 19% under standard light illumination.[63] Novel nanostructured anode/cathode materials with enhanced kinetics are applied for fuel cells, leading to lowered area surface resistance (ASR), high electron conductivity, large reaction surface and therefore improved power output.[64] Liang *et al.* from Stanford University reported a production of hybrid materials consisting of Co_3O_4 nanocrystals and Nitrogen-doped graphene. The prepared materials were served as catalysts for both oxygen reduction reaction and oxygen evolution reaction and exhibited highly catalytic activity.[65] Wang *et al.* produced multi-metallic nanoparticles made of gold, iron and platinum and witnessed high catalysis activity with high durability as compared to pure platinum catalysts.[66] Compared to a 100% fiberglass wind blades, light wind blades that are made of carbon fibers can not only allows the turbine systems to have a 38% reduction in weight and 14% decrease in cost, but also enables a more stable and safer operation. (especially in the case of area associated with constant high wind speeds.)[67]

On the other hand, in a sustainable energy generation system such as solar farm and wind farm, a large portion of the renewable energy is produced at a fluctuating rate. This situation attracted scientists to invent or improve energy storage technology for a desired constant energy supply. For instance, molten salts made with eutectic (e.g. sodium nitrate, calcium nitrate and potassium nitrate) with high specific heat capacity, low cost and wide operation temperature are intensively studied and employed as a thermal energy storage method into concentrated solar power (CSP) plants, allowing these plants to continuously supply electricity throughout the day and making CSP plants partially dispatchable.[68]–[70] Some other functional materials have also been extensively attempted and developed for high-performance rechargeable batteries,

aiming at increasing cell's capacity and stability, decreasing costs and improving its life cycle.[71] Kang *et al.* modified lithium nickel manganese oxide crystal structures and obtained unexpectedly high capacity with low material cost.[72] Zhou *et al.* demonstrated a fabrication of fibrous hybrid electrode consisting of graphene and sulfur nanocrystal for lithium-sulfur batteries and found excellent performance with long expectancy.[73]

Advances in terms of functional materials are countless and being constantly generated. Hereby, only a few examples are shown, but it is enough to understand the significance of advanced material in energy devices. As the performance of one energy system is mostly defined by its composed devices, a proper choice of materials is therefore fundamental and can definitely not be ignored.

2.2.1.2 Auxiliary materials for energy systems

Besides fundamental materials for energy devices, one should bear in mind that the promotion of auxiliary components and systems is also crucial in improving the overall performance of one energy system. Functional materials need to be coupled with some structural parts or current collectors such as conducting layers, insulating frames, porous voids or other external supporting structures in order to achieve proper functioning.

For example, busbars and fingers are necessary for a PV solar cell for current collecting and transmitting. Up to now, most manufacturers choose a state-of-the-art three busbar design for the collection of electricity generated by the solar cells. But some optimization can be done on this configuration for improvement. Braun *et al.* reported the necessity of designing novel busbars for improving solar cell performance. With an optimized structure, more light should be able to be reflected to the surface of the cell and then be absorbed.[74] Malevskaya *et al.* reported the influence of bus-bar material and configuration on solar cell's efficiency.[75] Apart from busbars and fingers, insulating layers are important for keeping the operation process safe and maintaining a constant power supply. Cheng *et al.* reported an application of mesoporous SiO₂ layers prepared by spin-coating as insulating layers for perovskite solar cells. The implementation of such layers is believed to give rises to cell power output via an enhanced absorption rate, a larger short circuit current density, a higher open circuit voltage and an increased fill factor.[76] Proper ceramic bearings designs are also reported to be able to save large amount of energy and extend the life of drive motor.[77]

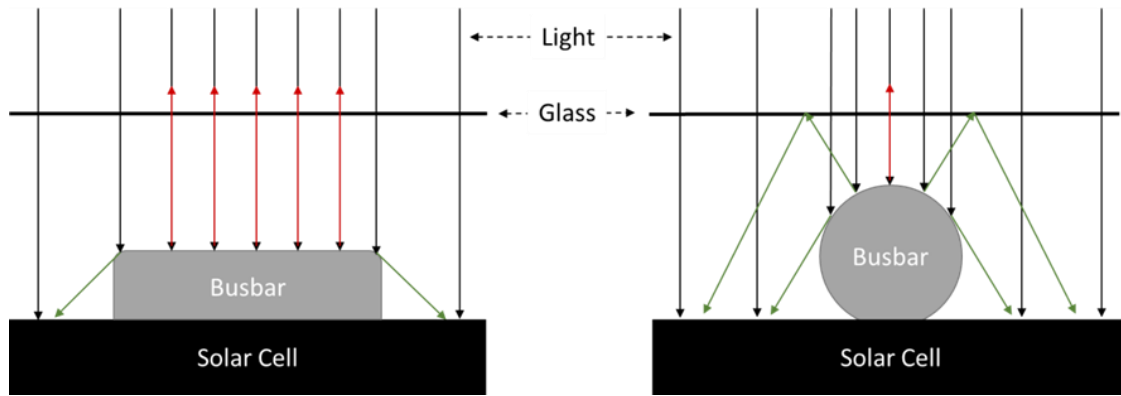


Figure 2-11 Schematic illustration of 3D geometrical optimized busbars for solar cells[74], with traditional rectangle busbars on the left and shape optimized busbar on the right

Consequently, one should not forget the importance of auxiliary components for energy devices and take the auxiliary materials into consideration when designing or developing an energy system.

2.2.2 Materials by microstructure

It should be noted that not only the composition of the material has a great influence on the performance of energy devices, but also the structure of those materials plays an important role in tuning properties. Numerous results have proved the importance of integrating micromaterials or nanomaterials to energy devices for adding favorable properties or improving overall performance.

For example, nano-scale Li-ion particles provide larger specific surface area, which results in an easier accessibility for ions to transport to the electrolyte and therefore a faster rate for charging/discharging the Li-ion batteries.[78] Nanocomposite and nanodome structures can be adopted in solar cells in order to reduce the Fresnel reflection while increase light transmission.[79] Well-designed nanostructured electrocatalysts and electrodes can achieve higher catalytic performance and consequently produce more power from a fuel cell system.[80] Enlightened by this idea, the scientific community has developed lots of methodologies for nanostructure materials.

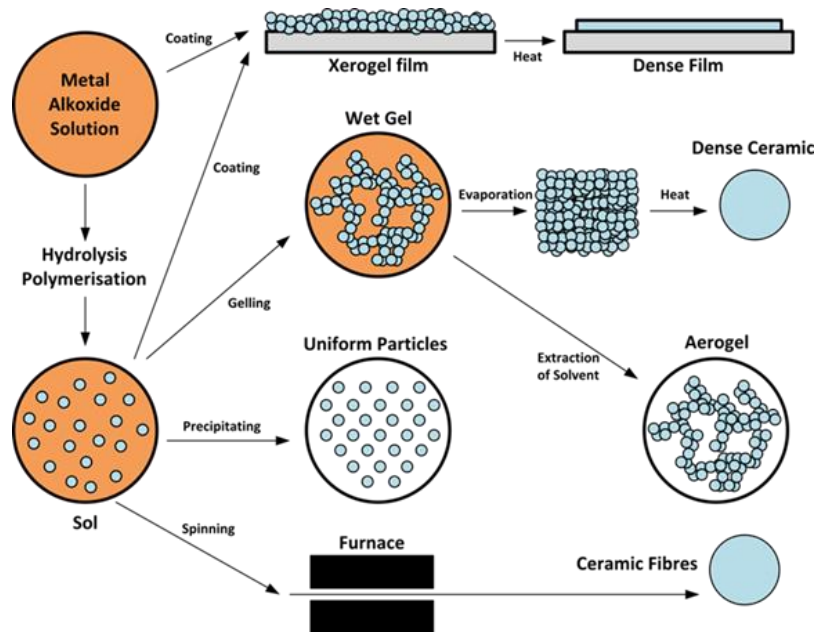


Figure 2-12 Schematic illustration of sol-gel process[81]

As one of the common ways to tune the microstructure of materials, sol-gel processing has been widely adopted as a way to produce solid ceramic materials with good microstructure from nano-sized particles. The process starts with dispersing solid particles (e.g. metal alkoxides) into a liquid solution, forming the “sol” solution. Later, with the help of partial evaporation of the solvent or some initiators, the “sol” undergoes a hydrolysis polymerization process and evolves towards the formation of a gel-like solution where both liquid and solid phase can be found. Depending on the need, various deposition methods can be adopted (e.g. spinning, gelling, coating and precipitating). The final solid product with desired features can be finally obtained after some post processing such as heat treatment or vacuum processing.[82] A schematic illustration of sol-gel processing can be found in Figure 2-12. It is a cost-effective and low energy demanding method which at the same time ensures homogeneity in the mixing on molecular levels while still guarantees an easy controllability of porosity and particle size. Because of these merits, various applications have been found in using sol-gel processing for the preparation of nanoscale powder, fibers or thin film material that can be useful for advanced energy devices.[83], [84]

Electrospinning is another method that have been widely used for the fiber production. It is a technique that relies on a high voltage power supply (often >20 kV) to electro spray polymer-fed solutions containing nanoparticles from a nozzle onto a conductive rotating drum. By doing so, materials which are originally in particles shape are stretched into fibers shape with a controlled diameter from submicrometer to nanometer.

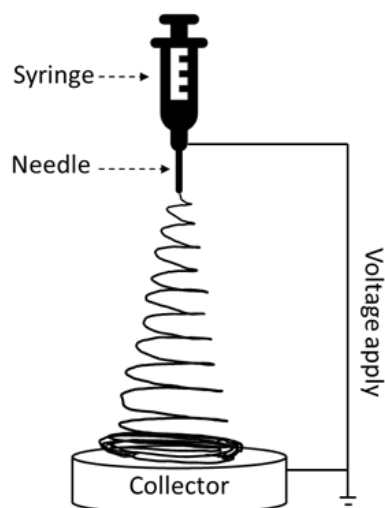


Figure 2-13 Schematic illustration of a simple electrospinning setup

In 2017, Phatharapeetranun *et al.* took advantage of this idea and managed to produce barium titanate (BTO) /PVDF nano-hybrids with enhanced dielectric properties. The group first used electrospinning process to generate high aspect ratio barium titanate nanofibers (BTNFs) with diameters of around 800 nm. The nanomaterials were then combined with 3DP for energy applications. After some post processing procedures, the BTNFs were mixed with the pure PVDF solution. By adopting FDM technique during the fabrication process, nano-hybrids materials with clear aligned fibers were created alongside the printing direction. This phenomenon of controllable alignment of nanofibers is believed to result in an improvement in terms of dielectric and piezoelectric properties, as the value from BTO/PVDF nano-hybrids is over ten times higher than that from the pure PVDF. Consequently, it is suggested that such designed BTNFs/PVDF nanohybrids can bring novel functionalities in dielectric components and in complex-shaped electric energy storage devices.[85] Guo *et al.* reported a work of the synthesize of nitrogen-doped carbon nanofibers (NCNFs) by electrospinning, where the as-prepared NCNFs demonstrated an efficient electrocatalytic activity in fuel cell system.[86] A novel piezoelectric nanogenerator based on lead zirconate titanate (PZT) NFs was also reported by Chen *et al.*, in which a considerable output voltage of 1.63V and power of 0.03 μ W was observed respectively, making this material an ideal choice for nano-scale energy generator applications.[87]

2.2.3 Summary of functional material for sustainable energy systems

Based on what has been discussed above, it is clear that the development of one energy device or system cannot be detached with the development of its relative materials. Future work should keep focusing on developing functional materials with different composition as well as analyzing the effect of microstructure that can bring benefits to energy applications.

2.3 Overview of 3D printing of functional material for energy systems

2.3.1 Solar energy systems

Solar energy, among all energy sources, is believed to be the most promising, clean and freely available energy sources for human beings.[88] The solar industry has been developing steadily in the past few decades and wide application such as PV-systems, concentrated solar plant and solar collectors have been implemented all over the world. However, some barriers still exist in the way of solar energy development. For instance, despite a high solar efficiency record of 46% (Fraunhofer ISE, Germany), most of the commercialized PV panels have a limited efficiency of up to 24%, which largely constraints the energy output from the designed PV plants.

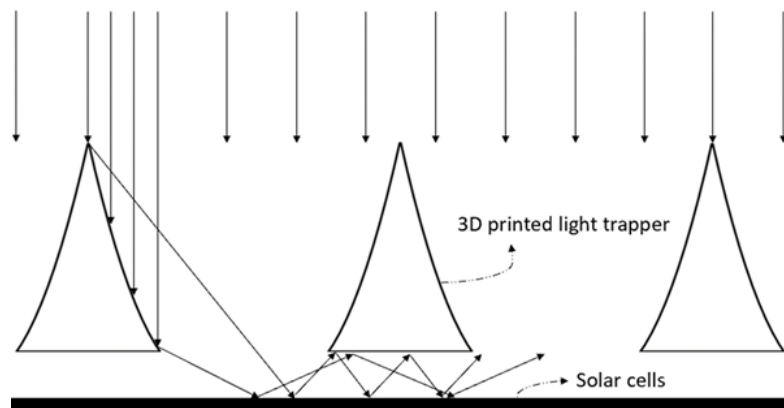


Figure 2-14 Schematic illustration of a 3D printed light trapper with solar cells

Some studies have been done on increasing solar efficiency by using 3D printing technology. Knott A *et al.* used Vat-based photopolymerization to fabricate periodic submicron intricate polymer structures, which are then used for 3D light trapping in dye-sensitized solar cells. Results shows that the proposed production method manage to incorporate high-degree design and enhances cell performance by around 25%.[89] Similarly, Lourens *et al.* printed external light traps for thin film solar cells and increased power output by around 13%.[90] Other innovative works have also been reported in manufacturing solar cells by using 3D printing technology.

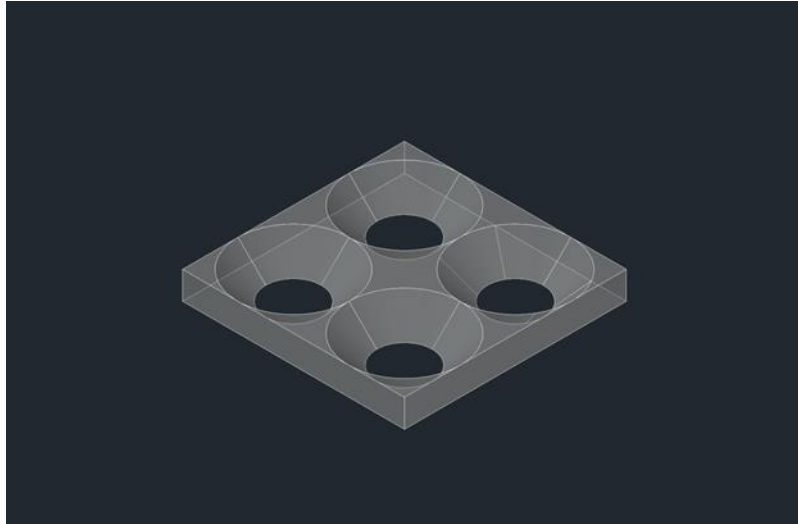


Figure 2-15 Schematic illustration of a CAD designed light trapper for solar cells

Lin *et al.* used inkjet printing technique to form thin film solar cells composed of kesterite $\text{Cu}_2\text{ZnSn}(\text{S}_x\text{Se}_{1-x})_4$ and optimized the ink formation to achieve a desirable efficiency.[91] Bag *et al.* used the same technique and demonstrated the fabrication of perovskite solar cells with high lead iodide loading, which achieved an efficiency comparable to that produced by spin coated technique.[92]

Using 3DP for solar industry can not only improve cell performance by an average rate of 20%, a report from Sculpteo also show that by taking advantage of 3D printing technology, the solar manufacturers can reduce their overall production cost by half.[93] Consequently, it is believed that the incorporation of 3D printing in solar energy technology is promising.

2.3.2 Thermoelectric energy systems

Clean electricity production is important for our societies. But it is clear that the produced energy has not been fully made use of by human beings. According to a report written by the U.S. Department of Energy, around 20%-50% of energy generation in America industry is lost as waste heat every year, although this lost energy has huge potential of being recycled and transformed into valuable electricity.[94] In this context, finding an economically and technologically feasible technology to recover waste heat and increase electricity efficiency becomes one interesting and promising research topic. This is where the thermoelectric generators (TEGs) are currently taking off.[95]

A thermoelectric generator is a solid-state semiconductor device that makes use of Seebeck effect and converts heat flux (e.g. temperature differences) directly into electricity. Basic science of this technology is referenced to the theory of thermoelement. The thermoelement forms from connections between p-type and n-type semiconductors. By linking a large number of the thermoelements in series and in

parallel, a thermoelectric module with proper voltage output and thermal conductivity can be created. The value of the power output mainly depends on the temperature difference between two surfaces and the properties of materials. However, external load resistance might also influence the power production.[96]–[99]

The thermoelectric generators are especially helpful to be applied into places where big temperature differences often occur. Some typical fields of application of TEGs are:[98]

- Waste heat recovery from industrial factories and power plants or exhaust gas from automobiles, ships and aircrafts;
- Solar thermoelectric generator such as classical solar concentrators or CHP power plant;
- Medical-based applications such as use body heat to power sensors and microelectronics;
- Geothermal energy.

By applying such technology, an additional electricity generation can be brought to the existing system or be added as a supplementary process, therefore increasing the overall fuel efficiency or providing a new vision to power generation. Conversely, when there is a voltage applied on such devices, a temperature difference can be created between two terminals and the device can therefore serve as a temperature controller.[99] Compared to other energy generation methods, the thermoelectric-based power generator has the following advantages:[98]

- Direct energy conversion from heat to electricity, therefore avoiding efficiency lost from using mechanical energy as an alternator;
- No moving parts in the generator, therefore require almost zero maintenance or any other extra operating cost;
- Quiet operation process and long operation lifespan;
- Robust, reliable and suitable for small scale energy production;
- Environmental friendly.

However, there are also many drawbacks of this technology. The most significant disadvantage of TEGs is its low semiconductor dimensionless figure-of-merit (Z_T is close to 1), which results in an overall low efficiency of less than 10%. When it comes to terrestrial application, specific structural requirements of the design can also make the system integration complicated. On the other hand, high-cost due to the use of rare earth materials and sophisticated production processes makes this technology less competitive compared to other energy generation methods.

Due to the above-mentioned features, the adoption of 3D printing is believed to facilitate the TEGs fabrication, both in terms of economic and technological aspects. For instance, a German company called Otego is currently running a business on polymer based thermoelectric generators via 3D printing. Inexpensive organic semiconductors that consist of an electrically conductive polymer called Poly(3,4-ethylenedioxythiophene) was selected as the TE material. Once the ink is prepared, ultra-thin foils were printed based on a roll-to-roll mechanism. The printed foils are environmental friendly and can be made in any shape to suit different applications.[100] Recently, their new product “oTEG”, an innovative energy converter, was released for a large range of applications in accordance with Industry 4.0.[101] Similarly, a group of research from Chalmers University of Technology in Sweden is developing a 6-years project called ThermoTex, aiming at producing energy from body heat via non-toxic, light-weight and inexpensive polymer-based TEGs. A feasibility study of production process between traditional weaving methods and emerging 3D-printing techniques is also being carried out to validate low-cost manufacturing.[102], [103]



Figure 2-16 Otego designed “oTEG”[100]

In 2015, Liang *et al.* managed to obtain electron-crystal phonon-glass thermoelectric materials with low thermal lost via SLA. The chosen material is $\text{Bi}_{0.5}\text{Sb}_{1.5}\text{Te}_3$ alloys, which is proved to be the optimum commercial thermoelectric materials at room ambient. In order to prepare the ink, Bi, Sb, and Te granules were mixed stoichiometrically and ball-milled for 100h. The obtained BST powder was then mixed with photo-resins and put into 3D printing with an SLA 3D printer. Interestingly, the printed objects demonstrated an ultralow value of thermal conductivity and shows a similar behavior of amorphous materials. However, the Z_T value is still too low to enable the wide application of such materials.[104]

Nan *et al.* from Tsinghua University reported novel $\text{Bi}_{0.5}\text{Sb}_{1.5}\text{Te}_3/\text{PLA}$ composite wires in 2018. The synthesized materials were mixed with different portion of multi-walled

carbon nanotubes, some silane coupling agent and plasticizer so as to improve their TE and mechanical properties. Results show that with proper doping, the designed material can reach an optimum Z_T value of 0.011 at room temperature and possess satisfactory mechanical properties. Even though this study did not do any practical 3D printing experiments, it still provide a valuable work for the PLA-based materials for FDM-based TE devices.[105] In the same year, Son and his colleagues introduced the production of conformal cylindrical TEGs via ME 3D printing. This reported method took advantage of 3D printing and managed to fabricate TEGs from all-inorganic materials into designed geometrical dimensions in order to perfectly fit heat sources. Bi_2Te_3 was used as the TE material while Sb_2Te_3 chalcogenidometallate (ChaM) ions was used as inorganic binders instead of traditional organic solvents. Due to the merit of ChaM ions, Bi_2Te_3 -based TE particles are able to be stabilized via electrostatic interactions, resulting in a solid-like ink with appropriate elasticity and enhanced colloidal stability. The prepared solution was printed by SLA for conformal TEGs with tailor-made shapes in order to fit specific structures of the heat sources. Results shows that the designed object demonstrated an outstanding TE performance (Low thermal conductivity, high electricity conductivity and high Z_T value). Based on proposed conformal cylindrical structure, a maximum output voltage of 27.0 mV and power of 1.62 mW were achieved at a temperature difference of 39 °C. Such values represent a great system integration potential as well as prove a pathway for a cost-effective fabrication process.[106]

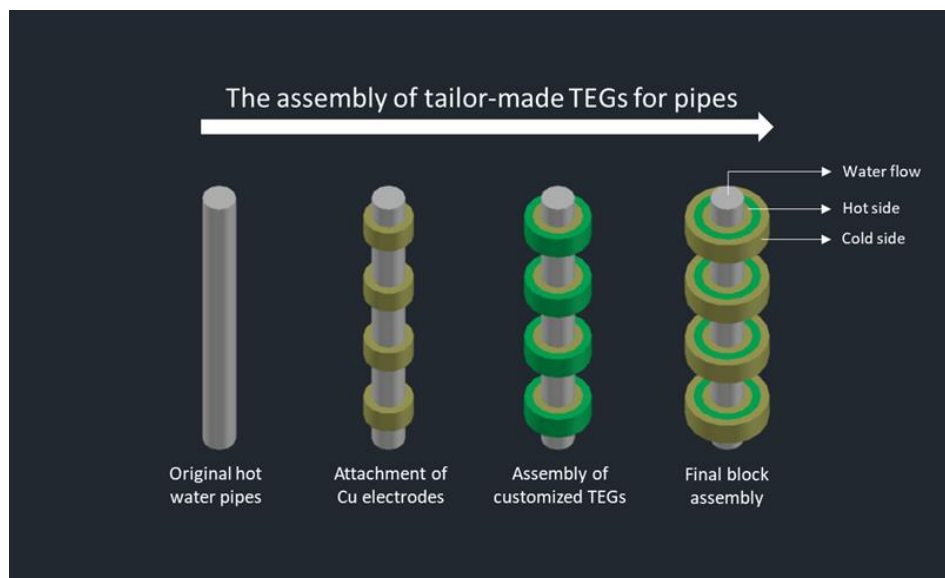


Figure 2-17 Example of 3D tailor-made TEGs for pipes, enlightened by Kim et al.[106]

The above-mentioned examples show that for TE materials or devices, 3D printing can not only serve as a manufacturing technique to makes the production cost-effective, but also enhance the mechanical and TE properties of devices by changing its material content.

2.3.3 Wind energy systems

Wind energy is another renewable source for energy production with capabilities of generating zero greenhouse gas (GHG) emission, chemical emission, or any other toxic waste.[107]

However, most commercialized large wind turbines, together with their supporting tall tower, require a large size of wind farm to operate and could pose a threat to the surrounding ecological environment.[107] In order to solve these problems, a miniature mobile wind energy harvester can be designed and put in places where the current commercialized wind turbines are suitable to operate (e.g. downtown with dense population or ventilation pipes with continuously air flow). For instance, Zhang *et al.* reported a miniature piezoelectric wind generator with suitable working air flow speed range and achieved a maximum power output of $0.86 \mu\text{W}$.[108]

In 2015, a 3D printed mobile wind turbine called AirEnergy 3D was delivered by a group of Polish engineers. The printed turbines are designed to be foldable and light for easy mobility and with the help of 3D printing technology, the overall production cost was controlled within 350 dollars. A maximum 300W power output, together with its in-built batteries, enables such product to stably charge to a dozen LEDs or five laptops at the same time. With these advantageous features, AirEnergy 3D is believed to be suitable for both in-home power supplement and outdoor power supply.[109], [110]

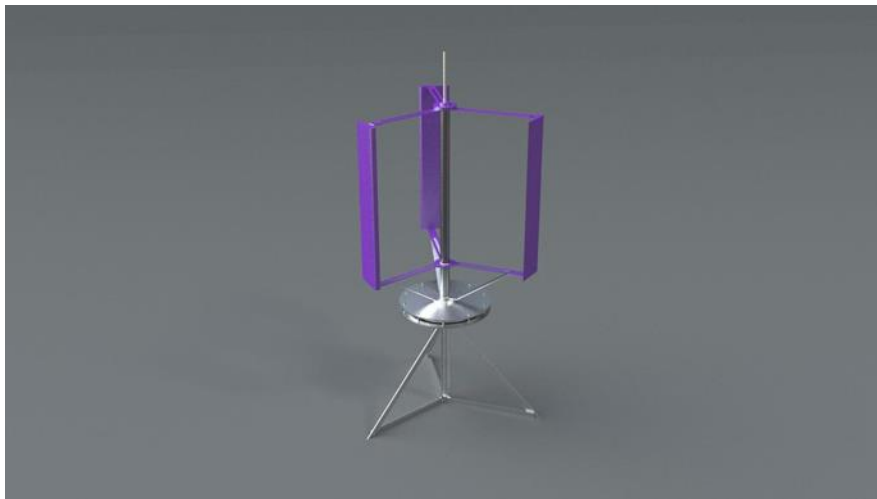


Figure 2-18 A working proof of concept of 3D printed mobile wind turbines [109]

In 2016, N. Han *et al.* designed and manufactured some small-scale wind harvesters by a ME-based 3D printer called MakerBot Replicator 2. Test results showed that each of these printed wind harvesters can generate power at 0.305 W with a maximum energy conversion efficiency of 6.59% and is able to supply the energy of four LED lights.[107]

Nonetheless, compared to other energy devices, very few application and progression are found in the adoption of 3D printing associated with wind energy, making this combination a promising field for future research and innovation.

2.3.4 Energy storage systems

In order to efficiently use the power generated by renewable energy sources, proper energy storage systems should be developed accordingly for solving the intrinsic drawback of renewables (e.g. intermittency). Despite the fact that current manufacturing methods have already successfully covered every single step of the production of energy storage systems, there remains some aspects that can be further improved. For example, the overall performance of the cell systems can be further enhanced by changing the layout of the materials while the production process could be optimized by implementing a cost-effective customized manufacturing.[111]

2.3.4.1 Batteries

One good solution to deal with this situation is to incorporate 3D printing into the production of energy storage devices. Compared to the conventional production methods, batteries manufactured by 3D printing has many advantages. Studies shows that 3D electrodes have higher areal energy density, shorter Li-ion transport length and lower tortuosity in comparison with 2D planar electrodes.[26], [112]–[114] Researcher also found out that by designing of complex interdigitated cells, the overall performance of 3D printed batteries could be improved with less capacity decay, better mechanical integrity as well as higher safety certainty.[115]

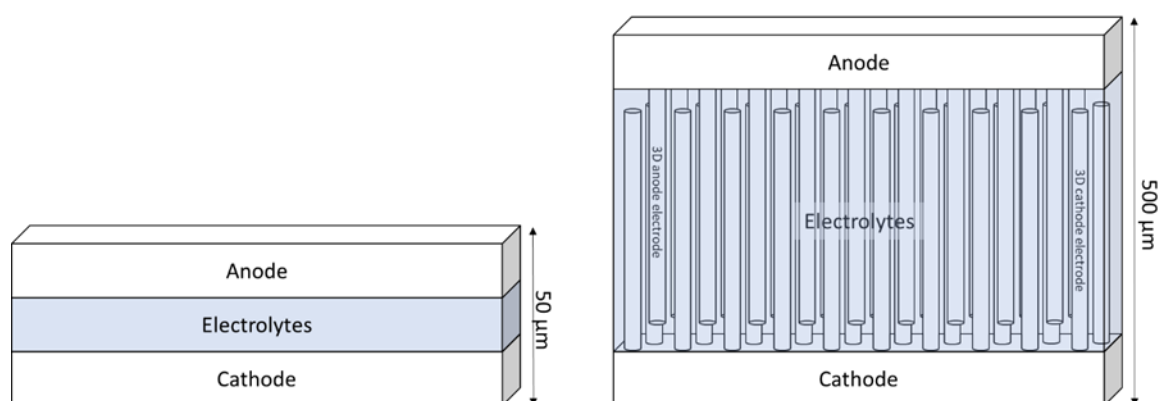


Figure 2-19 Representative configuration of 2D and 3D microbatteries

In 2013, Lewis and his colleagues demonstrated an interdigitated Li-ion microbattery architecture prepared by 3D printing.[116] Firstly, the anode ($\text{Li}_4\text{Ti}_5\text{O}_{12}$, LTO) and the cathode (LiFePO_4 , LFP) are printed layer-by-layer via direct printing technique on the golden current collector. Later, because of the designed graded volatility solvent system, the printed electrodes start solidifying. A post printing treatment was later introduced,

where a 600°C heating in inert gas was conducted in order to remove the organic contents and promote the sintering of nanoparticles. Liquid electrolyte was then prepared and loaded for electrochemical tests. Results show that a high areal energy density of 9.7 J/cm² and a good power density of 2.7 mW/cm² were obtained. Despite its high areal energy density, the high electrical resistivity in the battery makes this cell need further optimization.[26], [116]

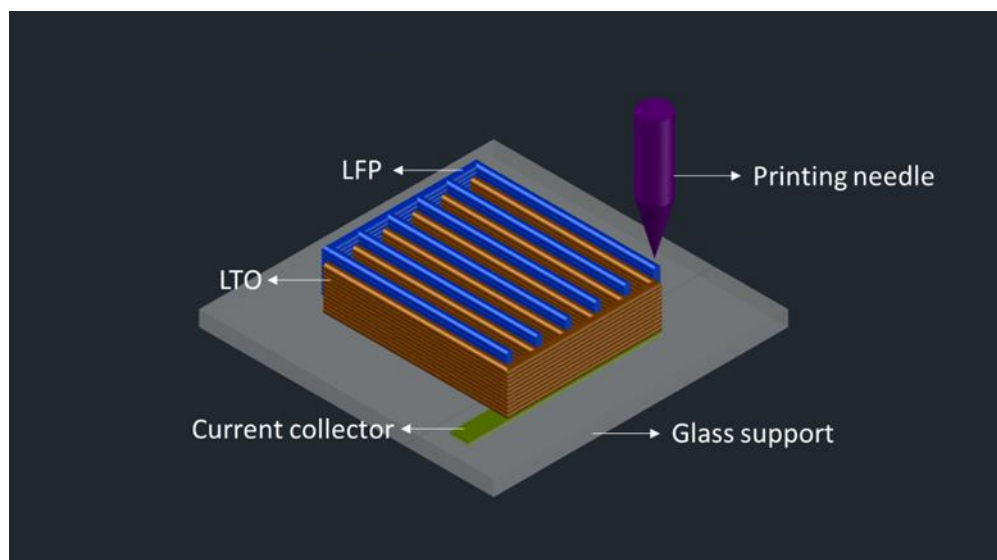


Figure 2-20 Schematic illustration of 3D interdigitated microbattery architectures, enlightened by Lewis's research[116]

With similar printing materials, Hu and his colleagues performed a work that introduced graphene oxide (GO) into electrodes materials in order to improve electron conductivity.[117] LTO/GO and LFP/GO inks were prepared separately and used to fabricate the electrodes. The increased viscosity of ink caused by added GO makes the following 3D printing process easier. Drying and annealing process were conducted after printing in order to solidify the electrodes and reduce GO for good electrical conductivity. An electrolyte consists of Al₂O₃ nanoparticles and poly(vinylidene fluoride)-co-hexafluoropropylene (PVDF-co-HFP) and was later prepared and printed between the annealed electrodes for a complete battery. Electrochemical tests revealed a charge capacity of 117 mAh/g and discharge capacity of 91 mAh/g with good stability.

In 2016, C. Foster *et al.* managed to fabricate complex 3D printed architectures by using graphene-based PLA filaments through an FDM 3D printer. The printed objects are used as electrodes for hydrogen production and Li-ion battery. Results show that the 3D printed electrodes demonstrate a considerably high catalytic activity towards hydrogen evolution reaction (HER), therefore providing a high competitiveness compared to platinum-based electrodes by cutting down the cost and simplifying the production process.[118]

Hu *et al.* developed 3D-printed Li-ion batteries whose cathodes consist of $\text{LiMn}_{0.21}\text{Fe}_{0.79}\text{PO}_4$ (LMFP) nanocrystal and carbon. The design of the cell takes advantage of higher energy density of 3D printed electrodes and theoretical increased working voltage due to increased material content. Electrochemical tests show the designed Li-ion batteries demonstrates the highest rate capability among all LMFP lithium ion batteries and are capable of retaining high reversible capacities with almost no decay.[111], [119] Consequently, it is believed that using 3D-printing technology can greatly promote future battery development.

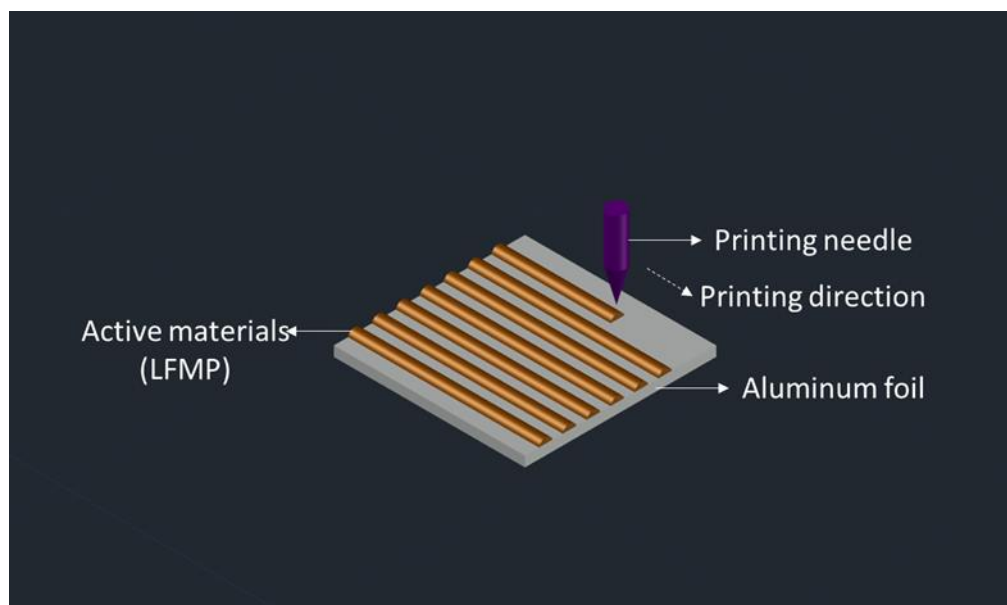


Figure 2-21 Schematic illustration of the preparation of 3D-printed electrodes for Li-ion batteries, enlightened by Hu et al.[119]

2.3.5 Super capacitors

Super capacitor is another well-known energy storage system. Compared to batteries, it has faster charging rate, higher power density and better recyclability but is lower in energy density and higher in cost.[120]

In 2016, Zhu *et al.* managed to produce a 3D-printable graphene composite aerogel for sandwich-type super capacitor applications. The printable ink was prepared by a mixture of graphene oxides (GOs), graphene nano platelets (GNP) and silica fillers. Direct-ink writing was used to build the super capacitor with periodic macroporous structure. The as-printed object was then sent to post processing (gelation, drying, heating and etching) and for performance test. Results show that printed supercapacitor has a superior gravimetric and volumetric energy densities over any other devices manufactured by traditional methods.[121]

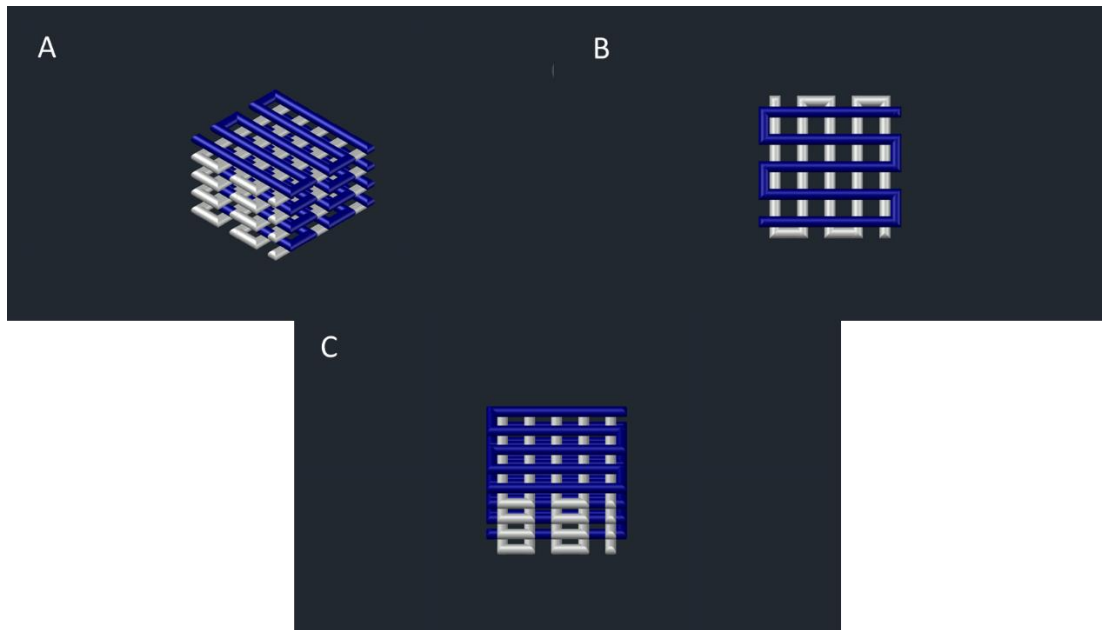


Figure 2-22 3D printed supercapacitors with periodic macroporous structure, enlightened by Zhu et al.[121]

2.3.6 Thermal energy systems

Traditionally, high-temperature environment is required for material synthesis and device processing. Such environment is normally accomplished by furnaces, which are generally considered to be bulky in size and low in energy efficiency. A 3D printed nano-heater, however, enables a high efficient thermal treatment with well heat distribution and low temperature gradient in materials.

In 2016, Hu *et al.* reported a 3D printable reduced graphene oxide (RGO) heater for functional thermal supply based on electrical Joule heating.[122] The study used water solved graphene oxide (GO) and direct ink writing as ink and printing technique, respectively. By applying electricity to the printed heater, a temperature of around 3000K with effective micrometer-level heating was achieved within 100ms. In this study, the 3D printing technology not only assists in designing tailor-made shapes with fast production time with low cost but also enables the printed heater to have a higher temperature and faster heating rate for effective heating compared to conventional thermal treatment.

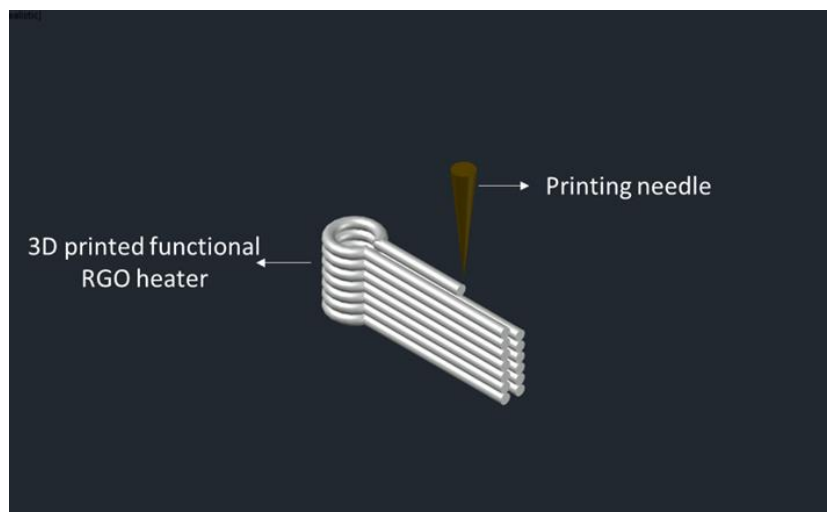


Figure 2-23 3D printed functional RGO heater, enlightened by Hu et al.[122]

In addition, the same research group also used similar methodology to develop a platform for high-temperature in-situ synthesis of metal nanoparticles inside a conductive 3D printed RGO matrix.[123] The idea is to mix the desired metal micro powders with RGO solution and make use of the high temperature generated by electricity shock in RGO to melt down the materials and use defects in designed RGO structure to prevent the molten metal from agglomerating. Because of the excellent thermal conductivity possessed by RGO, the following quenching process is rapid, therefore limiting the thermal treatment in a short time and hindering the particle from migration and surface oxidation. As a result, these designed materials have great potential in rapid energy conversion from chemical to thermal and produce work as energetic materials for explosive. On the other hand, the highly dispersed materials can be extremely beneficial for improving the performance of electrochemical energy storage systems or any other energetic devices.[26]

2.3.7 Fuel cells systems

Fuel cell is a type of electrochemical conversion device that produces electricity from fuels without combustion. Among many fuel cell choices, solid oxide fuel cell (SOFC) is being heavily studied and used at the industrial level. To start with, a SOFC uses solid oxide or ceramic material as its electrolyte and normally operates at high temperature. This high temperature condition allows the incoming fuels to react internally beforehand and promotes a highly active electrocatalysis process with non-precious metals. In addition, operating in such extreme environment further reduces the power lost from internal resistance and therefore improves overall performance. By introducing heat recovery and utilization to the system, the overall fuel efficiency can reach over 80%.[124] Due to such operating strategy and features, SOFC is exceedingly promising for high-power utility applications such as stationary CHP stations or large-scale electricity-generating plants.

However, a recent report reveals that in order to fabricate a complete SOFC stack, more than one hundred traditional manufacturing steps are required.[125] This often involves steps such as tape casting, screen printing, firing and so on which are usually considered low efficient, time-consuming and energy demanding. Plus, in order to achieve desired voltage and power output, each individual SOFC needs to be integrated in a complete SOFC stack which then requires several post manual assembly steps of joints, seals, etc. Such involvement of manual steps would, to some extent, damage the reliability and durability of the system. Moreover, various demands of electricity and heat from different commercial segments also require diverse capacities of the SOFC stacks. Therefore, finding a simple inexpensive customized production method that is also less manual involving and more efficient would be of benefit to the wide application of SOFCs. In this context, the implementation of cost-effective fabrication methods such as 3D printing for the production of SOFCs would be of interest.

Several works have been seen on the fabrication of the novel materials for SOFC. Gas-tight YSZ layers with low thickness (lower than 10 μm) and relatively high ionic conductivity have been studied and printed via inkjet printing on supporting substrates, which results in an improved cell performance for cells as well as low area specific resistance (ASR).[126], [127] In 2015, V. Esposito *et al.* reported ultra-thin ($\sim 1.2 \mu\text{m}$) YSZ electrolyte produced by inkjet printing from nanometric YSZ powders ($\sim 50 \text{ nm}$ in size) dispersed in an aqueous system. The printed electrolyte showed a negligible ASR value of less than $0.05 \Omega \cdot \text{cm}^2$ and was deposited on NiO/YSZ based anode and LSM/YSZ cathode for testing. The obtained SOFC exhibited close-to-theoretical open circuit voltage of 1.07-1.15V under dry hydrogen conditions and outstanding peak power density of above 1.5 W/cm^2 . [128]

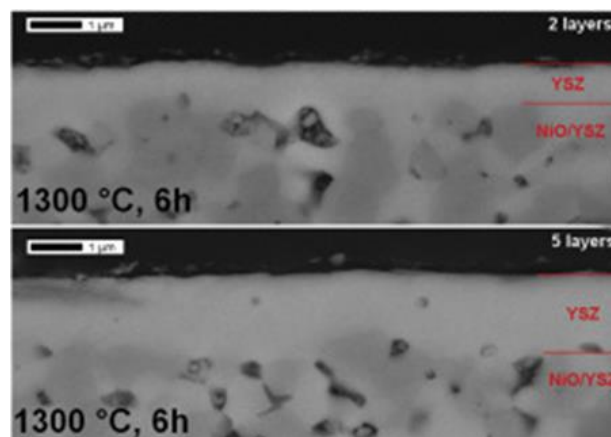


Figure 2-24 SEM observations of the inkjet printings of YSZ with 2-layer (up) and 5-layer (down) depositions after sintering at 1300 °C for 6 h. Reprinted from V. Esposito *et al.*[128]

Interesting fabrication of gadolinia-doped ceria, a novel electrolyte for intermediate temperature SOFCs, onto porous low-cost stainless steel was reported by Tomov *et al.* The research group demonstrated the possibility of producing 15 μm uniform electrolytes via direct ceramic inkjet printing by using in-house developed ink made of NiO, CGO and other necessary binders and solvents. This usage of such porous metal substrate is believed to be advantageous for SOFCs since they can provide excellent electrical conduction and mechanical strength while maintain good thermal distribution for rapid start-up/shut-down.[127] Similarly, Wang *et al.* proved the possibility of depositing dense CGO electrolytes onto porous substrates and optimized ink formation as well as inkjet printing regime.[129]

On the other hand, the ability of controlling the microstructure of electrodes and the quality of the interfaces from 3D printing can further improve the cell performance. Yashiro *et al.* produced controllable gadolinia doped ceria/lanthanum strontium cobalt ferrite functional layers with high triple phase boundary and improved cell performance by 30% compared with reference SOFCs.[130] Sukeshini *et al.* managed to enhance the performance of SOFC by creating microstructures among interfaces via aerosol jet printing, resulting in an almost doubled power output density compared to the reference cells.[131]

It is believed that the successful deposition of thin dense electrolytes via 3D printing onto commercial-accessible porous substrates will unlock the potential of all-type configurations of anodes and cathodes while cut down the production cost, therefore giving a promising commercialization for SOFCs.

Currently, there are also many researches going on in optimizing the production process of industrial SOFC stacks using 3D printing. In 2015, a project called Cell3Ditor was initiated by Catalonia Institute for Energy Research (IREC), which aims at three aspects: developing of proper 3D printer, analyzing proper formation of printing ink as well as ceramic materials and designing suitable system integration. The ultimate goal is to propose a two-step manufacturing process (printing and sintering) for the production of SOFC and replace current traditional manufacturing process. According to their plan, the proposed 3D printing technology will significantly reduce the energy and materials consumption of SOFC stacks production and cut down overall investment by 60%.[132], [133]

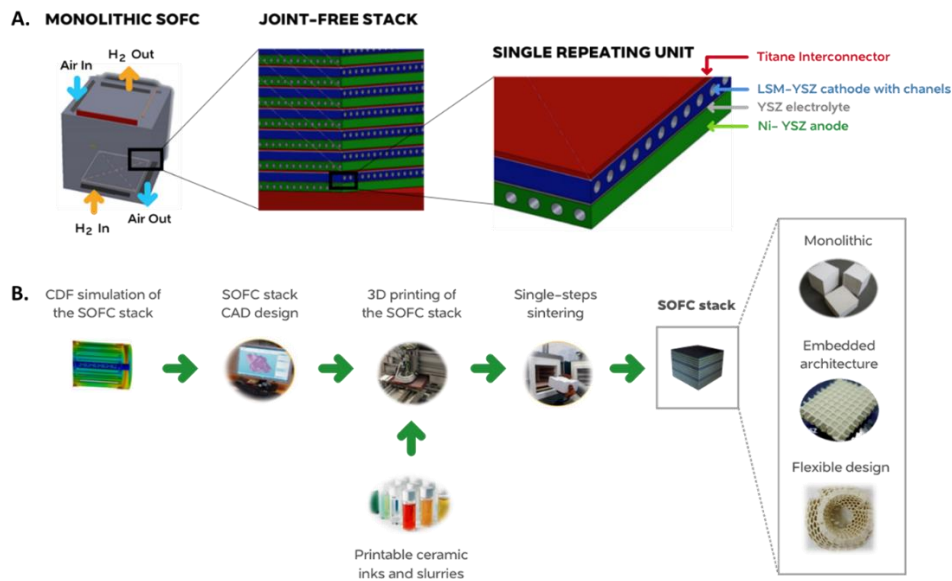


Figure 2-25 Schematic illustration of the Cell3Ditor project[134]

Nevertheless, based on current technology, it is still not convenient to produce SOFCs with high aspect ratio or with multi-material capabilities. Therefore, it is suggested that future work should not only focus on analyzing new materials for cell components, but also be done in developing hybrid 3D printers that are capable of building up high aspect ratio multi-materials cells with required accuracy on microscale.[21]

2.3.8 Sensors

Nowadays, the application of sensors can be found in almost every aspect of our lives. Ranging from medical biosensor for disease diagnosis to chemical sensor in toxic gas detection, these devices have been used widely for monitoring, testing or controlling purposes. However, an increased requirement from application expect future sensing technology to be more sensitive, specific and capable of withstanding extreme conditions and delivering multiple detection in a short time.[135] Nevertheless, traditional manufacturing methods of sensors are reported to be tedious, time-consuming and inflexible.[55] With the development of new and hybrid manufacturing methods, sensors with desired performance and specific features can be easily achieved.

For instance, Guo *et al.* constructed a novel helical structure made of PLA/MWCNT nano-composite via solvent-cast 3D printing. The printed object demonstrates an ideal performance for liquid-related sensing applications, as it was capable of trapping liquid within limited immersion time with excellent sensing sensitivity and selectivity. Such devices can be integrated with other sensing functions and be used for many other applications such as pollutant detection, remote controlling, etc.[136] Salamone *et al.* used FDM to print out complex structures for integrating with commercial sensors. The as-built nano environmental monitoring instruments have good reliability and are

reported to possess great potential for confined spaces application.[137] Zhou and his group used SLA to fabricate a part of ultrasonic transducer based on piezoelectric ceramic materials. Through some particular post-processing treatments, the printed components demonstrate excellent piezoelectric properties that can be of great value in areas such as biomedical imaging machines and energy harvesting technology.[138] Similarly, Woodward *et al.* fabricated a hollow spherical shell consist of piezoelectric ceramic via SLA. The printed sphere structures can generate ultrasound in MHz range when voltage is applied and can therefore be used in some specific conditions like hydrophones.[139]

Some other interesting work were found in various sensing application. In 2016, Suate-Gomez *et al.* performed a successful 3D fabrication of ear prosthesis, which was designed to serve as a multisensory unit for pressure and temperature sensing. The FDM fabricated artificial ears, which is composed of polyvinylidene fluoride (PVDF), were shown to be able to cover both aesthetics and functionality purposes. Testing results proved that the prosthesis can operate under a wide range of temperature (2 °C to 90 °C) and pressure (0 to 16350 Pa) with reliable response and sensitivity. This work is considered to be of great value to the hearing aid's manufacturing industry as it not only has a huge potential to response to sound as normal humans do, but also produce customized in-ear structure based on each patient demand and easily adjust the shape when needed, therefore delivering a higher level of comfortability and biocompatibility.[140]

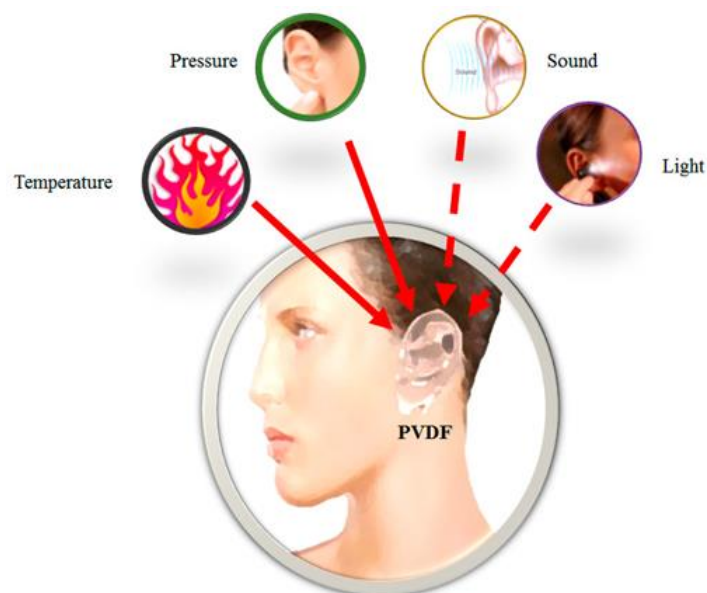


Figure 2-26 Schematic illustration of 3D fabrication of ear prosthesis proposed by Suate-Gomez et al.[140]

2.3.9 Summary of 3D printing of functional material for energy systems

Based on what has been discussed above, it is evident that 3D printing is currently being popularly used in various field of energy technology. Despite the fact that some limitation still exists, the implementation of 3D printings in energy technology shows a great potential in future applications in terms of customization, performance improvement, cost reduction and process simplification. Consequently, a case study is proposed in the following chapter to analyze one aspect of 3D printing for energy harvesting application.

CHAPTER 3. 3D printing of advanced functional materials for sustainable energy systems: a case study of ferroelectric composites for energy harvesting

3.1 Motivation

From what has been illustrated above, it is clear that 3D printing has many intrinsic advantages over traditional manufacturing methods and could offers a brand-new vision for the product manufacturing in terms of structural, functional and economic improvement. Particularly for energy devices, 3DP can bring multiple extraordinary benefits. For instance, an increasing demand of functionalization (especially nano-functionalization) required by advanced energy devices can be easily met by the implementation of 3DP, where some functional nanomaterials can be enriched and added into the 3D printing material during the fabrication process for performance enhancement. Also, 3DP in energy technology is capable of conjugating specific functionalities with geometrical complexity, which includes both tailored macrostructural shapes and designed micro or nano structural features. Moreover, as most energy technologies are built up from multiple materials and particularly from multiple functional composites, hybridized 3D printers that are also capable of dealing simultaneous multi-material processing give opportunities to further boost the developing of one energy system.

In the light of these merits, an experimental case study is elaborated based on functional materials for defining some general criteria in the field of 3DP for energy systems. The research materials in this work are selected to be piezoelectric materials, which have been widely used in a number of promising energy applications as well as treated as the functional core of energy harvesting technology. These features are particularly suitable for 3DP due to the following considerations:

- Customization requirement for end users;
- Complex shapes requirement for harvesting energy with 3D geometrical extension. (e.g. acoustic waves or vibrations propagating in the shape);
- Simple device architecture (e.g. two electrodes and one dielectric body);
- Applicable in many different energy systems such as sensors and transducers as well as stretchable smart wearing devices and some biomedical applications.

Among many material options, piezoelectric ceramics and polymers for energy harvesting have been intensively studied and explored.[85], [141], [142] To step forward, Polyvinylidene fluoride (PVDF) is one polymeric material that has been commonly used in energy technologies (e.g. sensors, transducers, capacitors, etc.) due to its high dielectric constant, outstanding physical strength and chemical stability. Barium titanate (BaTiO_3), on the other hand, has been used as a ceramic material in piezoelectric applications because of its non-toxicity, extraordinary piezoelectric and dielectric properties as well as easy processability. By loading the inorganic BaTiO_3 fillers into the organic PVDF matrix, it is possible to combine the advantageous features of both and obtain novel hybrid composites with enhanced properties.

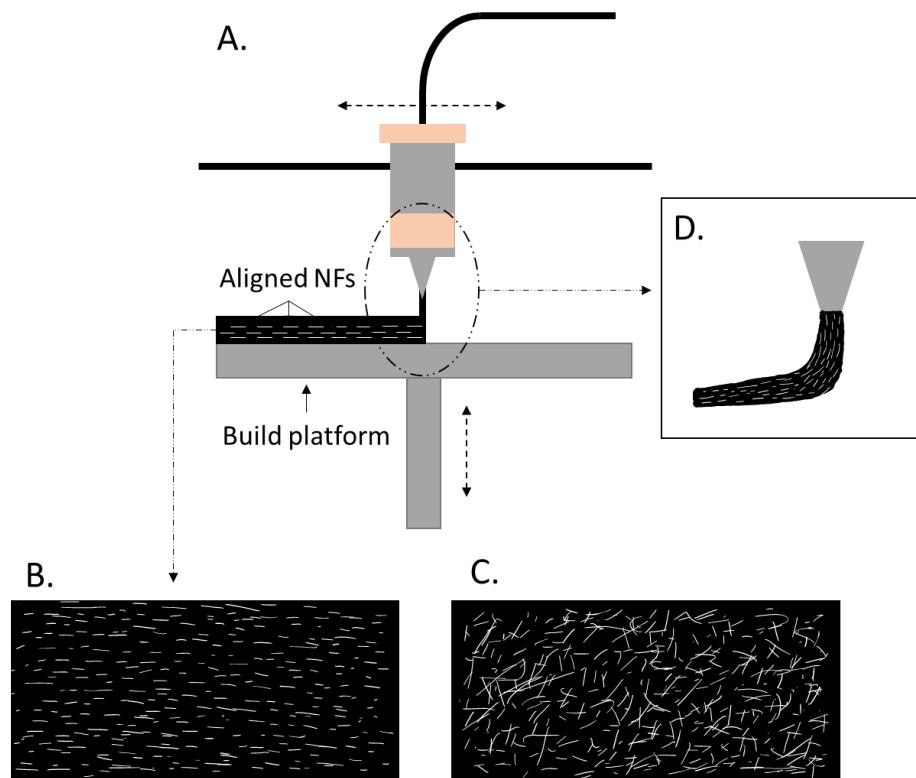


Figure 3-1 3D printed objects with intended fibers alignment A). Device diagram of an FDM 3D printer B). Desired highly-aligned fibers produced by 3DP C). Random oriented fibers often found in other manufacturing techniques D). Enlarged view at printing needle

Although lots of works have been done on the production of PVDF-BTO hybrid dielectric material, only a few considered 3DP.[85], [143]–[150] Additionally, since the internal arrangement and the anisotropy are also key points in the performance of one piezoelectric device, the adoption of 3DP is believed to give unique opportunities to control the geometrical features of the printed materials at a multiscale level. This concept of producing shape-free objects that are controllable in both short and long range was, for the first time, explored by aligning elongated BaTiO_3 fibers in PVDF matrix via 3DP in 2017.[85] A schematic illustration of the designed idea can be found in Figure 3-1.

Most traditional manufacturing method can only control the macro structure (e.g. shape) of the items but cannot modify their micro structure (e.g. microfibers alignment). This study creatively exploits the viscoelastic effect between each flow layers and the printing needles to produce hybrid PVDF-BTO composite with designed shape and observes significant dielectric performance enhancement. Ideally, 3DP is expected to provide a platform for tuning the microstructure of one material and achieving high degree of functionality. In addition, by depositing the layers in different ways (e.g. cubes with fully aligned fibers or crossed oriented fibers), objects with a same macro structure are expected to exhibit different properties (e.g. mechanical strength, dielectric/piezoelectric response and so on.). Figure 3-2 illustrates the idea of generating items with multiple printing direction and microlevel fibers alignment.

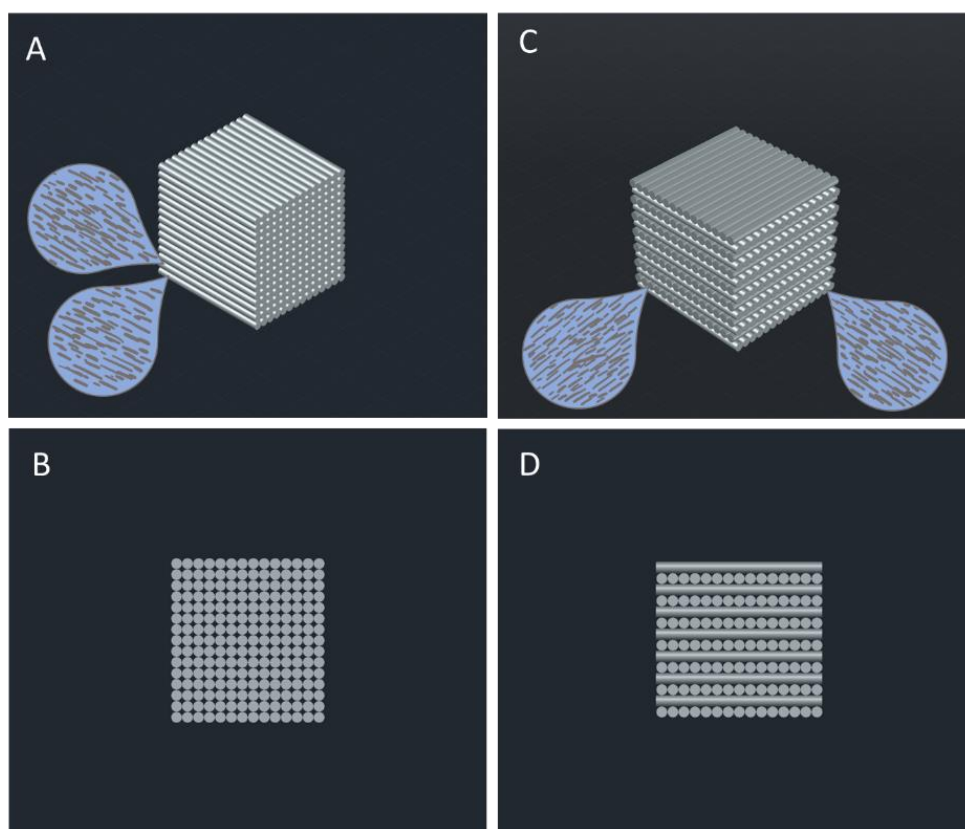


Figure 3-2 Design of two different printing scenario A). Overall view of one-direction-printing with same-aligned microstructure on each layer; B). Right-side view of one-direction-printing; C). Overall view of two-direction-printing with cross-aligned microstructure on each layer; D). Right-side view of two-direction-printing

Consequently, using 3DP to print out shape-free hybrid PVDF-BTO composite with devised microstructure and improve its related properties would be of interest to the energy harvesting industry. Among all possible 3DP methods, fused deposition modeling (FDM) is selected as the best solution for our work due to its high flexibility with the material compositions, low cost, easy controllability and low-energy requirement.

In order to validate the proposal, the experimental work is designed and conducted as following. Firstly, sol-gel processing and electrospinning technique are used to produce proper BTO microfibers with reference to existing examples.[85] Secondly, the as-prepared BTMFs are loaded to the PVDF solution, hoping to improve the dielectric and piezoelectric property of the composite and increase printability. Afterward, FDM technique is selected to fabricate objects from the designed STL file. Lastly, some characterizations are conducted to validate the result of proposal.

3.2 Experiment

3.2.1 List of equipment

The detail of used equipment throughout the experiments are listed below:

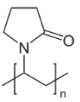
Table 3-1 List of experiment equipment

Test	Usage	Type
Scanning Electron Microscopy (SEM)	Characterization	Low-magnification, Table-top TM3000, Hitachi
Scanning Electron Microscopy (SEM)	Characterization	High-magnification, ZEISS SUPRA
Optical Microscope	Characterization	OLYMPUS SZX9 & DeltaPix
X-Ray Diffraction (XRD)	Characterization	Bruker D8 Robot Tools X-ray diffraction, Bruke
Thermo Gravimetical Analysis (TGA)	Characterization	Netzsch STA 409C/CD,
Rheology Test	Characterization	Anton Paar rheometer
Dielectric Test	Characterization	Solartron 1260A, Solartron Analytical
3D Printer	Printing	INKREDIBLE CELLINK
Electrospinning	Shaping	RT Advanced, Linari engineering
Furnace	Calcination/Sintering	-

3.2.2 List of materials

The detail of used materials throughout the experiments are listed below:

Table 3-2 List of experiment materials

Name	Chemical formula	Form/Type	Specification	Source
Barium acetate	Ba(CH ₃ COO) ₂	Powder/Salt	Purity >98%	Sigma-Aldrich
Acetic acid	CH ₃ COOH	Liquid/Acid	Purity >98%	Sigma-Aldrich
Titanium isopropoxide	Ti(OCH(CH ₃) ₂) ₄	Liquid/Alkoxide	Purity >98%	Sigma-Aldrich
Polyvinyl pyrrolidone; PVP		Powder/Polymer	Average Mw ~1,300,000	Sigma-Aldrich
Polyvinylidene fluoride; PVDF		Powder/Polymer	Average Mw ~534,000	Sigma-Aldrich
Ethanol; EtOH	C ₂ H ₅ OH	Liquid/Solvent	Purity >98%	Sigma-Aldrich
N-methyl-2-pyrrolidone; NMP	C ₅ H ₉ NO	Liquid/Solvent	Purity >98%	Sigma-Aldrich
Argon	Ar	Gas/Inert	Purity >98%	AGA

All the chemicals were analytical reagent grade and used as received without further treatment.

3.2.3 The 3D printer

The printers available for this project are INKREDIBLE and BIOX, produced by a Swedish 3D company called CELLINK. The equipment was acquired by kind support of the H.C. Ørsted's Fond (Denmark), under the frame of the “*High precision 3D printing of electromechanically active components for miniaturized sonic devices - 3SONIC*”. These machines use FDM as their core technology and each has several print heads, therefore enabling multi-materials processing. By linking an external pneumatic pump to their print heads, the printing materials are pushed outside of the syringe and constructed as a 3D item.

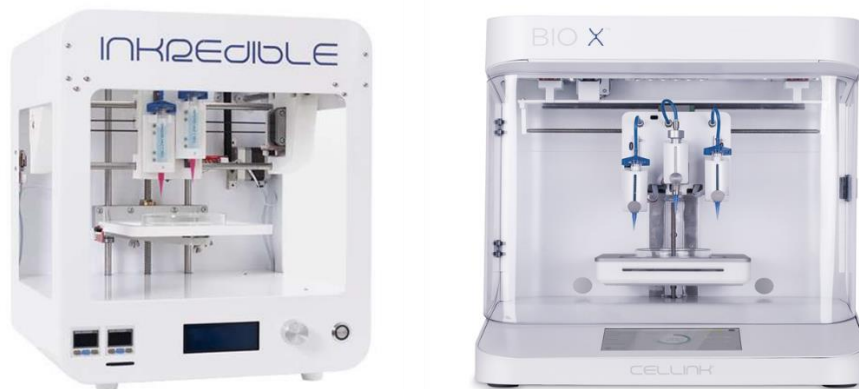


Figure 3-3 Digital view of CELLINK INKREDIBLE on the left and CELLINK BIOX on the right

Although these printers are originally designed for bio-related printing process, they have many features that are beneficial to this project. In particular, the CELLINK INKREDIBLE is reported to be the most cost-effective printer in its class currently available in the market.[151] Besides, the built-in clean chamber can produce a highly filtered air flow with positive pressure for extrusion, making the printer extremely suitable to deal with contamination-sensitive printing pastes. The equipped dual print heads pave the way for in-situ multi-material processing without switching cartridges or pausing the printing process. The embedded LCD controllers also enable the machine to be used as standalone units for printing three-dimensional object, making it convenient to reproduce complex shape structures. Based on the above-mentioned features, the CELLINK INKREDIBLE is mainly selected as the printer in our experiment for producing 3D-objects.

To generate the model of 3D structure. AutoCAD 2018 and Slic3r (1.2.7) were used for the design of the configuration. A stereolithography (STL) file of the devised structure was firstly generated by AutoCAD and then imported onto Slic3r, from which the G-code of the configuration was exported and finally sent to the 3D printer.

Typical setup of the printer should respect the following procedures:

1. Attach the syringe (containing printing materials) to an air pump pipe;
2. Lower the build plate and place the desired substrate onto the platform;
3. Fix the syringe onto the printing position;
4. Open the air pump but retain a closed air valve;
5. Choose the X-Y calibration option in the menu from control panel for positioning the printer head to the middle-point of the platform;
6. Open the air valve and test appropriate printing pressure via control knob until continuous flow is achieved;
7. Mark the optimized printing pressure and close the air valve;
8. Choose the Z calibration option in the menu from control panel and manually adjust the vertical axis to an appropriate position (set the needle 1mm away from the substrate) on Z-axis and calibrate the Z-position to zero;
9. Begin 3D printing.

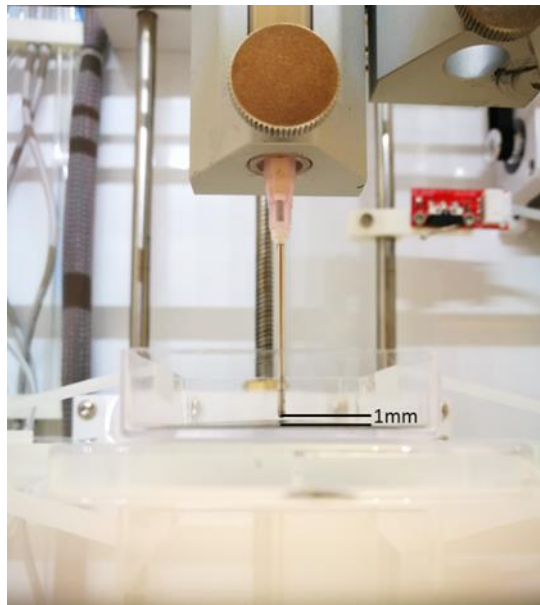


Figure 3-4 Adjusting Z axis for the 3D printer

By opening the channel between pump and syringe and adjusting the pressure value manually from the knob built on the 3D printer, a rough proper pressure value is found when a constant extrusion of material is witnessed. After fixing the printing pressure and choosing the already prepared STL file that has been imported into the printer, the 3D printing process can begin.

3.3 Preparation of the starting materials: BaTiO₃ microfibers (BTMFs)

3.3.1 Preparation of spinning solution

In order to prepare the materials for electrospinning, solution with proper concentration and viscosity should be prepared accordingly. To start, Ba(CH₃COO)₂ was dissolved in CH₃COOH under vigorous stirring at the temperature of 50°C until homogenous salt solution is obtained. Titanium isopropoxide was then slowly added into the prepared Ba(CH₃COO)₂/CH₃COOH solution under purging argon to obtain the cationic (Ba and Ti) precursor solution. In the meantime, homogenous PVP/EtOH solution was prepared and slowly added into the cationic precursor solution. The mixture was continuously stirred with the help of magnetic bars until the final homogenous viscous solution was obtained. Herein, to prepare the electrospinning precursor microfibers of BaTiO₃, the mole ratio of the concentration of the cations in spinning solution was controlled at 0.113 g/mL and the mole ratio of the acid per alkoxide was fixed at 11. Meanwhile, the concentration of the polymer in spinning solution was altered at 0.025 g/mL and 0.050 g/mL to find out optimized condition for electrospinning. Figure 3-5 shows the arrangement of the glassware during the electrospinning solution preparation and the flow chart of each preparation step.

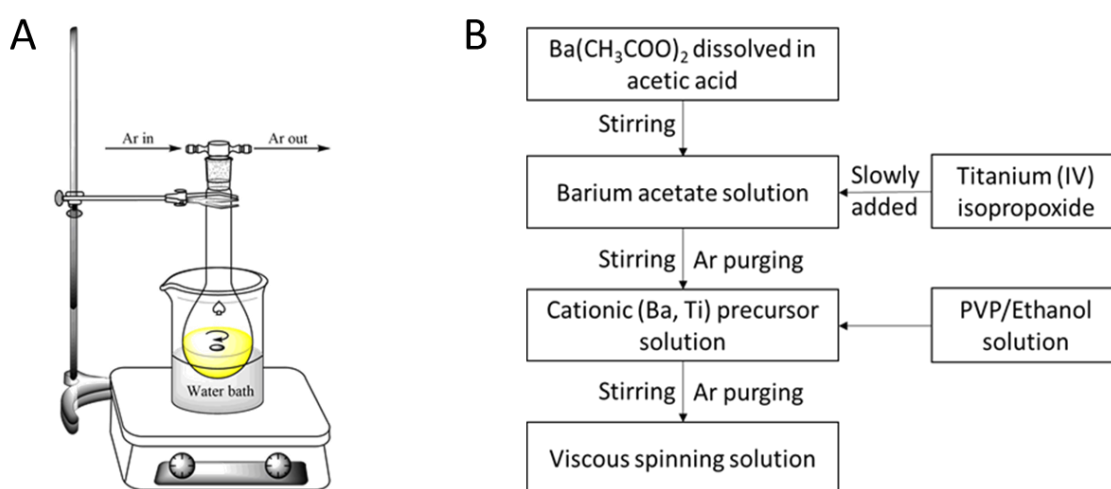


Figure 3-5 Electrospinning solution preparation process A). Glassware arrangement B). Flow chart of the preparation of the viscous spinning solution

3.3.2 Electrospinning and calcination process

RT Advanced (Linari Engineering) electrospinning equipment was herein used for electrospinning. The above-prepared spinning solution was loaded into a glass syringe with a metallic needle. The spinning distance (tip-to-collector) was fixed at 12 cm and the feeding rate was controlled at 1 ml/h. The microfiber produced during the electrospinning was collected by using a grounded rotating drum which spins at a speed of 100 rpm.

After aging the as-spun microfibers overnight in atmospheric air, the calcination process was performed at 800 °C for 1 h, with heating rate of 5 °C/min in atmospheric air, aiming at achieving organic-free ceramic microfiber products. After the thermal treatment, the size of the produced microfibers was modified by crushing using ball milling and controlled by mesh sieving. The final obtained product was then ready to be used as fillers in the micro-composite materials. A detailed flow chart showing the electrospinning process and calcination process is shown in Figure 3-6.

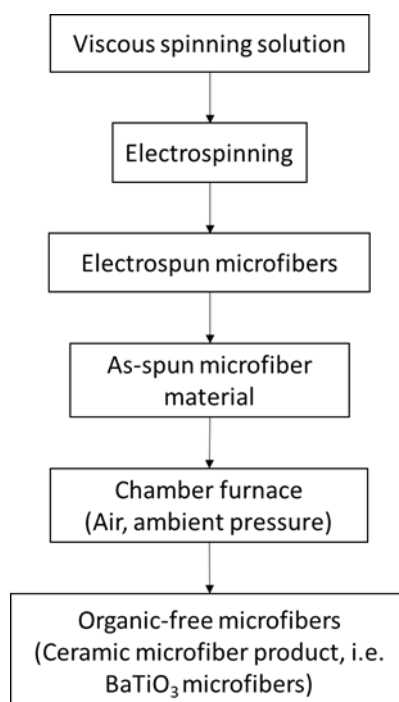


Figure 3-6 Flow chart of the electrospinning process and related post-processing procedures

3.4 3D printing of the BTMFs/PVDF hybrid material

3.4.1 Computer aided design of printing object

To start with, a digital model of sample structure was designed via AutoCAD 2017. To simplify the process, the structure was built up in a shape of cube with an area of 1 cm² and with a thickness of three-layers (about 6 mm). The deposition of more layers was not performed in our experiments as in principle it can be easily achieved by a repetition of crossed bilayers. Figure 3-7 shows one example of the CAD design of object. The file was later exported into STL style and sent to Slic3r for the generation of G-code, which was then sent to the INKREDIBLE 3D printer.

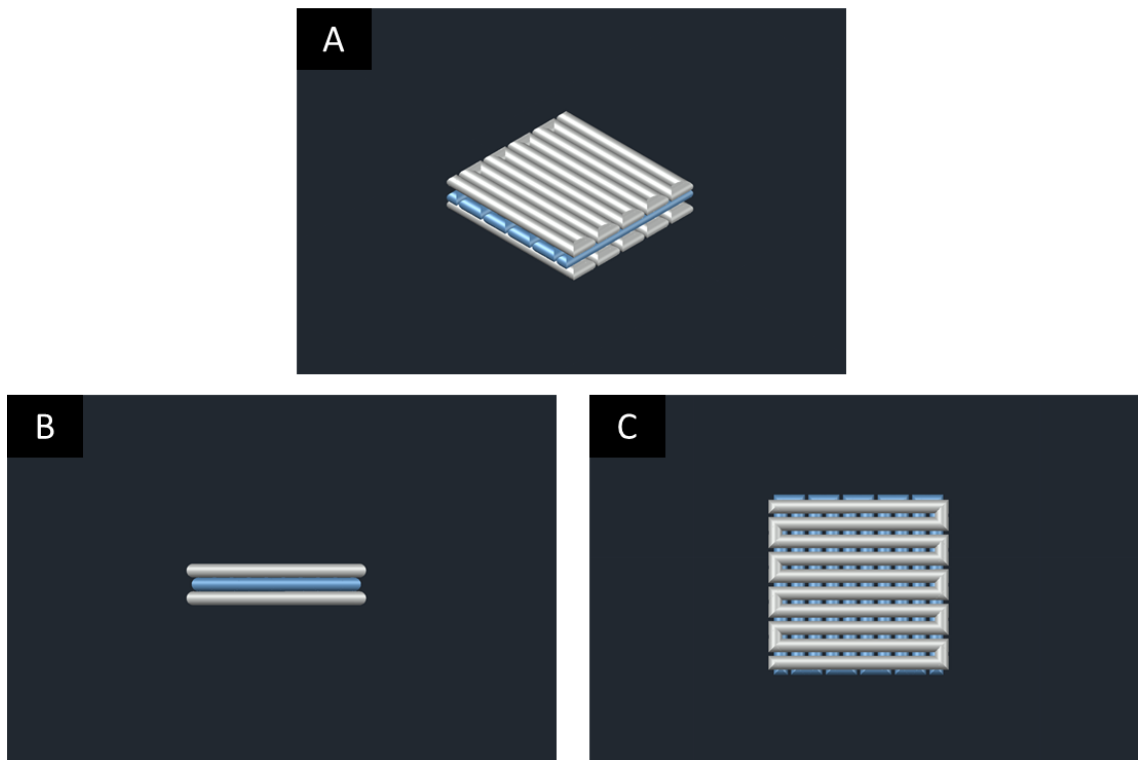


Figure 3-7 Computer aided design of printing object A). Overview B). Front view C). Top view

3.4.2 Preparation of printing pastes

In our experiment, N-methyl-2-pyrrolidone (NMP) was used as the solvent to dissolve the purchased PVDF powder. Firstly, the solution of PVDF in NMP was prepared by fixing the PVDF concentration of 20 wt% in order to match with the viscosity range of the thick paste materials for CELLINK INKREDIBLE (5000 - 100000 mPa s). In order to have a homogenous solution, a magnetic bar was used to stir the whole solution in a closed chamber at temperature of 50°C for 2 h. Afterwards, the size-controlled microfibers were loaded into the as-prepared PVDF/NMP solution and a magnetic bar was used to stir the obtained solution for 1 h. Figure 3-8 depicts the preparation of the

printing pastes. The resulting mixture was then subjected to ultrasonic agitation at frequency of 24 kHz for 30 min for further dissolving. The paste obtained was ready to be 3D printed. In order to study the effect of fiber loading concentration in composite, the ceramic particle loaded in the composite was controlled at 4.5 vol%, 20 vol% and 25 vol%, respectively.

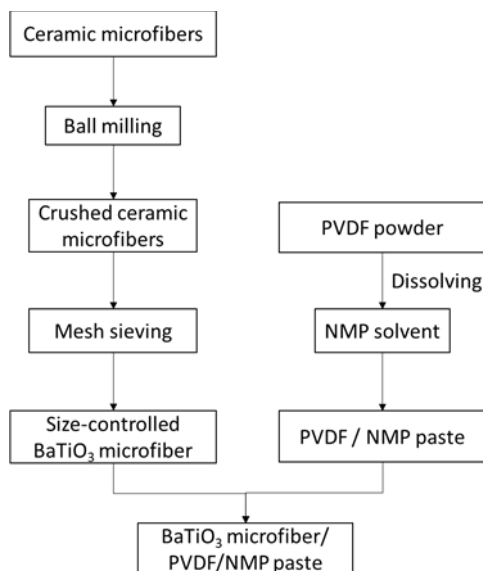


Figure 3-8 Flow chart of the preparation of 3D printing paste

3.4.3 3D printing of designed objects

After loading the as-prepared 3D ink into special plastic syringes, calibration process was done by following the procedures illustrated in section 3.2.3. A nozzle with a diameter of 2.12 mm was used throughout the test. In our experiment, no heating is needed to serve to the printing head as the printing paste used during printing process is already in a viscous paste-like form. The final printing process was performed in atmospheric air and at room temperature.

3.5 Characterizations

The thermal property of the electrospun microfiber product was evaluated with the aid of Thermo Gravimetric Analysis (TGA) and Differential Thermal Gravimetric (DTG) analysis (Netzsch STA 409C/CD, Germany). This analysis can provide useful information about possible physical phenomenon and chemical reactions during the heat-treatment process and measure the mass change of as-synthesized materials under different temperature over time. The collected data can be used to depict the thermal decomposition behavior of the as-spun BaTiO₃ microfibers and be used to optimize the post-processing procedure. The TGA/DTG analysis was performed in air flux from room temperature to 1200 °C at a heating rate of 1 °C/min.

The morphologies of the as-prepared microfibers and 3D printed hybrid materials were investigated by scanning electron microscopes (TM3000 Tabletop SEM, Hitachi, at an accelerating voltage of 15 kV with a backscattered electron detector and field emission scanning electron microscopy (FE-SEM), Supra, Carl Zeiss, Germany).

The crystallographic features of the produced ceramic microfibers were studied by XRD (XRD: Bruker D8 Robot Tools X-ray diffraction, Bruker, Germany). The analysis was carried out with a scan speed of $0.01^\circ 2\theta/\text{min}$ at a 2θ range of 10° to 90° .

The rheology test of the pure PVDF and the BTMFs/PVDF hybrid material were carried out by Anton Paar rheometer (MCR 302) using rotational modes at a constant temperature of 21°C . A 41-angle parallel-parallel spindle measuring system was utilized with a diameter of 50 mm (PP50) and at gap distance of 0.5 mm under a solvent trap. Pretreatment was done before performing the rheological measurement of the gels following three steps: the pre-shear at 0.1 s^{-1} for 1 min, 1 min at rest (0 s^{-1} shear rate), and the third step at 1 s^{-1} for 1 min. Meanwhile, the flow-curve measurements were carried out in step mode using 60 steps with a waiting time of 10 s. The shear rates were investigated from 1 s^{-1} up to 100 s^{-1} in the up-ramp, and from 100 s^{-1} to 1 s^{-1} in the down-ramp.

The dielectric constant (k) of the pure PVDF and the BTMFs/PVDF hybrid material with different loadings were investigated under the help of an Impedance/Gain-Phased Analyzer (Solartron 1260A, Solartron Analytical, UK). In order to complete the test, silver electrodes were painted onto the tested surface. The dielectric measurement was then conducted at room temperature in the perpendicular direction.(i.e. electric field direction is orthogonal to the fibers' orientation.) The frequency of the test was controlled with a range between 0.1 kHz to 1 MHz together with an applied biasing voltage of 0.2V. The obtained electrical impedance values were then used to calculate the capacitance and the dielectric constant of the material following the below equations.

$$C_p = \frac{1}{2 \times \pi \times f \times X_c} \quad (1)$$

$$k = \frac{C_p \times t}{A \times \epsilon_0} \quad (2)$$

where C_p is the capacitance of the material (F), f is the frequency (Hz), X_c is the capacitive resistance (Ω), t is the thickness of the material (m), A is the area of the electrode (m^2) and the ϵ_0 is the vacuum permittivity ($8.854 \times 10^{-12}\text{ F/m}$).

CHAPTER 4. Result and discussion

4.1 Characterizations of the BTMFs

4.1.1 Thermal properties

Thermo gravimetric analysis and differential thermal gravimetric analysis were conducted to test the thermal properties of the as-prepared materials and used to optimize the heat treatment process.

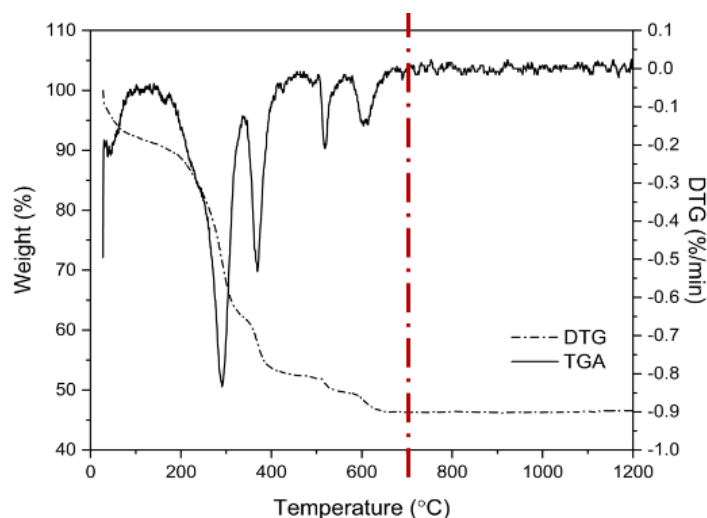


Figure 4-1 TGA/DTG analysis

As can be seen from Figure 4-1, a change of weight occurs as soon as a thermal treatment is applied. About 10% of initial weight is lost between room temperature and 180 °C, mainly due to the evaporation of residual moisture and solvents such as ethanol (boiling point at 78 °C) and acetic acid (boiling point at 118 °C). A significant mass loss (about 35%) is observed between 180 °C to 410 °C, together with a peak mass loss rate of 0.83%/min at around 290 °C. This is probably due to the oxidation and decomposition of unreacted organic precursors inside the synthesized material.[152] Another DTG peak is found from 500 °C to 560 °C, possibly corresponding to the further decomposition of the main chains of remaining PVP and the transformation of the intermediate phase BaCO_3 . [153] The last mass lost is found between 570 °C to 660 °C, indicating the crystallization of as-spun BaTiO_3 microfibers.[85] Totally, about 53% weight loss is observed during the heat-treatment process and no further lost is found at temperature after 700 °C, indicating that the organic-free fibers with complete crystallization could be obtained after calcination at 700 °C. Although the calcination process seems to be fully completed at 750 °C, hereby we choose 800 °C to be the final calcination temperature in order to obtain a thorough pure and fully-transformed BTMFs.

4.1.2 Morphology

Figure 4-2 depicts the physical photos of the electrospun materials before and after calcination at 800°C, respectively. It can be seen from the graph that the as-spun material has a similar color with the as-calcinated material. However, in terms of their mechanical property, the former material is more flexible in shape while the latter tends to be more fragile and brittle. This phenomenon can be explained by the removal of organic compounds from the samples, as the leftover material are mainly made of inorganic BaTiO₃ ceramics.

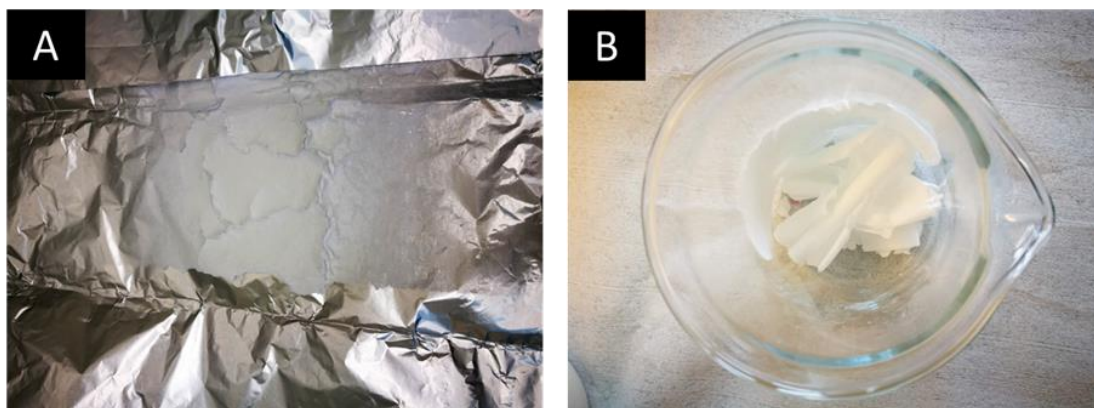


Figure 4-2 Physical photos of A). as-spun material B). as-calcinated material

Scanning electron microscopy was then used to observe the morphology of the as-spun BTMFs and the calcined samples. Since the electrospinning parameters have a big impact on the final product, different electrospinning conditions are analyzed to obtain the optimized electrospinning condition. Figure 4-3 and Figure 4-4 show the electrospinning results under different voltages and binder concentrations, respectively.

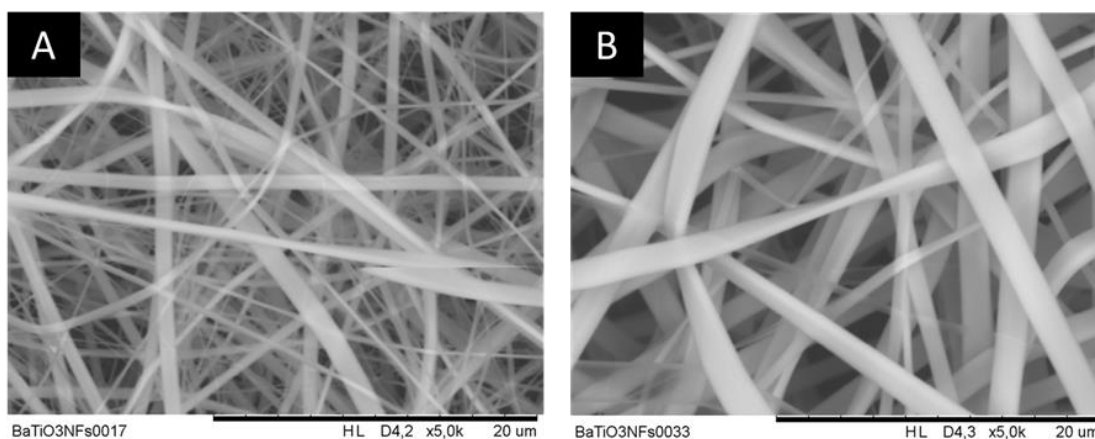


Figure 4-3 Electrospinning with applied voltage at 15 kV and binder concentration at A). 0.025 g/ml B). 0.050 g/ml

As can be seen from Figure 4-3, micro-sized fibers are obtained after electrospinning. However, results from higher binder concentration tend to have less fibers when a same

voltage is applied. Despite the fact that produced fibers from high concentration are more evenly distributed, the productivity from the mentioned group is really low, which is most likely due to a higher viscosity of the spinning solution. Considering that the size distribution can be further modified by varying electrospinning voltage, the lower binder concentration at 0.025 g/ml is chosen to maintain proper productivity.

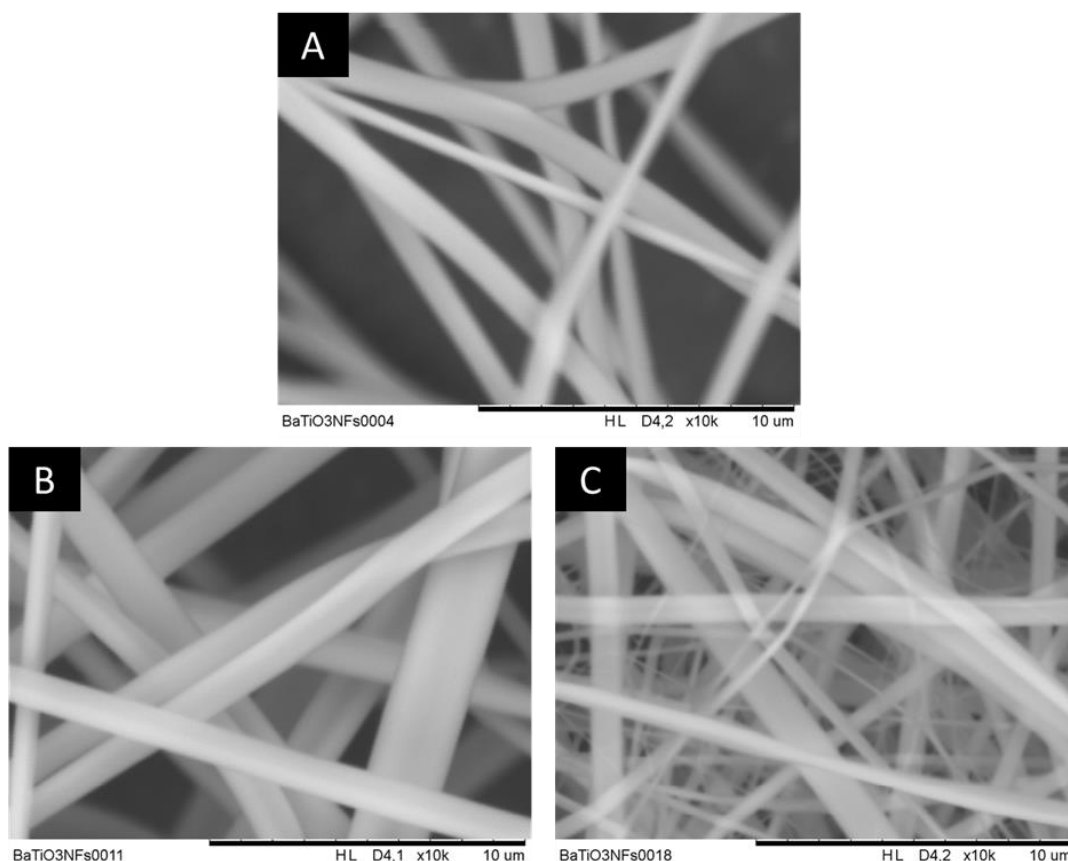


Figure 4-4 Electrospinning with binder concentration at 0.025 g/ml and applied voltage at A). 10 kV B). 15 kV C). 20 kV

Figure 4-4 represents the result of electrospinning at a binder concentration of 0.025 g/ml with different applied voltage (e.g. 10 kV, 15 kV, 20 kV). As can be seen from the graph, microfibers produced by a voltage of 20 kV are largest in quantity but most distributed in fibers' diameter. By comparison, an electrospinning voltage of 10 kV gives the lowest productivity to the fibers. When the applied voltage is fixed at 15 kV, the outcome tends to be optimized as the produced fibers are more similar in size (*vs.* high voltage condition) and richer in quantity (*vs.* low voltage condition). As a result, an applied voltage of 15 kV is selected to be our final electrospun voltage value.

After setting the final optimized condition of binder concentration at 0.025 g/ml and applied voltage at 15 kV for electrospinning, the as-prepared fibers are sent to post-processing treatment and then to high-resolution SEM for further characterization.

Figure 4-5 shows the surface morphologies of the as-synthesized fibers and their 800 °C calcined correspondences, respectively.

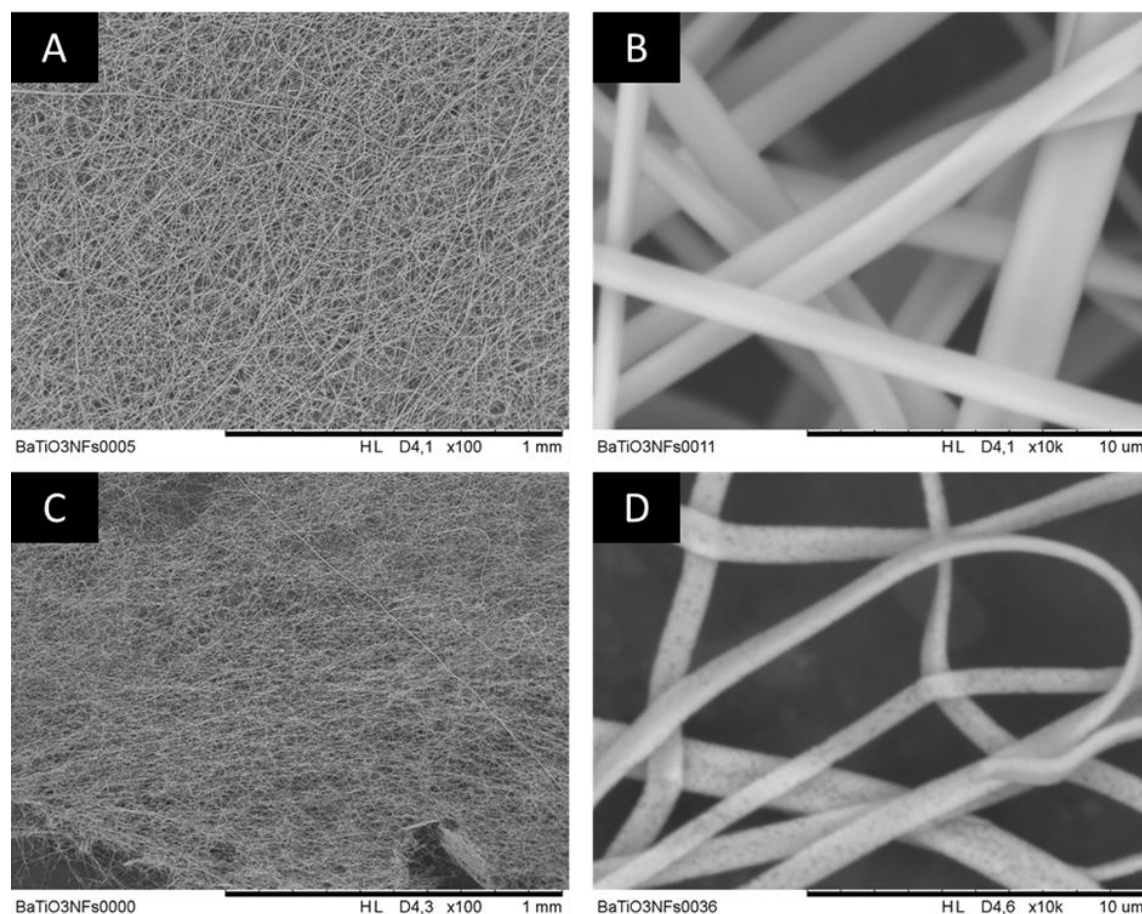


Figure 4-5 SEM figures of A). B). as-spun BTMFs and C). D). calcinated BTMFs

Clearly, the as-spun microfibers exhibit relatively smoother and more uniform surfaces while the calcined microfibers tend to have a higher surface roughness. In terms of orientation, both materials are randomly-oriented with no major domination. Shrinkage phenomenon is observed during the calcination process, as the cross-sectional area of microfibers is expected to decrease after calcination. To estimate the size of produced microfibers from the SEM images, 25 fibers in different areas were randomly selected. In general, the fiber's width lowers from around $2.15 \pm 0.07 \mu\text{m}$ to $1.20 \pm 0.05 \mu\text{m}$ while fiber's thickness drops from $0.60 \pm 0.03 \mu\text{m}$ to $0.40 \pm 0.04 \mu\text{m}$. This condition can be attributed to the decomposition of the trapped organic components and the crystallization of desirable BaTiO₃ (As discussed in section 4.1.1). By calculation, an average cross-sectional area reduction of more than 60% is estimated.

The morphology of the grinded material was also observed and presented in Figure 4-6. Clearly, after ball milling and mesh sieving, the length of BTMFs are reduced but the material still remains a relatively high aspect ratio.

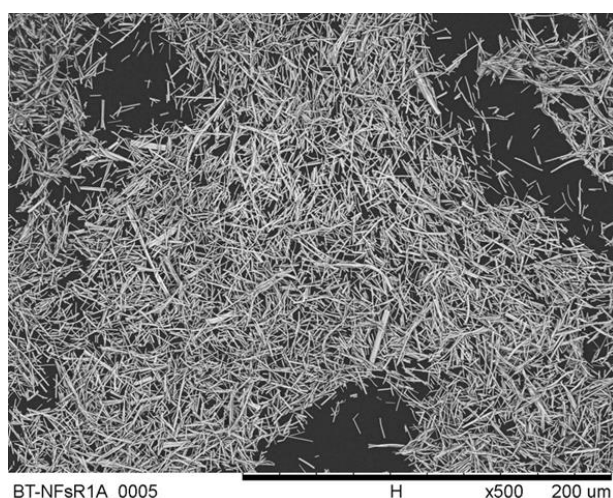


Figure 4-6 SEM figure of grinded BTMFs

4.1.3 Crystallography

In order to further validate the as-calcinated BaTiO_3 powder, X-ray diffraction test is done to qualitatively analyze the phases and composition of the material. With reference to the result from TGA, the 800°C thermal treated material is sent to test.

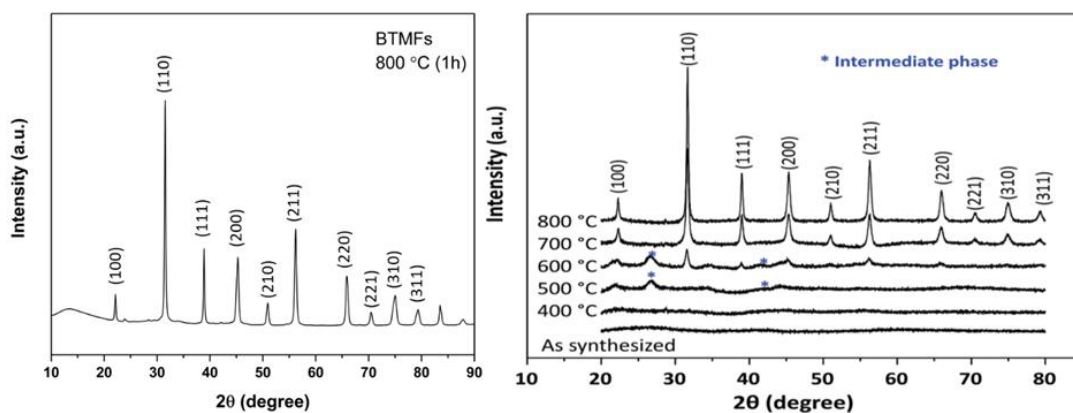


Figure 4-7 XRD characterization of the as-prepared materials (Left) and reference XRD pattern (Right)[85]

The 800°C calcined BTMFs diffraction patterns are presented in Figure 4-7. Ten characteristic peaks at 2θ range from 20° to 80° were found in our sample. Obviously, the diffraction pattern represents evident narrow peaks with sharp signals, indicating a high-quality of crystalline composition in the material. The result was compared with previous work done by N. Phatharapeetranun *et al.*[85] and it is found out that all peaks match perfectly to the reference paper in terms of position and intensity. Therefore, a conclusion can be drawn that the pure perovskite BaTiO_3 material was successfully produced.

4.2 Characterizations of 3D printed BTMFs/PVDF hybrid materials

In order to have good printability with the FDM technique, the maximum solid loading in the ink is normally controlled under 50 wt%.[154], [155] Indeed, an increased concentration of solid loading leads to higher viscosity and shear stress values, which always results in an unstable extrusion flow or blockage at the printer nozzle during the printing. Consequently, the loading of BTMFs in this work is designed to be 4.5 vol%, 20 vol% and 25 vol%. Herein, several tests are done to further characterize the properties of the BTMFs/PVDF hybrid materials.

4.2.1 Rheology

Previous report has demonstrated the importance of using proper printing needles during 3D printing process.[85] However, restrained by the limited selection of equipment, only a 2.12 mm needle was used during our experiment. In order to analyze the performance of printing ink, a series of rheology tests were conducted to measure ink's viscosity.

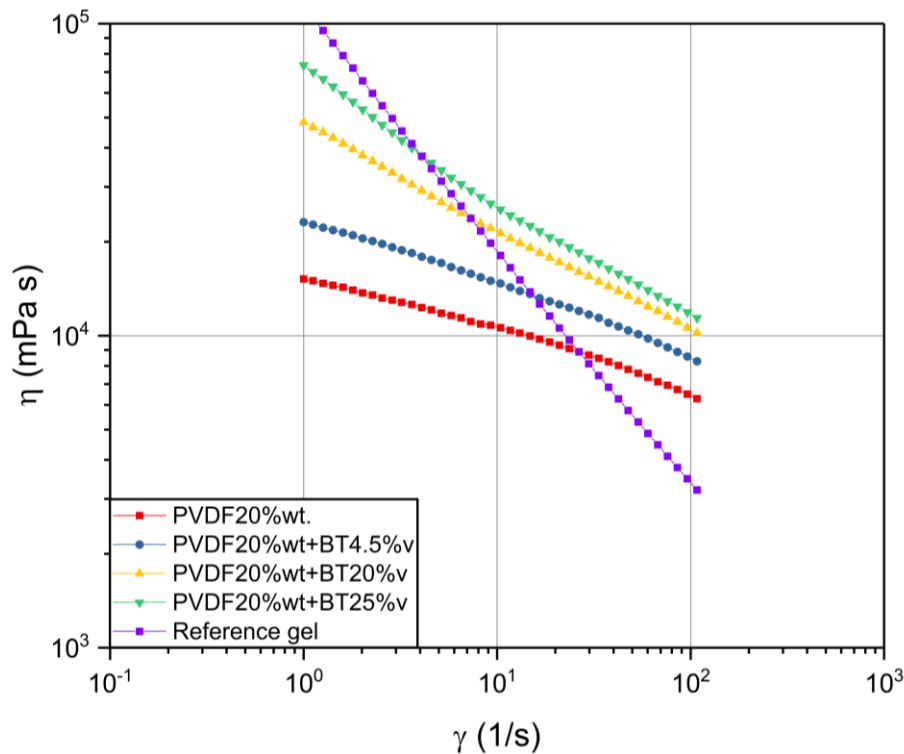


Figure 4-8 Result of rheology test-viscosity test

Figure 4-8 illustrates the relationship between the shear rate (γ , on X axis) and the viscosity (η , on Y axis) for reference gel, pure PVDF and hybrid material with different BTMFs loadings. As expected, a clear trend is found that as the loading concentration rises, the viscosity of the hybrid material increases. This can be explained by the flow

hindering effect due to the presence of BTMFs.[85], [156] However, compared to the reference gel, the change of shear rate seems to have a less influence on the viscosity of pure PVDF or on our hybrid material. On the other hand, all samples demonstrate a shear thinning behavior, which can be proved by the negative slopes of viscosity curves. Interestingly, the highest loading of 25 vol% BTMFs does not only show the strongest shear thinning effect, but also possess the highest viscosity among all samples. This phenomenon is further validated by calculating the flow index (n) of the sample.

In a rheology test, the flow index (n) is often used as a parameter to judge the differential behavior between the experiment material and the Newtonian material ($n=1$). By plotting the shear rate and the shear stress based on double logarithmic form of the power law, the value of flux index can be obtained as the slope of its fitted straight line. As a result, the obtained value can be used to explain the flowing mechanism of one system.

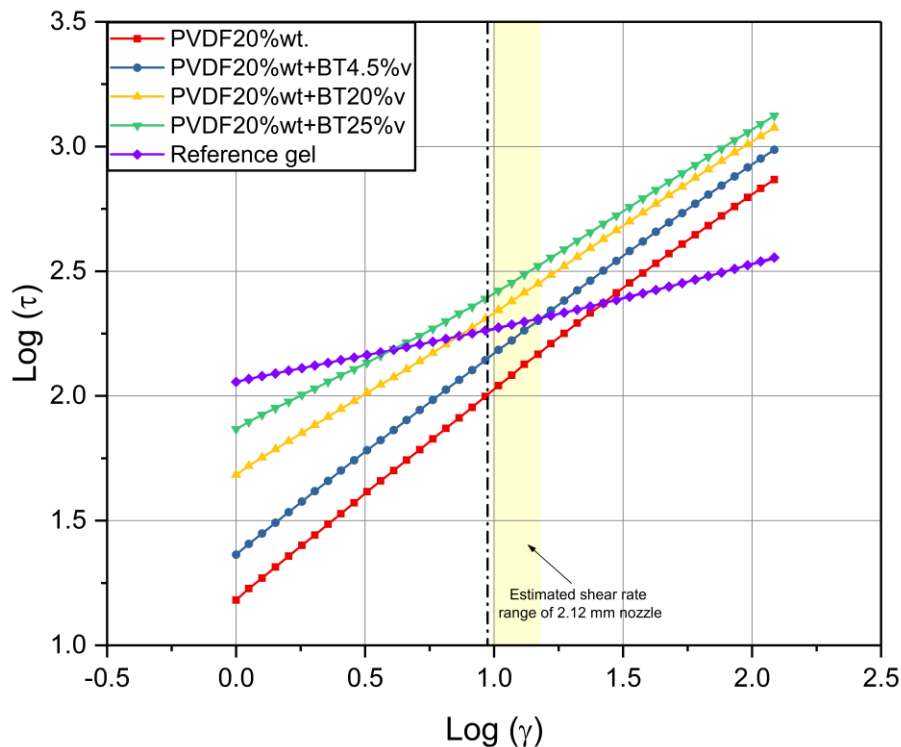


Figure 4-9 Result of rheology test-double logarithmic power law plot for showing flow index

Figure 4-9 illustrates the relationship between the shear rate ($\dot{\gamma}$, on X axis) and the shear stress (τ , on Y axis) for reference gel, pure PVDF and its composites with different BTMF loadings. Clearly, a linear tendency is found in the plotted graph. However, some evident inflection points (occurs when $\log(\dot{\gamma})$ is equal to 0.95) were found in all curves, meaning that a multiple flow index profile with different values of n exist.[85] Interestingly, instead of being influenced by the loading concentration, the position of

the inflection point is determined by the shear rate value. With the help of linear regression, the values of flow indexes are calculated and presented in Table 4-1.

Table 4-1 Flow indexes for the pure PVDF, reference gel and the hybrid materials

Flow index Samples	n ₁		n ₂	
	Value	Standard Error	Value	Standard Error
PVDF20	0.84	0.1%	0.77	0.4%
PVDF-BTMFs-4.5% vol%	0.80	0.2%	0.75	0.3%
PVDF-BTMFs-20% vol%	0.63	0.1%	0.68	0.2%
PVDF-BTMFs-25% vol%	0.52	0.2%	0.65	0.1%
Reference gel	0.21	0.0%	0.26	0.2%

It can be seen from Table 4-1 that for both situations, hybrid material with higher BTMFs loading has lower flow index value. Nevertheless, materials with low BTMFs loading demonstrate higher flow index values at low shear rate range while the situation is vice versa for high loading materials. This difference between flow rate values could result in very distinct outcomes to the end-product with rather different shape of the materials after deposition.

A thin needle normally has a higher shear rate than its thick correspondence. As a result, when dealing with a shear-thinning material (e.g. our BTMFs/PVDF hybrid composite) by a thinner needle, the extruding material are in a state of lower viscosity. Consequently, the printing flow is in a higher level of unstable circumstance and can be easily disturbed by any other factors. As a result, the fibers contained in the composite are less likely to be influenced by the internal friction between the flows and therefore tends to have less degree of alignment. Subsequently, materials with higher viscosity and lower level of shear thinning behavior are preferred during the printing process. Concerning our experiment, PVDF with 25 vol% BTMFs loadings should supposedly be the optimal solution.

On the other hand, since the value of our samples are very different from that of the reference gel, it is evident that the printing situation is not at its optimum condition. Further optimization on the PVDF rheology would therefore be needed to modify the printing ink rheology. Despite the differences, in our work, all the materials resulted printable, although some spilling effect occurs after deposition (see section 4.2.3).

4.2.2 Crystallography

The XRD analysis of the printed composite material was then conducted to observe the change of crystallography of the as-prepared material with different fiber loadings.

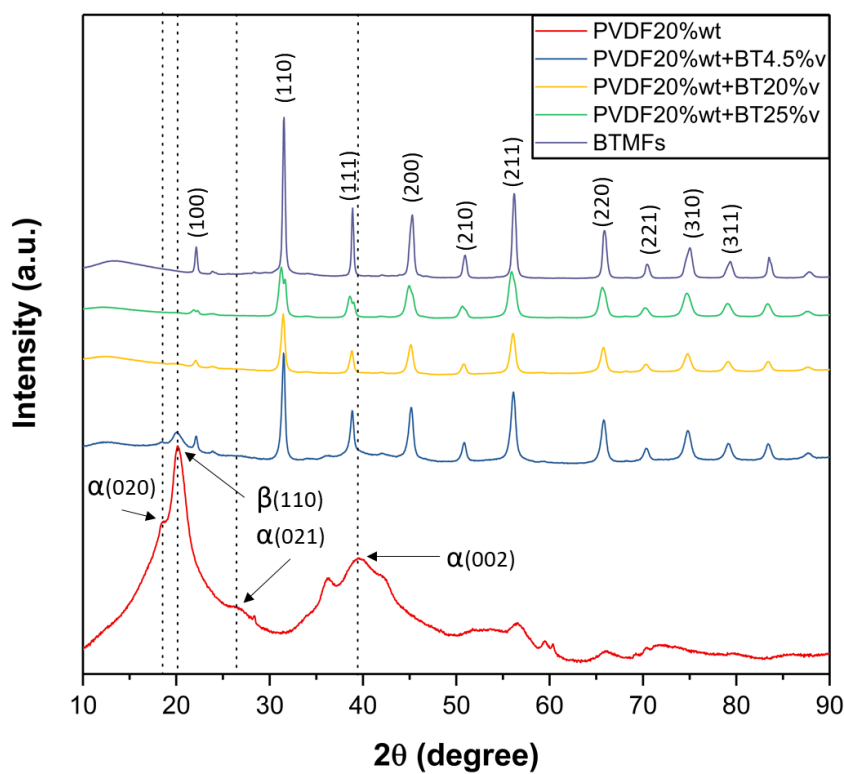


Figure 4-10 XRD pattern of pure PVDF, BTMFs and hybrid printing materials

As it can be seen in Figure 4-10, the XRD pattern for pure PVDF contains broad humps rather than any sharp diffraction peaks, which means the purchased PVDF is in an amorphous form. Nonetheless, several characteristic peaks in the patterns indicates a semi-crystalline nature of PVDF. The peaks at 2θ values of 18.47° , 26.41° and 39.47° can be attributed to the (020), (021), and (002) reflections of the α phase of pure PVDF while the peak at 20.15° corresponds to the β phase of pure PVDF.[85], [157]. Compared to the α phase PVDF, the β phase PVDF has a better piezoelectric property.[158] When it comes to the diffraction patterns of BTMFs/PVDF hybrid materials, all sharp characteristic peaks corresponding to the perovskite BTO structures were noticed. In the 4.5 vol% BTMFs loading sample, a small peak at 20.15° was found, indicating the existence of β phase PVDF in the composite. With the continuous increase of BTMFs loading, the intensities of both α and β PVDF's peak in the hybrid material decrease. When the maximum loading of 25 vol% is reached, the XRD pattern of PVDF can be barely observed, while a broad peak was detected at low angles at around 13.54° because of the influence of BTMFs. However, there is no significant difference of the diffraction patterns between the 20 vol% and 25 vol% loadings, probably due to a dominant amorphous phase of the PVDF.

4.2.3 Morphology

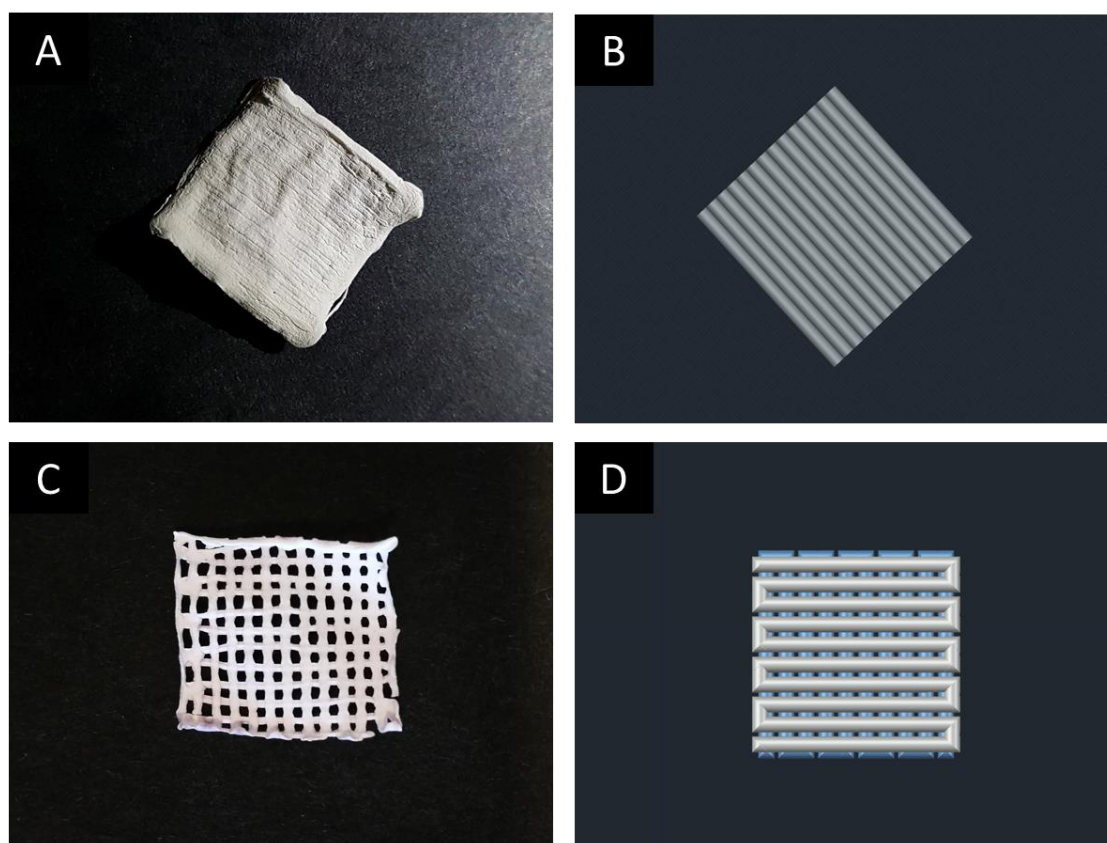


Figure 4-11 Comparison of A). physical view of the one direction printed object (3 layers) after drying and its B). digital design model vs. B). physical view of the crossed printed object (3 layers) after drying and its D). digital design model

The macro structures of the printed objects were firstly observed by optical microscope. Figure 4-11 shows the physical photo and digital designed model of the one-direction printed object and crossed printed object (both with a size of 1 cm * 1 cm * 2 mm after drying). Clearly, repeated lined pattern was found on the one-direction 3D object and a solid intersected structure was successfully produced via the crossed printing, meaning that the printed materials are capable of maintaining their structure and not collapsing after printing and drying. Shape distortion in the printed object was spotted due to the combined effects of drying of the polymers and a residual flowing of the printing after depositions. Despite the limits, the result was promising and, as discussed in section 4.2.1, opened to optimization. This is of great importance to the microstructure configuration as a collapse of macrostructure could induce a random flow of the microfibers.

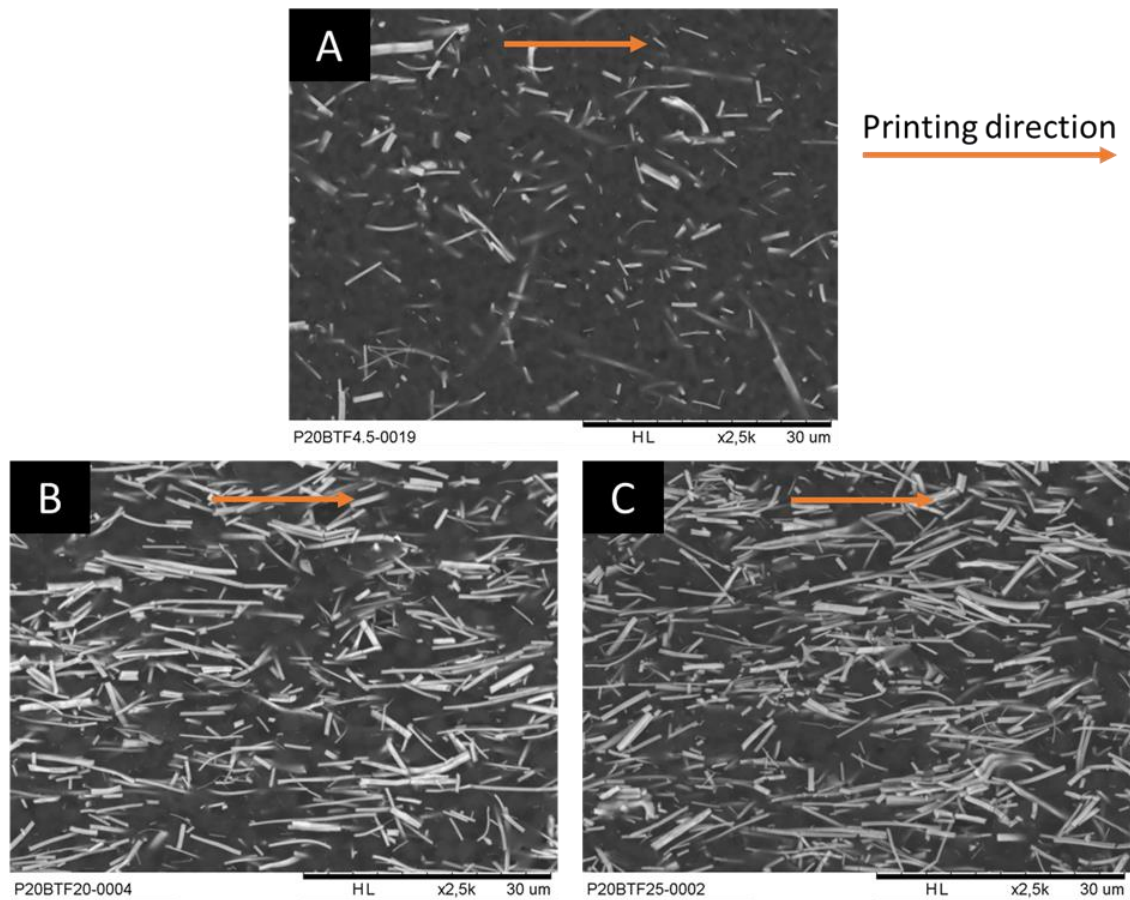


Figure 4-12 SEM figures showing the alignment of BTMFs in 3D-printed materials with different loading A). 4.5 vol% BTMFs C). 20 vol% BTMFs C). 25 vol% BTMFs

In order to further observe the microstructure of the printed material, the morphology of BTMFs/PVDF 3D hybrid materials was characterized by SEM. As can be seen from Figure 4-12, barium titanate microfibers were averagely distributed in the PVDF matrix. No agglomeration was found in the final object, indicating the solution was produced in a well-dispersed state. Clearly, a random orientation of fibers was found out for the sample with 4.5 vol% BTMFs loading. However, in the high BTMFs loading samples, a high degree of fiber orientation was observed alongside the printing direction. This phenomenon of fiber alignment can be explained by the viscoelastic effects during the printing process, where the friction between flow layers and between surface layer and the extruders triggered the orientation of fibers.[85]

From this result, we can say that 3D-printed objects with complex macro-shape and designed micro-structure (e.g. controllable fiber alignment in polymer matrix) have been successfully produced by FDM.

4.2.4 Dielectric property

The dielectric performance of the materials is one of the basic properties to be investigated for piezoelectric applications. To some extent, the dielectric properties can reflect the performance of one piezoelectric material. That is to say, there is a coexistence of dielectric and piezoelectric property in the composite and for most cases, it is almost impossible to have one excellent performance in one property while the other property stays poor. For validating this relationship, Dr. Robert Newnham proposed an mathematical model and demonstrated an positive correlation between the polarization electrostriction coefficient and the dielectric polarization rate.[159] Moreover, in our case, due to the low BTO content loaded in the hybrid composite, while the effect of fibers alignment in the composite is difficult to be detected by change in the piezoelectric coefficient of the samples, the dielectric constant (permittivity) is selected to be tested due to its sensitivity to the ceramic-polymer mixing.



Figure 4-13 Sample of 3D printed BTMFs/PVDF hybrid material with silver electrodes for dielectric testing

To facilitate the dielectric test of the material, simple BTMFs/PVDF rods with a width of 2 mm and a length of 5 mm were designed and printed. After painting on silver electrodes, the surface condition was checked by optical microscope and the active surface conducting area was measured by digital camera. Later, the prepared dielectric samples were sent to final tests. Figure 4-13 shows the physical view of one sample tested object.

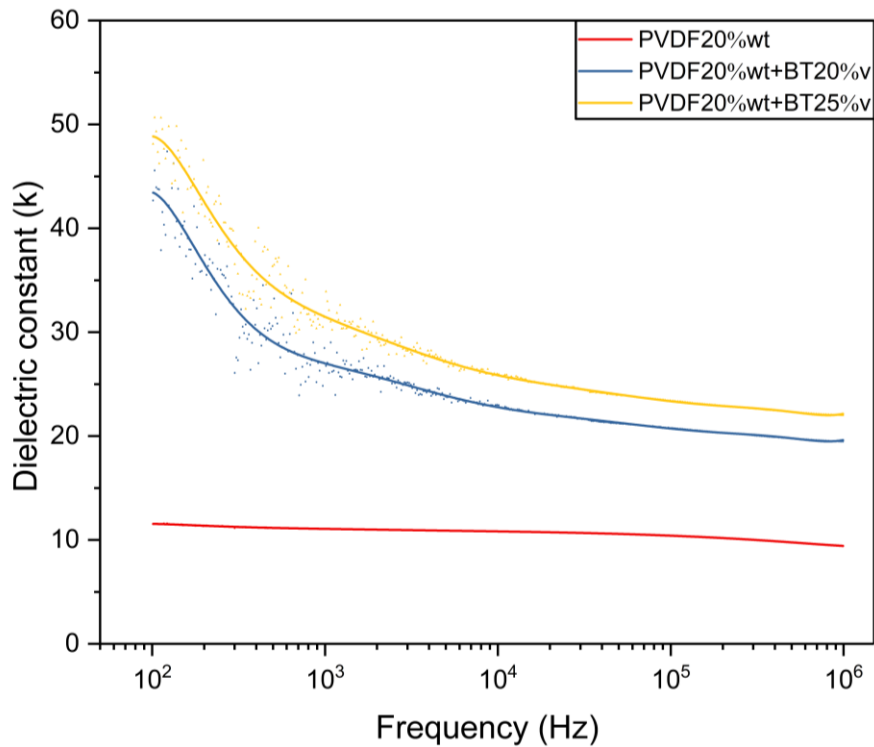


Figure 4-14 Frequency dependence of the dielectric constant of the 3D printed hybrid material

Figure 4-14 shows the result of the dielectric test of the 3D printed hybrid material with frequency at the horizontal axis and dielectric constant at the vertical axis. Obviously, as the frequency increases, the dielectric constants of all samples decrease. By loading more BTMFs into the pure PVDF matrix, an increment of k value was observed. Particularly, considerably high values of dielectric constant were found at the low frequency range for samples with 20 vol% and 25 vol% BTMFs loadings. This tendency can be explained by the Maxwell-Wagner-Sillars polarization effect (interfacial polarization effect), where space charges are built up and accumulated at the interfaces by following the applied electric field direction, resulting in to a high polarization phenomenon and high k value. Contrarily, the dielectric constant demonstrates a much less significant value and almost linear trend at the high frequency range. In all cases, samples with BTMFs loadings exhibit a higher value compared to that of the pure PVDF material.

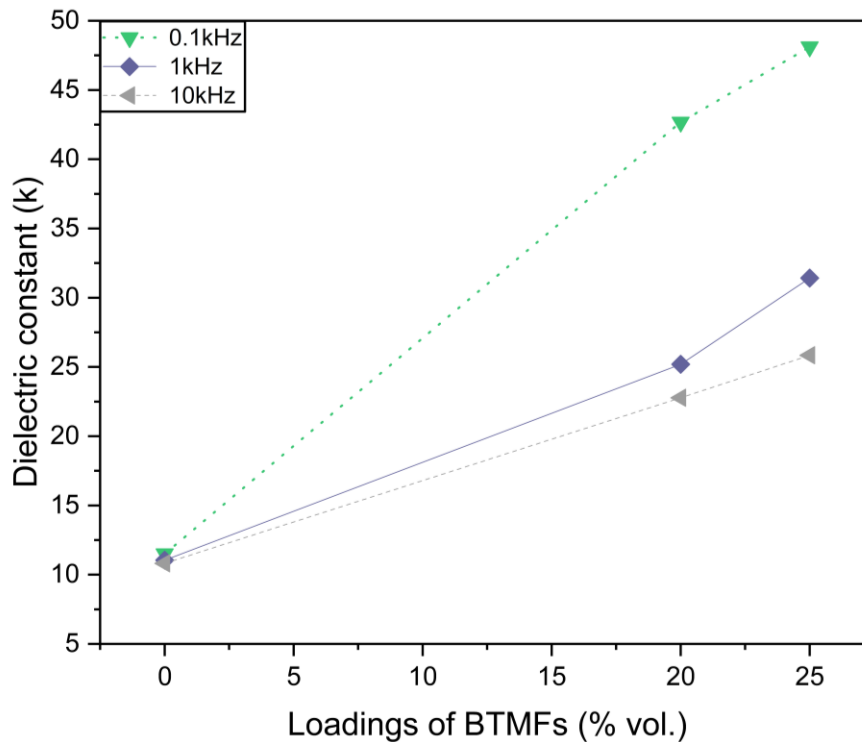


Figure 4-15 Dielectric constant comparison of BTMFs/PVDF composites with different BTMFs loadings at 0.1 kHz, 1 kHz and 10 kHz, room temperature

To further understand the effect of BTMFs loading on dielectric constant, a loading comparison was made by investigating targeted k value at 0.1 kHz, 1 kHz and 10 kHz from all samples. As it can be seen from Figure 4-15, an evident trend of dielectric constant enhancement was noticed by filling larger portion of BTO microfibers into the polymer matrix. When the frequency was controlled at 10 kHz, the value of pure PVDF, hybrid materials with 20% loading and hybrid materials with 25% loading are 10, 22 and 26, respectively. At a lower frequency value of 1 kHz, the dielectric constant of 3D printed material experiences an almost three-time increment from 11 in pure PVDF polymer to 31 in 25%vol BTMFs loading composite. This outcome can be explained by the additional loadings of barium titanium in the composite, as the dielectric value of former material is reported to be high (at around 1000).[156]

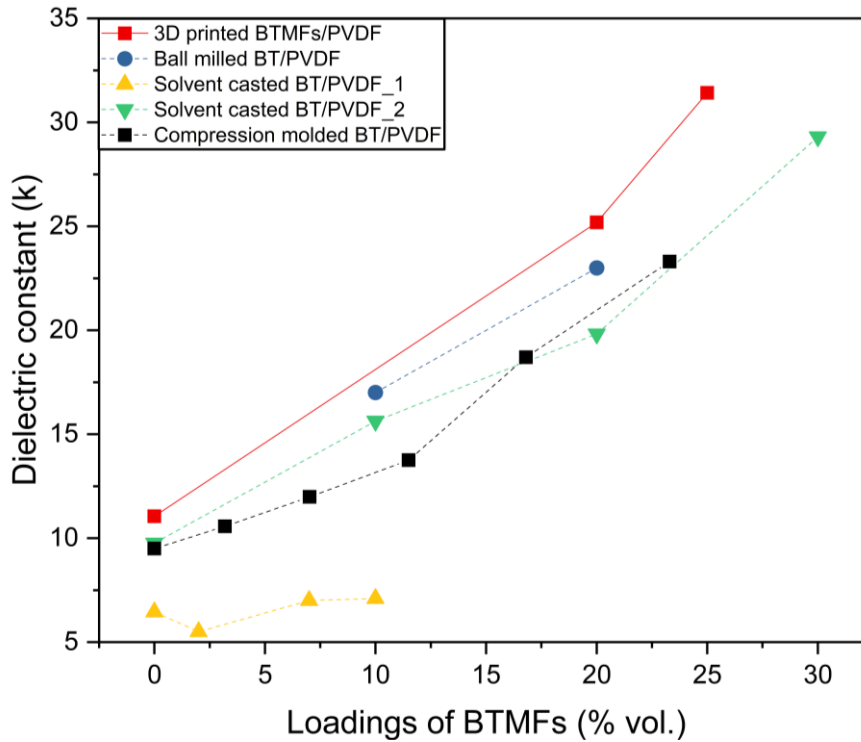


Figure 4-16 Dielectric constant comparison between the 3D-printed BTMFs/PVDF hybrid material and the reported BTO/PVDF composites at 1 kHz, room temperature

By evaluating the k value with previous reported work done by the others, the advantage of using 3D printing to produce high-performance BTO/PVDF composite can be validated. Figure 4-16 compares the dielectric constant of BTO nanoparticle/PVDF hybrid material produced by ball milling[160], compression molding[144], solvent casting[161], [162] and 3D printing. As expected, our 3D-printed BTMFs/PVDF hybrid material demonstrates an optimum performance in dielectric constant as its value is consistently higher than any other examples throughout all loading range. This fact can be attributed to the implementation of high-aspect-ratio microfiber in the polymer matrix, which introduces an increased amount of enlarged hybrid interfaces between the organic polymer matrix and the inorganic ceramic filler.[85], [163] It is therefore concluded that using 3D printing to generate object with controlled fiber alignments is of benefit to enhance the dielectric constant of such product.

CHAPTER 5. Business case analysis

As it has been demonstrated in the experimental work, a BTMFs/PVDF based hybrid material with enhanced dielectric properties was successfully fabricated by a following procedures of sol-gel processing technology, electrospinning and 3D printing. Although only dielectric properties are tested in the characterization, the piezoelectric performance of such hybrid material is also expected to be improved. In order to move such achievement from laboratory to market, a business-related research is conducted to identify the potential application area. Herein, several potential industries that can be of interest to our results are identified and listed.

5.1 Energy storage system

Firstly, dielectric materials with high energy density are promising candidates for high-performance energy storage devices due to their small size, light weight and outstanding cycling efficiency. One typical application for our experiment materials is capacitors. By inserting a 3D printed dielectric between two capacitor plates, not only the capacitance can be increased, but also the need for sophisticated structure can be meet. By doing so, it is possible to obtain complex-shaped embedded capacitors with enhanced performance. Applications can be found in the startup of hybrid vehicles cars, for complementing traditional batteries, etc.

5.2 Smart wearable industry

A report from the International Data Corporation revealed that around 125.5 million wearable devices were purchased by the public in 2017 and the corresponding number is expected to increase to 240.1 million in five years.[164] Consultants from Research Nester also anticipated that a total market value of over 52.5 billion US dollar will be reached in the smart wearable industry by the end of 2024, providing lots of opportunities and valuation to the industry.[165] For our shape free piezoelectric material, some interesting applications for wearable devices could be proposed.

For instance, smart shoes for assisting running dynamics and testing plantar pressure serves as an interesting example. Nowadays, since the smart watches and fitness trackers are now the main players of the wearable device market, an increased interest can be found in sports activity monitoring and alerting. By embedding the designed-shape piezoelectric energy harvester (PEH) into soles with wireless module and data processing package, smart shoes can be manufactured for health monitoring, providing real-time data for individuals on precise steps counting and foot pressure distribution

censoring. Conversely, one can even expect using this type of shoes to adjust wrong walking patterns or act as a buffer to protect ankles. Therefore, this kind of designs are of particular interest to those who are exposed to intensive labor work or sport training, as dangerous injury may occur more frequently.

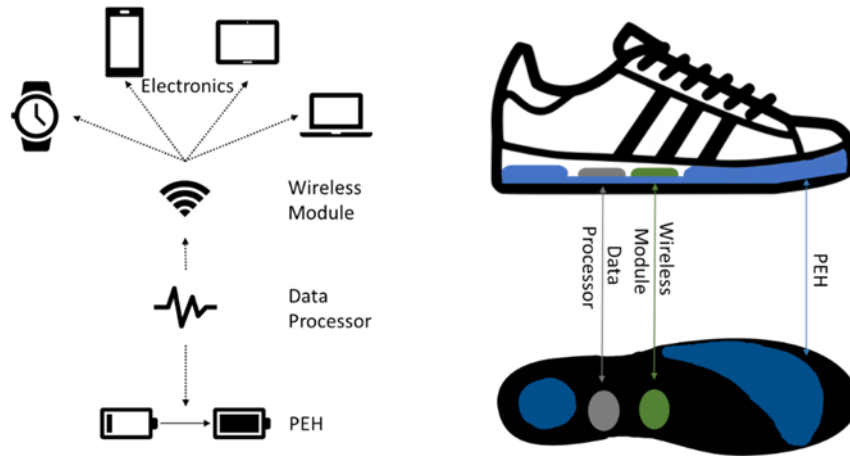


Figure 5-1 PEH applications in smart shoes

Similarly, if micro energy storage systems and charging modules are incorporated, the shoes can also be utilized as an electricity generator for wireless charging. Once someone put pressure on the soles, power will be supplied to the energy storage systems. The energy can be released later to electronics when needed. In addition, by introducing a wireless charging module, it is also possible to achieve real-time charging and abandon the traditional cable-to-electronics process.

5.3 Medical industry

In the medical sector, customized artificial prosthesis with complex shapes are often needed for the disabled based on their own biological features. This concept fits very well with 3D printing, where devised structures can be easily modelled and generated.

One example to apply our 3D printed PEH into the medical industry is the ear prosthesis. As the structure of inner ear varies from one to the other, a devised complex PEH generated by 3D printing can perfectly fits one's physiological need and be used as a hearing aid for those who have disability in detecting and recognizing sound. Similar work has been performed by Gómez et al, who also used a 3D printed ear prosthesis as a temperature and pressure sensor by transforming the mechanical force into electrical stimulation.[140] Of course, this was done under the help of some other auxiliary components, which gives electrical signal to patients' nervous system and therefore compensating their tactile sensation.

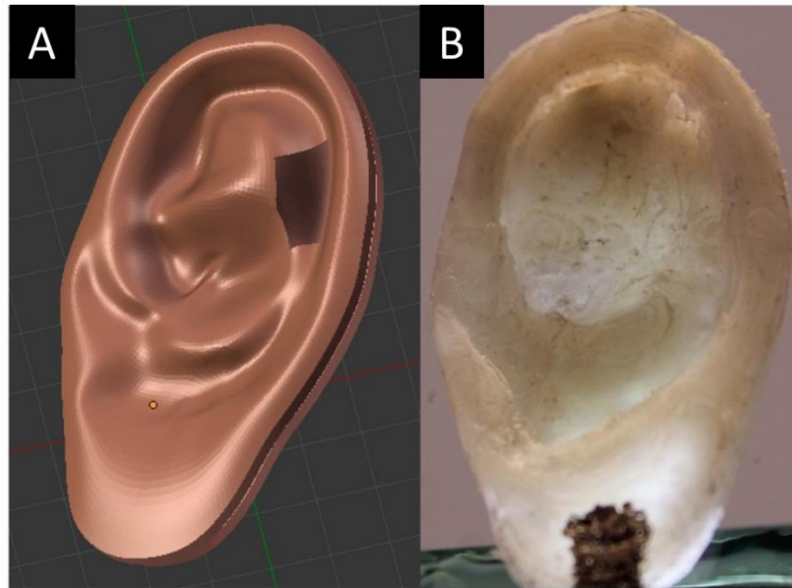


Figure 5-2 3D printed ear prosthesis for temperature and pressure sensing by Gómez et al.[140] A). Computer-aided designed ear prosthesis B). 3D printed ear prosthesis

Patients who have cardiac diseases can also be our targeted group. For instance, a printed PEH can be placed on the heart of the cardiac patient in order to act as an emergency power for pacemaker or provide electricity to the implanted defibrillator for avoiding the repeated change of batteries.

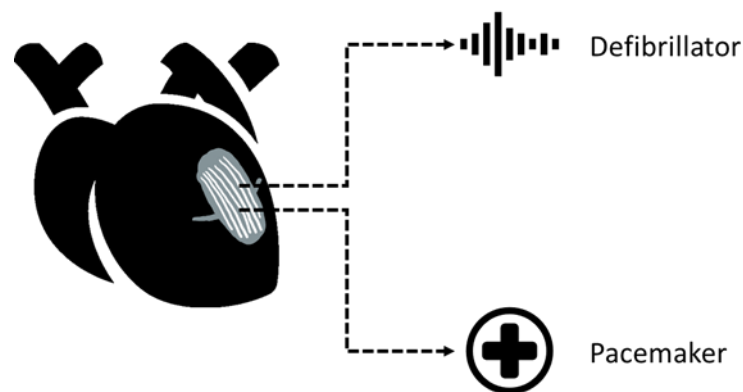


Figure 5-3 PEHs applications on heart to power defibrillator and pacemaker

On the other hand, the printed piezoelectric material can be used for bone or tissue healing detection. The idea is implant micro/nano-sized piezo-based sensors into patient's body (e.g. knees, ankles, etc.) and monitor the process of the healing status of injured bones and their surrounding tissues. As the tissues and bones grow, the pressure applied on the sensor changes, which provides useful information to doctors who will later decide the following treatment process for the patients. Also, by early adoption of these sensors, one can expect an early diagnose of abnormal changes in their teeth/bone density and stiffness so as to avoid diseases such as osteoporosis. Besides, such idea can

be further extended into a preventive detection of one's detrimental habits, which can be reflected by their physical movements such as gait patterns.

5.4 Wind energy industry

As it known to all, blades vibrations can be usually found during the normal operation process of one wind turbine. This phenomenon causes a power output reduction due to the loss of some kinetic energy. This situation makes PEHs innovatively applicable in wind turbines.

By introducing PEHs into the wind turbines, the wasted energy can be partially recovered to the system in two different ways. From one aspect, the PEHs can be employed on the blades of the turbine, where incoming wind can constantly apply changing bending force on the materials. Together with the vibration effect, certain amount of electricity is expected to be re-generated to the system. From another aspect, the PEHs can be implemented on the rotary axis of the turbines, where the rotary force changes continuously. Consequently, a continuously altering power could be produced. As a result, the overall performance of one wind farm is expected to increase.

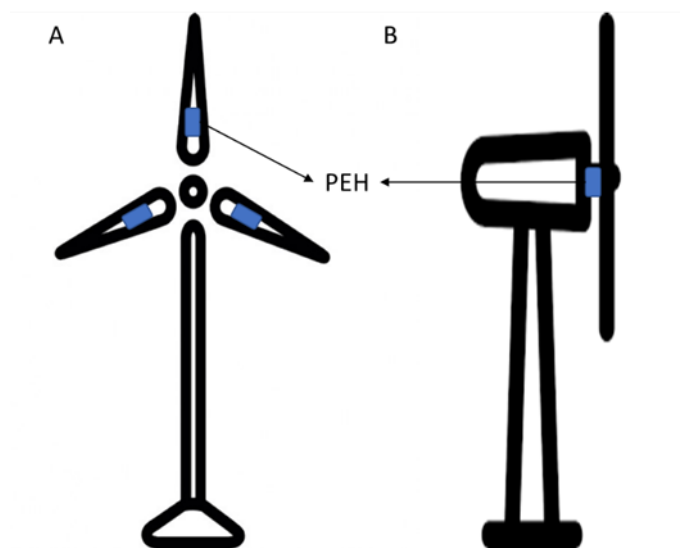


Figure 5-4 PEHs applications on wind turbines A). PEHs using bending force B). PEHs using rotary motion

Besides, as several studies have already reported the novel wind turbine design based on the piezoelectric material, a 3D printed piezoelectric turbines with shape free structure and supposedly enhanced piezoelectric property is expected to give both structural flexibility and better performance to the system.[166], [167]

5.5 Automotive industry

In terms of PEHs application in vehicles, an energy recovery system can be proposed and built up. With 3DP technology, customized shape can be designed and built up for each individual car. A schematic configuration of the designed energy recovery system can be found in Figure 5-5. The mechanism of such system is to harness the kinetic energy released by road-induced vibration. As the main body of the car moves vertically on rugged roads, the mechanical force applied between the body and the wheels varies continuously. By incorporating PEHs into cars, this constantly fluctuating mechanical force can be transformed by piezoelectric material into electrical energy, which can be used for direct consumption or for future usages. Reversely thinking, when a certain level of voltage is applied on the material, the PEHs can be utilized as auxiliary components (e.g. buffers) for car dampers in order to provide a better driving experience. As a result, a higher fuel efficiency and a smoother driving process can be obtained. In addition, as validated by some other studies, such power can be utilized for powering wireless sensors, transmitters, transducers and so on.[168], [169]

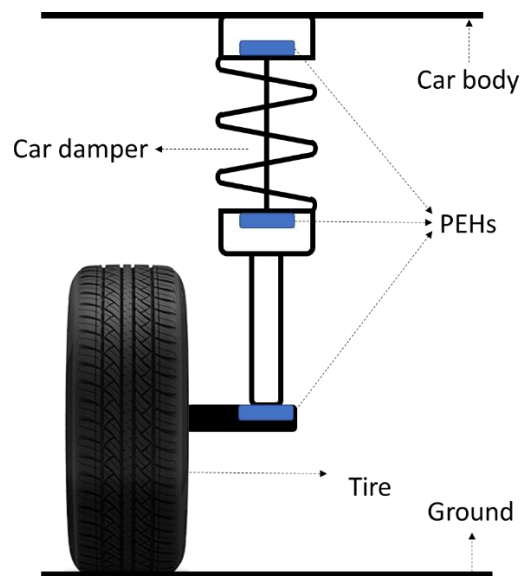


Figure 5-5 PEHs applications on automotive

CHAPTER 6. Overall conclusion

To summarize, the work load of this thesis can be divided into three phases. Firstly, a comprehensive review of 3D printing technique and its applications in energy technology was conducted. Later, a novel experiment based on piezoelectric material was devised and approached by material synthesis, computer aided design, printing pastes preparation, 3D printing and post processing. In detail, a functional hybrid energy material consisting of the barium titanate microfibers (BTMFs) fillers and the polyvinylidene fluoride (PVDF) matrix was designed and processed by a representative 3D printing technique called fuse deposition modelling (FDM). Phase composition, fibers structures, ink rheology, fibers alignment and dielectric constant were then analyzed with different solid loadings and characterized by various equipment. Through XRD, it is found out that barium titanate with single perovskite phase was successfully produced after 800 °C thermal treatment. By mixing the as-prepared barium titanate (BTO) into PVDF matrix, a hybrid material with typical BTO characteristic peaks was obtained. Through SEM, BTMFs with high-yield production and consistent size were fabricated by electrospinning and sol-gel process. By mixing the BTMFs fillers into the PVDF matrix before printing, a high degree of well-distributed fibers with clear alignment was obtained in the 3D object. Through dielectric test, the electrical response of the designed material was analyzed. Specifically, the hybrid composite with 25 vol % BTMFs loading demonstrates a high dielectric constant in the perpendicular direction of around 31 at the frequency of 1 kHz and around 26 at the frequency of 10 kHz at room temperature while the same test from pure PVDF material only has an according value of 11 and 10, respectively. Although only dielectric properties are tested in the characterization, the piezoelectric performance of such hybrid material is also expected to be improved. These characteristics represent a stepping stone towards the wide application of 3D printing in energy technology of the future. A potential application analysis of the prepared functional materials was therefore conducted. It is found out that the shape free BTMFs/PVDF composite can be utilized in several industries, ranging from energy storage, smart shoes and microbatteries in the medical sector to kinetic energy recovery system in renewable energy and automobile industry.

As a result, it is believed that the 3D printing provides great opportunities for the development of advanced functional materials. Apart from enabling complex geometrical processability, this technology can give additional functionalities to energy devices. The experimental work uncovers a new pathway for the manufacturing of high-performance energy material based on flexible piezoelectric composite that have promising applications in future energy harvesting and sensing technologies.

CHAPTER 7. Future work

Although works have been done on a successful manufacturing of three-dimensional dielectric material with controllable microfiber alignment and high dielectric constant, some significant workload can be identified and done in the future.

First of all, as shown in the rheology test, the printing work was conducted in a non-optimized condition. It was witnessed that some of the printed material tend to splash after extruding. They failed to maintain its designed structure and lost the desired property within a short period. Even though this problem was temporarily settled by the variation of the printing pressure, it is suggested to solve this issue from a fundamental point of view by modifying the rheology of the ink similar to the reference gel's and using different size of needles to change printing shear rate. As such, the printability and probably the dielectric constant of the object could be improved.

Secondly, it will be interesting to evaluate the degree of fiber alignment at a three-dimensional level, which can be done by a usage of focused ion beam (FIB) SEM. As the observation of the material from its top view and cross-sectional view can be simultaneously conducted, it will be possible inspect the printed material at a solid level rather than a surface level. The result will be helpful for understanding and maybe predicting the potential performance of the product.

In addition, a more detailed variation of filler loadings in printing ink should be studied to define a larger range of possible loadings and to identify the specific loading with best testing result. Afterwards, the piezoelectric test of the material should be conducted to validate the assumption of piezoelectric performance enhancement. Moreover, it will be meaningful to construct a structure with more complex shape and test its performance on the proposed real-life applications.

CHAPTER 8. References

- [1] BP Global, *BP Statistical Review of World Energy*, 67th ed. BP Global, 2018.
- [2] World Energy Council, “World Energy Resources,” @WECouncil, vol. 2007, pp. 1–1028, 2016.
- [3] E. A. Rosa, G. E. Machlis, and K. M. Keating, “Energy and Society,” *Annual Review of Sociology*, vol. 14. Annual Reviews, pp. 149–172.
- [4] S. Suman, “Hybrid nuclear-renewable energy systems: A review,” *J. Clean. Prod.*, vol. 181, pp. 166–177, Apr. 2018.
- [5] W. Ma, X. Xue, and G. Liu, “Techno-economic evaluation for hybrid renewable energy system: Application and merits,” *Energy*, vol. 159, pp. 385–409, Sep. 2018.
- [6] S. Guo, Q. Liu, J. Sun, and H. Jin, “A review on the utilization of hybrid renewable energy,” *Renew. Sustain. Energy Rev.*, vol. 91, pp. 1121–1147, Aug. 2018.
- [7] N. Scarlat, J.-F. Dallemand, F. Monforti-Ferrario, M. Banja, and V. Motola, “Renewable energy policy framework and bioenergy contribution in the European Union – An overview from National Renewable Energy Action Plans and Progress Reports,” *Renew. Sustain. Energy Rev.*, vol. 51, pp. 969–985, Nov. 2015.
- [8] S. A. M. Tofail, E. P. Koumoulos, A. Bandyopadhyay, S. Bose, L. O’Donoghue, and C. Charitidis, “Additive manufacturing: scientific and technological challenges, market uptake and opportunities,” *Mater. Today*, vol. 21, no. 1, pp. 22–37, 2018.
- [9] H. Shao, L. He, H. Lin, and H.-W. Li, “Progress and Trends in Magnesium-Based Materials for Energy-Storage Research: A Review,” *Energy Technol.*, vol. 6, no. 3, pp. 445–458, Mar. 2018.
- [10] V. J. L. Vouldis I, Millet P, “Novel materials for energy applications,” Brussels, 2008.
- [11] Z. Abdmouleh, R. A. M. Alammari, and A. Gastli, “Review of policies encouraging renewable energy integration & best practices,” *Renew. Sustain. Energy Rev.*, vol. 45, pp. 249–262, May 2015.
- [12] T. M. Letcher, *Storing energy: with special reference to renewable energy sources*. Elsevier, 2016.
- [13] F. Zhang *et al.*, “3D printing technologies for electrochemical energy storage,” *Nano Energy*, vol. 40, no. May, pp. 418–431, Oct. 2017.
- [14] A. C. Luna, N. L. Diaz, M. Graells, J. C. Vasquez, and J. M. Guerrero, “Cooperative energy management for a cluster of households prosumers,” *IEEE Trans. Consum. Electron.*, vol. 62, no. 3, pp. 235–242, Aug. 2016.

- [15] B. C. Gross, J. L. Erkal, S. Y. Lockwood, C. Chen, and D. M. Spence, "Evaluation of 3D printing and its potential impact on biotechnology and the chemical sciences," *Anal. Chem.*, vol. 86, no. 7, pp. 3240–3253, 2014.
- [16] T. D. Ngo, A. Kashani, G. Imbalzano, K. T. Q. Nguyen, and D. Hui, "Additive manufacturing (3D printing): A review of materials, methods, applications and challenges," *Compos. Part B Eng.*, vol. 143, no. December 2017, pp. 172–196, Jun. 2018.
- [17] M. Kamran and A. Saxena, "A Comprehensive Study on 3D Printing Technology," *MIT Int. J. Mech. Eng.*, vol. 6, no. August 2016, pp. 63–69, 2016.
- [18] S. Ford and M. Despeisse, "Additive manufacturing and sustainability: an exploratory study of the advantages and challenges," *J. Clean. Prod.*, vol. 137, pp. 1573–1587, 2016.
- [19] A. Zhakeyev, P. Wang, L. Zhang, W. Shu, H. Wang, and J. Xuan, "Additive Manufacturing: Unlocking the Evolution of Energy Materials," *Adv. Sci.*, vol. 1700187, p. 1700187, 2017.
- [20] Ernst & Young Gmbh (EY), "How Will 3D Printing Make Your Company the Strongest Link in the Value Chain? - EY's Global 3D printing Report 2016," *Ernst Young Gmbh*, pp. 1–26, 2016.
- [21] J. C. Ruiz-Morales *et al.*, "Three dimensional printing of components and functional devices for energy and environmental applications," *Energy Environ. Sci.*, vol. 10, no. 4, pp. 846–859, Apr. 2017.
- [22] H. Tokoro *et al.*, "External stimulation-controllable heat-storage ceramics," *Nat. Commun.*, vol. 6, no. 1, p. 7037, Dec. 2015.
- [23] V. Kronhardt *et al.*, "High-temperature Thermal Storage System for Solar Tower Power Plants with Open-volumetric Air Receiver Simulation and Energy Balancing of a Discretized Model," *Energy Procedia*, vol. 49, pp. 870–877, Jan. 2014.
- [24] I. Grinberg *et al.*, "Perovskite oxides for visible-light-absorbing ferroelectric and photovoltaic materials," *Nature*, vol. 503, no. 7477, pp. 509–512, Nov. 2013.
- [25] International Organization for Standardization, "ISO/ASTM 52900:2015 - Additive manufacturing -- General principles -- Terminology," 2015. [Online]. Available: <https://www.iso.org/standard/69669.html>. [Accessed: 18-Jul-2018].
- [26] K. Fu, Y. Yao, J. Dai, and L. Hu, "Progress in 3D Printing of Carbon Materials for Energy-Related Applications," *Adv. Mater.*, vol. 29, no. 9, 2017.
- [27] Z. Zhou, I. Salaoru, P. Morris, and G. J. Gibbons, "Development of a direct feed fused deposition modelling technology for multi-material manufacturing," *AIP Conf. Proc.*, vol. 1769, no. 2016, 2016.
- [28] D. Espalin, J. Ramirez, F. Medina, and R. Wicker, "Multi-Material, Multi-Technology FDM System," *Proc. Solid Free. Fabr. Symp. Work.*, pp. 828–835, 2012.
- [29] R. Jones *et al.*, "Reprap - The replicating rapid prototyper," *Robotica*, vol. 29, no. 1 SPEC. ISSUE, pp. 177–191, 2011.

- [30] Modellus, “Resolution and Tolerance comparison - 3D Printing - Talk Manufacturing,” *3D Hubs*, 2016. [Online]. Available: <https://www.3dhubs.com/talk/t/resolution-and-tolerance-comparison/7982/2>. [Accessed: 17-Aug-2018].
- [31] F. Grieser, “What Resolution Can 3D Printers Print?,” *All3DP*, 2015. [Online]. Available: <https://all3dp.com/3d-printer-resolution/>. [Accessed: 17-Aug-2018].
- [32] 3D printing from scratch, “Types of 3D printers or 3D printing technologies overview | 3D Printing from scratch.” [Online]. Available: <http://3dprintingfromscratch.com/common/types-of-3d-printers-or-3d-printing-technologies-overview/>. [Accessed: 08-Aug-2018].
- [33] R. B. Wicker and E. W. MacDonald, “Multi-material, multi-technology stereolithography: This feature article covers a decade of research into tackling one of the major challenges of the stereolithography technique, which is including multiple materials in one construct,” *Virtual Phys. Prototyp.*, vol. 7, no. 3, pp. 181–194, 2012.
- [34] R. B. Wicker and E. W. MacDonald, “Multi-material, multi-technology stereolithography,” *Virtual Phys. Prototyp.*, vol. 7, no. 3, pp. 181–194, Sep. 2012.
- [35] M. Molitch-Hou, “Overview of additive manufacturing process,” *Addit. Manuf.*, pp. 1–38, Jan. 2018.
- [36] R. Xie and D. Li, “Research on the curing performance of UV-LED light based stereolithography,” *Opt. Laser Technol.*, vol. 44, no. 4, pp. 1163–1171, Jun. 2012.
- [37] 3D Systems Inc, “3D Systems ProJet SLA 6000 3D printers.” [Online]. Available: <https://www.3dsystems.com/3d-printers/projet-6000-hd>. [Accessed: 08-Aug-2018].
- [38] 3D Hubs, “2018 Best 3D Printer Guide,” 2018. [Online]. Available: <https://www.3dhubs.com/best-3d-printer-guide>. [Accessed: 08-Aug-2018].
- [39] DOE/LAWRENCE LIVERMORE NATIONAL LABORATORY, “LLNL researchers develop high-quality 3-D metal parts using additive manufacturing | EurekAlert! Science News,” *The global source for science news*, 2014. [Online]. Available: https://www.eurekalert.org/pub_releases/2014-06/dlnl-lrd061614.php. [Accessed: 17-Jul-2018].
- [40] S. Sun, M. Brandt, and M. Easton, *Powder bed fusion processes: An overview*. Elsevier Ltd, 2016.
- [41] Wikipedia, “Selective laser melting,” 2018. [Online]. Available: https://en.wikipedia.org/wiki/Selective_laser_melting. [Accessed: 17-Jul-2018].
- [42] Wikipedia, “Selective laser sintering,” 2018. [Online]. Available: https://en.wikipedia.org/wiki/Selective_laser_sintering. [Accessed: 17-Jul-2018].
- [43] C. Y. Yap *et al.*, “Review of selective laser melting: Materials and applications,” *Appl. Phys. Rev.*, vol. 2, no. 4, p. 041101, Dec. 2015.
- [44] Kevin Eckes, “How multi-powder deposition will transform industrial 3D printing,” *Aerosint SA*, 2018. [Online]. Available:

- <https://medium.com/@aerosint/how-multi-powder-deposition-will-transform-industrial-3d-printing-fa7c83631091>. [Accessed: 17-Jul-2018].
- [45] V. Bhavar, P. Kattire, V. Patil, S. Khot, K. Gujar, and R. Singh, “A review on powder bed fusion technology of metal additive manufacturing,” in *4th International conference and exhibition on Additive Manufacturing Technologie*, 2014, no. April 2016.
- [46] Dragonator, “Focus SLS printer,” *Thingiverse*, 2013. [Online]. Available: <https://www.thingiverse.com/thing:33697/#instructions>. [Accessed: 08-Aug-2018].
- [47] Additively, “Material Jetting,” 2018. [Online]. Available: <https://www.additively.com/en/learn-about/material-jetting>. [Accessed: 17-Jul-2018].
- [48] I. Gibson, D. Rosen, and B. Stucker, *Additive Manufacturing Technologies*. 2015.
- [49] J. Y. Lee, J. An, and C. K. Chua, “Fundamentals and applications of 3D printing for novel materials,” *Appl. Mater. Today*, vol. 7, pp. 120–133, 2017.
- [50] J. Kechagias, P. Stavropoulos, A. Koutsomichalis, I. Ntintakis, and N. Vaxevanidis, “Dimensional Accuracy Optimization of Prototypes produced by PolyJet Direct 3D Printing Technology,” *2014 Int. Conf. Ind. Eng. (INDE '14)*, no. December, pp. 61–65, 2014.
- [51] J. M. Lee, M. Zhang, and W. Y. Yeong, “Characterization and evaluation of 3D printed microfluidic chip for cell processing,” *Microfluid. Nanofluidics*, vol. 20, no. 1, p. 5, Jan. 2016.
- [52] H. Yang *et al.*, “Performance evaluation of ProJet multi-material jetting 3D printer,” *Virtual Phys. Prototyp.*, vol. 12, no. 1, pp. 95–103, Jan. 2017.
- [53] A. M. R. G. Loughborough University, “Sheet Lamination | Additive Manufacturing Research Group | Loughborough University.” [Online]. Available: <http://www.lboro.ac.uk/research/amrg/about/the7categoriesofadditivemanufacturing/sheetlamination/>. [Accessed: 24-Jul-2018].
- [54] Elizabeth Engler Modic, “Directed energy deposition (DED) vs powder bed fusion (PBF) - Aerospace Manufacturing and Design,” *Aerospace manufacturing and design*, 2018. [Online]. Available: <http://www.aerospacemanufacturinganddesign.com/article/optomec-directed-energy-versus-powder-bed-070318/>. [Accessed: 24-Jul-2018].
- [55] Y. Ni, R. Ji, K. Long, T. Bu, K. Chen, and S. Zhuang, “A review of 3D-printed sensors,” *Appl. Spectrosc. Rev.*, vol. 52, no. 7, pp. 623–652, 2017.
- [56] 3DCeram, “CERAMAKER, turnkey line for 3D printing,” *3DCeram*, 2018. [Online]. Available: <http://3dceram.com/ligne-cle-main-limpression-3d/imprimantes-equipements-limpression-3d/>. [Accessed: 13-Aug-2018].
- [57] Stephen Mraz, “Hybridized 3D-Printed Part Combines Plastic and Metal,” *Machine design*, 2014. [Online]. Available: <https://www.machinedesign.com/3d-printing/hybridized-3d-printed-part-combines-plastic-and-metal>. [Accessed: 08-

- Aug-2018].
- [58] Cell3Ditor, “New CERAMAKER hybrid 3D printer (from 3DCERAM) employed for the Cell3Ditor project -,” *Youtube*, 2018. [Online]. Available: <https://www.youtube.com/watch?v=TLB0iEvKjAQ>. [Accessed: 17-Aug-2018].
- [59] C. Bounioux, E. A. Katz, and R. Yerushalmi - Rozen, “Conjugated polymers - carbon nanotubes-based functional materials for organic photovoltaics: A critical review,” *Polym. Adv. Technol.*, vol. 23, no. 8, pp. 1129–1140, 2012.
- [60] Eva Bundgaard, “Polymer solar cells,” *Plasticphotovoltaics org*. [Online]. Available: <http://plasticphotovoltaics.org/lc/lc-polymersolarcells.html>. [Accessed: 18-Jul-2018].
- [61] S. Xiao, Q. Zhang, and W. You, “Molecular Engineering of Conjugated Polymers for Solar Cells: An Updated Report,” *Adv. Mater.*, vol. 29, no. 20, p. 1601391, May 2017.
- [62] Z. Wu *et al.*, “n-Type Water/Alcohol-Soluble Naphthalene Diimide-Based Conjugated Polymers for High-Performance Polymer Solar Cells,” *J. Am. Chem. Soc.*, vol. 138, no. 6, pp. 2004–2013, Feb. 2016.
- [63] F. Bella *et al.*, “Improving efficiency and stability of perovskite solar cells with photocurable fluoropolymers,” *Science (80-.)*, vol. 354, no. 6309, pp. 203–206, Oct. 2016.
- [64] B. Peng and J. Chen, “Functional materials with high-efficiency energy storage and conversion for batteries and fuel cells,” *Coord. Chem. Rev.*, vol. 253, no. 23–24, pp. 2805–2813, Dec. 2009.
- [65] Y. Liang *et al.*, “Co₃O₄ nanocrystals on graphene as a synergistic catalyst for oxygen reduction reaction,” *Nat. Mater.*, vol. 10, no. 10, pp. 780–786, Oct. 2011.
- [66] C. Wang *et al.*, “Multimetallic Au/FePt₃ Nanoparticles as Highly Durable Electrocatalyst,” *Nano Lett.*, vol. 11, no. 3, pp. 919–926, Mar. 2011.
- [67] T. U. Daim, E. Bayraktaroglu, J. Estep, D. J. Lim, J. Upadhyay, and J. Yang, “Optimizing the NW off-shore wind turbine design,” *Math. Comput. Model.*, vol. 55, no. 3–4, pp. 396–404, Feb. 2012.
- [68] T. Bauer, N. Breidenbach, N. Pfleger, D. Laing, and M. Eck, “OVERVIEW OF MOLTEN SALT STORAGE SYSTEMS AND MATERIAL DEVELOPMENT FOR SOLAR THERMAL POWER PLANTS.”
- [69] N. Breidenbach, C. Martin, H. Jockenhöfer, and T. Bauer, “Thermal Energy Storage in Molten Salts: Overview of Novel Concepts and the DLR Test Facility TESIS,” *Energy Procedia*, vol. 99, pp. 120–129, Nov. 2016.
- [70] M. Liu *et al.*, “Review on concentrating solar power plants and new developments in high temperature thermal energy storage technologies,” *Renew. Sustain. Energy Rev.*, vol. 53, pp. 1411–1432, Jan. 2016.
- [71] F. Cheng, J. Liang, Z. Tao, and J. Chen, “Functional materials for rechargeable batteries,” *Adv. Mater.*, vol. 23, no. 15, pp. 1695–1715, 2011.
- [72] K. Kang, “Electrodes with High Power and High Capacity for Rechargeable Lithium Batteries,” *Science (80-.)*, vol. 311, no. 5763, pp. 977–980, Feb. 2006.

- [73] G. Zhou *et al.*, “Fibrous Hybrid of Graphene and Sulfur Nanocrystals for High-Performance Lithium–Sulfur Batteries,” *ACS Nano*, vol. 7, no. 6, pp. 5367–5375, Jun. 2013.
- [74] S. Braun, G. Micard, and G. Hahn, “Solar cell improvement by using a multi busbar design as front electrode,” *Energy Procedia*, vol. 27, pp. 227–233, 2012.
- [75] A. V. Malevskaya, D. A. Malevski, and N. D. I. Ioffe, “Related content Optimizing back surface field for improving Voc of (Al)GaInP solar cell Influence of GaInP ordering on the performance of GaInP solar cells Effect of bus-bar material and configuration on the efficiency of GaInP/GaAs/Ge solar cells,” *J. Phys.*, 2016.
- [76] N. Cheng *et al.*, “Application of mesoporous SiO₂ layer as an insulating layer in high performance hole transport material free CH₃NH₃PbI₃ perovskite solar cells,” *J. Power Sources*, vol. 321, pp. 71–75, Jul. 2016.
- [77] Jessica Shapiro, “Ceramic Bearings Save Energy, Extend Life,” *Machine design*, 2009. [Online]. Available: <https://www.machinedesign.com/bearings/ceramic-bearings-save-energy-extend-life>. [Accessed: 16-Aug-2018].
- [78] P. Simon and Y. Gogotsi, “Materials for electrochemical capacitors,” *Nat. Mater.*, vol. 7, no. 11, pp. 845–854, Nov. 2008.
- [79] T. Song, “Graphene-Tapered ZnO Nanorods Array as a Flexible Antireflection Layer,” *J. Nanomater.*, vol. 2015, pp. 1–6, Oct. 2015.
- [80] M. Liu, C. Zhang, and W. Chen, “Novel Nanomaterials as Electrocatalysts for Fuel Cells,” *Nanomater. Green Energy*, pp. 169–204, Jan. 2018.
- [81] Claudionico, “Schematic representation of the different stages and routes of the sol-gel technology,” *Wikimedia*, 2013. [Online]. Available: <https://commons.wikimedia.org/w/index.php?curid=29869440>. [Accessed: 17-Aug-2018].
- [82] C. J. Brinker and G. W. Scherer, *The Physics and Chemistry of Sol–Gel Processing*, 1st ed. Academic Press, 1990.
- [83] A. Dehghanhadikolaie, J. Ansary, and R. Ghoreishi, “Sol-gel process applications : A mini-review,” *Proc. Nat. Res. Soc.*, vol. 2, no. 02008, 2018.
- [84] L. C. Klein, “Opportunities for sol-gel materials in fuel cells,” Rutgers, 2002.
- [85] N. Phatharapeetranun, B. Ksapabutr, D. Marani, J. R. Bowen, and V. Esposito, “3D-printed barium titanate/poly-(vinylidene fluoride) nano-hybrids with anisotropic dielectric properties,” *J. Mater. Chem. C*, vol. 5, no. 47, pp. 12430–12440, 2017.
- [86] Q. Guo, D. Zhao, S. Liu, S. Chen, M. Hanif, and H. Hou, “Free-standing nitrogen-doped carbon nanotubes at electrospun carbon nanofibers composite as an efficient electrocatalyst for oxygen reduction,” *Electrochim. Acta*, vol. 138, pp. 318–324, Aug. 2014.
- [87] X. Chen, S. Xu, N. Yao, and Y. Shi, “1.6 V Nanogenerator for Mechanical Energy Harvesting Using PZT Nanofibers,” *Nano Lett.*, vol. 10, no. 6, pp. 2133–2137, Jun. 2010.

- [88] N. Kannan and D. Vakeesan, "Solar energy for future world: - A review," *Renew. Sustain. Energy Rev.*, vol. 62, pp. 1092–1105, Sep. 2016.
- [89] A. Knott, O. Makarovskiy, J. O'Shea, Y. Wu, and C. Tuck, "Scanning photocurrent microscopy of 3D printed light trapping structures in dye-sensitized solar cells," *Sol. Energy Mater. Sol. Cells*, vol. 180, pp. 103–109, Jun. 2018.
- [90] L. Van Dijk, E. A. P. Marcus, A. J. Oostra, R. E. I. Schropp, and M. Di Vece, "3D-printed concentrator arrays for external light trapping on thin film solar cells," *Sol. Energy Mater. Sol. Cells*, vol. 139, pp. 19–26, Aug. 2015.
- [91] X. Lin *et al.*, "Inkjet-printed CZTSSe absorbers and influence of sodium on device performance," *Sol. Energy Mater. Sol. Cells*, vol. 180, pp. 373–380, Jun. 2018.
- [92] M. Bag, Z. Jiang, L. A. Renna, S. P. Jeong, V. M. Rotello, and D. Venkataraman, "Rapid combinatorial screening of inkjet-printed alkyl-ammonium cations in perovskite solar cells," *Mater. Lett.*, vol. 164, pp. 472–475, Feb. 2016.
- [93] Lucie Gaget, "3D printed solar panels: Meet the revolution," *Sculpteo*, 2018. [Online]. Available: <https://www.sculpteo.com/blog/2018/01/24/3d-printed-solar-panels-meet-the-renewable-energy-revolution/>. [Accessed: 08-Aug-2018].
- [94] I. 2008. Industrial Technologies Program Prepared by BCS, "Waste Heat Recovery: Technology and Opportunities in U.S. Industry," 2008.
- [95] J. D. Koenig, "Next step in manufacturing," *Nat. Energy*, vol. 3, no. 4, pp. 259–260, 2018.
- [96] R. Ahiska and H. Mamur, "A review: Thermoelectric generators in renewable energy," *Int. J. Renew. Energy Res.*, vol. 4, no. 1, pp. 128–136, 2014.
- [97] Alphabet energy, "How Thermoelectric Generators Work - Alphabet Energy," *Alphabet Energy, Inc.*, 2018. [Online]. Available: <https://www.alphabetenergy.com/how-thermoelectrics-work/>. [Accessed: 08-Jul-2018].
- [98] D. Champier, "Thermoelectric generators: A review of applications," *Energy Convers. Manag.*, vol. 140, pp. 167–181, 2017.
- [99] D. Patel and P. S. B. Mehta, "Review of Thermoelectricity to Improve Energy Quality," *Int. J. Emerg. Technol. Innov. Res.*, vol. 2, no. 3, p. 847, 2015.
- [100] Otego GmbH, "Thermoelectric Generators (TEG) for Energy Harvesting Applications | otego," 2018. [Online]. Available: <https://www.otego.de/en/>. [Accessed: 09-Jul-2018].
- [101] OTEGO GmbH, "Microenergy Supply without Battery and Cable," *KIT press release*, no. 036, Karlsruhe, pp. 1–3, 05-Apr-2018.
- [102] Christian Müller, "Woven and 3D-Printed Thermoelectric Textiles," Göteborg, 1, 2015.
- [103] European Research Council, "3D printing wearable thermoelectric textiles," Göteborg, 1, 2015.
- [104] M. He, Y. Zhao, B. Wang, Q. Xi, J. Zhou, and Z. Liang, "3D Printing Fabrication

- of Amorphous Thermoelectric Materials with Ultralow Thermal Conductivity,” *Small*, vol. 11, no. 44, pp. 5889–5894, 2015.
- [105] J. Wang, H. Li, R. Liu, L. Li, Y. H. Lin, and C. W. Nan, “Thermoelectric and mechanical properties of PLA/Bi_{0.5}Sb_{1.5}Te₃ composite wires used for 3D printing,” *Compos. Sci. Technol.*, vol. 157, pp. 1–9, 2018.
- [106] F. Kim *et al.*, “3D printing of shape-conformable thermoelectric materials using all-inorganic Bi₂Te₃-based inks,” *Nat. Energy*, vol. 3, no. 4, pp. 301–309, 2018.
- [107] N. Han, D. Zhao, J. U. Schluter, E. S. Goh, H. Zhao, and X. Jin, “Performance evaluation of 3D printed miniature electromagnetic energy harvesters driven by air flow,” *Appl. Energy*, vol. 178, pp. 672–680, 2016.
- [108] Z. Zhang *et al.*, “A miniature airflow energy harvester from piezoelectric materials Related content Packaging strategy for maximizing the performance of a screen printed piezoelectric energy harvester A miniature airflow energy harvester from piezoelectric materials,” *J. Phys. Conf. Ser. OPEN ACCESS*, 2013.
- [109] ALEKSANDRA STANISLAWSKA, “Printed wind turbine - Poland.pl,” *Polska*, 2014. [Online]. Available: <https://polska.pl/science/achievements-science/printed-wind-turbine/>. [Accessed: 14-Aug-2018].
- [110] Jon Fingas, “3D-printed wind turbine puts 300W of power in your backpack,” *Engadget*, 2014. [Online]. Available: <https://www.engadget.com/2014/08/17/airenergy-3d-wind-turbine/?guccounter=1>. [Accessed: 14-Aug-2018].
- [111] X. Tian, J. Jin, S. Yuan, C. K. Chua, S. B. Tor, and K. Zhou, “Emerging 3D-Printed Electrochemical Energy Storage Devices: A Critical Review,” *Adv. Energy Mater.*, vol. 7, no. 17, pp. 1–17, 2017.
- [112] J. H. Pikul, H. Gang Zhang, J. Cho, P. V Braun, and W. P. King, “High-power lithium ion microbatteries from interdigitated three-dimensional bicontinuous nanoporous electrodes,” *Nat. Commun.*, vol. 4, p. 1732, May 2013.
- [113] H. Zhang, X. Yu, and P. V. Braun, “Three-dimensional bicontinuous ultrafast-charge and -discharge bulk battery electrodes,” *Nat. Nanotechnol.*, vol. 6, no. 5, pp. 277–281, May 2011.
- [114] J. Liu *et al.*, “High Volumetric Capacity Three-Dimensionally Sphere-Caged Secondary Battery Anodes,” *Nano Lett.*, vol. 16, no. 7, pp. 4501–4507, Jul. 2016.
- [115] S. Ferrari, M. Loveridge, S. D. Beattie, M. Jahn, R. J. Dashwood, and R. Bhagat, “Latest advances in the manufacturing of 3D rechargeable lithium microbatteries,” *J. Power Sources*, vol. 286, pp. 25–46, 2015.
- [116] K. Sun, T. S. Wei, B. Y. Ahn, J. Y. Seo, S. J. Dillon, and J. A. Lewis, “3D printing of interdigitated Li-ion microbattery architectures,” *Adv. Mater.*, vol. 25, no. 33, pp. 4539–4543, 2013.
- [117] K. Fu *et al.*, “Graphene Oxide-Based Electrode Inks for 3D-Printed Lithium-Ion Batteries,” *Adv. Mater.*, vol. 28, no. 13, pp. 2587–2594, 2016.
- [118] C. W. Foster *et al.*, “3D Printed Graphene Based Energy Storage Devices,” *Sci.*

- Rep.*, vol. 7, no. October 2016, pp. 1–11, 2017.
- [119] J. Hu *et al.*, “3D-Printed Cathodes of $\text{LiMn}_{1-x}\text{Fe}_x\text{PO}_4$ Nanocrystals Achieve Both Ultrahigh Rate and High Capacity for Advanced Lithium-Ion Battery,” *Adv. Energy Mater.*, vol. 6, no. 18, pp. 1–8, 2016.
- [120] Santiago Miret, “Storage Wars: Batteries vs. Supercapacitors | BERC,” *Berkeley Energy & Resources Collaborative*, 2013. [Online]. Available: <http://berc.berkeley.edu/storage-wars-batteries-vs-supercapacitors/>. [Accessed: 21-Jun-2018].
- [121] C. Zhu *et al.*, “Supercapacitors Based on Three-Dimensional Hierarchical Graphene Aerogels with Periodic Macropores,” *Nano Lett.*, vol. 16, no. 6, pp. 3448–3456, 2016.
- [122] Y. Yao *et al.*, “Three-Dimensional Printable High-Temperature and High-Rate Heaters,” *ACS Nano*, vol. 10, no. 5, pp. 5272–5279, 2016.
- [123] Y. Chen *et al.*, “Ultra-fast self-assembly and stabilization of reactive nanoparticles in reduced graphene oxide films,” *Nat. Commun.*, vol. 7, pp. 1–9, 2016.
- [124] FuelCellToday, “FCT - Fuel Cell Technologies - SOFC,” *FuelCellToday*, 2018. [Online]. Available: <http://www.fuelcelltoday.com/technologies/sofc>. [Accessed: 11-Jul-2018].
- [125] M. R. Weimar, L. A. Chick, D. W. Gotthold, and G. A. Whyatt, “Cost Study for Manufacturing of Solid Oxide Fuel Cell Power Systems,” no. September, p. 50, 2013.
- [126] C. Li, H. Shi, R. Ran, C. Su, and Z. Shao, “Thermal inkjet printing of thin-film electrolytes and buffering layers for solid oxide fuel cells with improved performance,” *Int. J. Hydrogen Energy*, vol. 38, no. 22, pp. 9310–9319, Jul. 2013.
- [127] R. I. Tomov *et al.*, “Direct ceramic inkjet printing of yttria-stabilized zirconia electrolyte layers for anode-supported solid oxide fuel cells,” *J. Power Sources*, vol. 195, no. 21, pp. 7160–7167, Nov. 2010.
- [128] V. Esposito *et al.*, “Fabrication of thin yttria-stabilized-zirconia dense electrolyte layers by inkjet printing for high performing solid oxide fuel cells,” *J. Power Sources*, vol. 273, pp. 89–95, Jan. 2015.
- [129] C. Wang, S. C. Hopkins, R. I. Tomov, R. V. Kumar, and B. A. Glowacki, “Optimisation of CGO suspensions for inkjet-printed SOFC electrolytes,” *J. Eur. Ceram. Soc.*, vol. 32, no. 10, pp. 2317–2324, Aug. 2012.
- [130] N. Yashiro, T. Usui, and K. Kikuta, “Application of a thin intermediate cathode layer prepared by inkjet printing for SOFCs,” *J. Eur. Ceram. Soc.*, vol. 30, no. 10, pp. 2093–2098, Aug. 2010.
- [131] A. M. Suresh *et al.*, “Aerosol Jet Printing and Microstructure of SOFC Electrolyte and Cathode Layers,” *Electrochem. Soc.*, vol. 35, no. 1, pp. 2151–2160, 2011.
- [132] CELL3DITOR, “COST-EFFECTIVE AND FLEXIBLE 3D PRINTED SOFC

- STACKS FOR COMMERCIAL APPLICATIONS,” 2016. [Online]. Available: <https://www.fch.europa.eu/project/cost-effective-and-flexible-3d-printed-sofc-stacks-commercial-applications>. [Accessed: 11-Jul-2018].
- [133] A. Tarancón, “Development of cost effective manufacturing technologies for key components or fuel cell systems,” *Fuel Cells Bull.*, no. 10, p. 12, Oct. 2016.
- [134] CELL3DITOR, “About CELL3DITOR,” *CELL3DITOR*, 2018. [Online]. Available: <http://www.cell3ditor.eu/about/>. [Accessed: 17-Aug-2018].
- [135] Y. Xu *et al.*, *The Boom in 3D-Printed Sensor Technology*, vol. 17, no. 6. 2017.
- [136] S.-Z. Guo, X. Yang, M.-C. Heuzey, and D. Therriault, “3D printing of a multifunctional nanocomposite helical liquid sensor,” *Nanoscale Commun. Cite this Nanoscale*, vol. 7, p. 6451, 2015.
- [137] F. Salamone, L. Belussi, L. Danza, M. Ghellere, and I. Meroni, “Design and development of nEMoS, an all-in-one, low-cost, web-connected and 3D-printed device for environmental analysis,” *Sensors (Basel)*, vol. 15, no. 6, pp. 13012–27, Jun. 2015.
- [138] Z. Chen *et al.*, “3D printing of piezoelectric element for energy focusing and ultrasonic sensing,” *Nano Energy*, vol. 27, no. December 2017, pp. 78–86, 2016.
- [139] D. I. Woodward, C. P. Purssell, D. R. Billson, D. A. Hutchins, and S. J. Leigh, “Additively-manufactured piezoelectric devices,” *Phys. Status Solidi Appl. Mater. Sci.*, vol. 212, no. 10, pp. 2107–2113, 2015.
- [140] E. Suaste-Gómez, G. Rodríguez-Roldán, H. Reyes-Cruz, and O. Terán-Jiménez, “Developing an Ear Prosthesis Fabricated in Polyvinylidene Fluoride by a 3D Printer with Sensory Intrinsic Properties of Pressure and Temperature,” *Sensors (Basel)*, vol. 16, no. 3, Mar. 2016.
- [141] K. S. Ramadan, D. Sameoto, and S. Evoy, “A review of piezoelectric polymers as functional materials for electromechanical transducers,” *Smart Mater. Struct.*, vol. 23, no. 3, p. 033001, Mar. 2014.
- [142] Y. Zhang *et al.*, “PVDF–PZT nanocomposite film based self-charging power cell,” *Nanotechnology*, vol. 25, no. 10, p. 105401, Mar. 2014.
- [143] H. Kim, F. Torres, D. Villagran, C. Stewart, Y. Lin, and T.-L. L. B. Tseng, “3D Printing of BaTiO₃/PVDF Composites with Electric In Situ Poling for Pressure Sensor Applications,” *Macromol. Mater. Eng.*, vol. 302, no. 11, pp. 1–6, Nov. 2017.
- [144] Y. C. Li, S. C. Tjong, and R. K. Y. Li, “Dielectric properties of binary polyvinylidene fluoride/barium titanate nanocomposites and their nanographite doped hybrids,” *Express Polym. Lett.*, vol. 5, no. 6, pp. 526–534, 2011.
- [145] M. Olszowy, “Piezoelectricity and dielectric properties of PVDF/BaTiO₃ composites,” Szczyrk, 1997.
- [146] D. Ramesh, “One-step fabrication of biomimetic PVDF-BaTiO₃ nanofibrous composite using DoE,” *Mater. Res. Express*, vol. 5, no. 8, p. 85308, 2018.
- [147] J. Fu, Y. Hou, M. Zheng, Q. Wei, M. Zhu, and H. Yan, “Improving Dielectric Properties of PVDF Composites by Employing Surface Modified Strong

- Polarized BaTiO₃ Particles Derived by Molten Salt Method,” *ACS Appl. Mater. Interfaces*, vol. 7, no. 44, pp. 24480–24491, 2015.
- [148] V. Corral-Flores and D. Bueno-Baqués, “Flexible Ferroelectric BaTiO₃ – PVDF Nanocomposites,” in *Ferroelectrics - Material Aspects*, V. Corral-Flores and D. Bueno-Baqués, Eds. Mexico: InTech, 2009, p. 518.
- [149] H. Kim, T. Fernando, M. Li, Y. Lin, and T.-L. B. Tseng, “Fabrication and characterization of 3D printed BaTiO₃ /PVDF nanocomposites,” *J. Compos. Mater.*, p. 002199831770470, 2017.
- [150] V. Corral-Flores, D. Bueno-Baqués, and R. F. Ziolo, “Hybrid BaTiO₃-PVDF Piezoelectric Composites for Vibration Energy Harvesting Applications,” *MRS Proc.*, vol. 1325, pp. 3–7, 2011.
- [151] 3DPrinting.com, “INKREDIBLE – The Most Cost Effective Desktop 3D Bioprinter Available - 3D Printing.” [Online]. Available: <https://3dprinting.com/bio-printing/inkredible-the-most-cost-effective-desktop-3d-bioprinter-available/>. [Accessed: 06-Aug-2018].
- [152] S. Kumar, G. L. Messing, and W. B. White, “Metal Organic Resin Derived Barium Titanate: I, Formation of Barium Titanium Oxycarbonate Intermediate,” *J. Am. Ceram. Soc.*, vol. 76, no. 3, pp. 617–624, 1993.
- [153] S. Maensiri, W. Nuansing, J. Klinkaewnarong, P. Laokul, and J. Khemprasit, “Nanofibers of barium strontium titanate (BST) by sol-gel processing and electrospinning,” *J. Colloid Interface Sci.*, vol. 297, no. 2, pp. 578–583, 2006.
- [154] J. A. Lewis, J. E. Smay, J. Stuecker, and J. Cesarano, “Direct ink writing of three-dimensional ceramic structures,” *J. Am. Ceram. Soc.*, vol. 89, no. 12, pp. 3599–3609, 2006.
- [155] F. Castles *et al.*, “Microwave dielectric characterisation of 3D-printed BaTiO₃/ABS polymer composites,” *Sci. Rep.*, vol. 6, no. March, pp. 1–8, 2016.
- [156] D. Wu, J. Wang, M. Zhang, and W. Zhou, “Rheology of carbon nanotubes-filled poly(vinylidene fluoride) composites,” *Ind. Eng. Chem. Res.*, vol. 51, no. 19, pp. 6705–6713, 2012.
- [157] S. Yu, W. Zheng, W. Yu, Y. Zhang, Q. Jiang, and Z. Zhao, “Formation mechanism of β -phase in PVDF/CNT composite prepared by the sonication method,” *Macromolecules*, vol. 42, no. 22, pp. 8870–8874, 2009.
- [158] Wikipedia, “Polyvinylidene fluoride,” *Wikipedia*, 2018. [Online]. Available: https://en.wikipedia.org/wiki/Polyvinylidene_fluoride. [Accessed: 01-Sep-2018].
- [159] N. Yavo *et al.*, “Large Nonclassical Electrostriction in (Y, Nb)-Stabilized δ -Bi₂O₃,” *Adv. Funct. Mater.*, vol. 26, no. 7, pp. 1138–1142, 2016.
- [160] Y. Niu, K. Yu, Y. Bai, and H. Wang, “Enhanced dielectric performance of BaTiO₃/PVDF composites prepared by modified process for energy storage applications,” *IEEE Trans. Ultrason. Ferroelectr. Freq. Control*, vol. 62, no. 1, pp. 108–115, 2015.
- [161] R. H. Upadhyay and R. R. Deshmukh, “Investigation of dielectric properties of newly prepared β -phase polyvinylidene fluoride-barium titanate nanocomposite

- films,” *J. Electrostat.*, vol. 71, no. 5, pp. 945–950, 2013.
- [162] K. Yu, H. Wang, Y. Zhou, Y. Bai, and Y. Niu, “Enhanced dielectric properties of BaTiO₃/poly(vinylidene fluoride) nanocomposites for energy storage applications,” *J. Appl. Phys.*, vol. 113, no. 3, 2013.
- [163] L. Nicole, C. Laberty-Robert, L. Rozes, and C. Ement Sanchez, “Hybrid materials science: a promised land for the integrative design of multifunctional materials,” *Nanoscale*, vol. 6, pp. 6267–6292, 2014.
- [164] FRAMINGHAM, “Worldwide Wearables Market to Nearly Double by 2021, According to IDC,” *International Data Corporation (IDC)*, 2017. [Online]. Available: <https://www.idc.com/getdoc.jsp?containerId=prUS42818517>. [Accessed: 21-Aug-2018].
- [165] Research nester, “Smart Wearable Device Market Size: Global Industry Demand, Growth, share & Forecast 2024,” *Research nester*, 2018. [Online]. Available: <https://www.researchnester.com/reports/smart-wearable-device-market-global-demand-analysis-opportunity-outlook-2024/380>. [Accessed: 21-Aug-2018].
- [166] R. A. Kishore, S. Priya, and V. Tech, “Piezoelectric wind turbine,” vol. 8690, no. March, pp. 1–8, 2013.
- [167] S. J. Oh, H. J. Han, S. B. Han, J. Y. Lee, and W. G. Chun, “Development of a tree-shaped wind power system using piezoelectric materials,” *Int. J. Energy Res.*, vol. 34, no. 5, pp. 431–437, Apr. 2010.
- [168] B. Lafarge, C. Delebarre, S. Grondel, O. Curea, and A. Hacala, “Analysis and optimization of a piezoelectric harvester on a car damper,” *Phys. Procedia*, vol. 70, pp. 970–973, 2015.
- [169] Q. Zhu and Y. Li, “Piezoelectric Energy Harvesting in Automobiles,” *Ferroelectrics*, vol. 467, no. 1, pp. 33–41, 2014.